11

Magmatism in the Netherlands: expression of the northwest European rifting history

Manfred J. van Bergen, Geert-Jan Vis, Wim Sissingh, Janne M. Koornneef & Isaac Brouwers*

*Corresponding author: M.J.vanBergen@uu.nl

ABSTRACT

The presence of igneous rocks in about 100 wells drilled for hydrocarbons, mainly concentrated in the eastern provinces of the Netherlands, the western onshore and offshore areas and in the northern offshore testify to the significance of magmatic activity in the geological history of the Netherlands. Intrusive rocks, mainly emplaced into Carboniferous and younger sedimentary rocks dominate over lavas and other extrusive products. Prominent exceptions are two buried Late Jurassic volcanoes. The Zuidwal volcano under the Waddenzee consists of thick extrusive deposits and associated subsurface features that collectively define a well-developed volcanic centre. The recently discovered Mulciber volcano is a complex on the rim of the Central Graben below the North Sea.

Radiometric ages have been determined on samples from 25 wells, but most of the currently available results are inaccurate due to ubiquitous effects of alteration. Despite this limitation, additional stratigraphic, geochemical and petrological evidence indicates that magmatism in the Netherlands was largely periodic and followed a pattern of intermittent activity in the North Sea region and adjacent areas in late Paleozoic, Mesozoic and Cenozoic times.

Samples from ca. 15 core intervals studied in detail suggest that a large majority of igneous rocks in the Dutch subsurface have a mafic composition and a moderate to high alkali content. Geochemical signatures are consistent with a within-plate tectonic setting throughout the successive episodes of magmatism, of which the Carboniferous – early Permian and Late Jurassic periods were the most productive. The lithospheric rifting processes that have dominated the northwest European geological history since Paleozoic times provided favourable conditions for melt generation, the emplacement of intrusive magma bodies and associated volcanism.

<< Porphyritic trachyte lava in the upper Carboniferous Step Graben Formation in well F04-02-A (offshore, Dutch Central Graben). Photo: Geert-Jan Vis.

DOI: 10.5117/9789463728362_ch11

Introduction

Igneous rocks are not readily associated with the low-lying, mostly flat landscapes of the Netherlands where surface outcrops of any hard rock are rare and restricted to the rolling countryside near the eastern border and to the south-easternmost part of the country. The only noticeable igneous rocks are building materials that were imported from surrounding countries over many centuries. Columnar basalts, traditionally used for the reinforcement of dikes, are well-known examples.

Nonetheless, the long geological history of the lowlands has known episodes of strong magmatic activity, as is evidenced by a surprisingly rich hidden record in the subsurface across the country, both on land and below the sea. Striking illustrations are the buried Zuidwal and Mulciber volcanoes, which were active in Late Jurassic times. In strong contrast, volcanic activity is ongoing in the Caribbean Netherlands at the present day. The latest eruption of the Quill volcano on the island of Statia was around 250 AD, and that of Mount Scenery on Saba as recent as in 1640 AD or shortly before.

The first discovery of igneous rock in the Dutch subsurface dates back to 1923 when a dolerite intrusion was encountered in an exploration well near Corle in the east of the country (Tesch, 1925, 1928; Tomkeieff & Tesch, 1931). Several years later, similar intrusive rocks were found in the Meddeho and Hupsel wells nearby (Tesch & Van Voorthuysen, 1944). In all of these cases, the intrusion was encountered in Carboniferous shales at current depths of between 957 and 1320 m. Since then, a diversity of intrusive and extrusive igneous rocks has been found in numerous wells drilled mainly by the hydrocarbon industry, both onshore and offshore.

Based on published, unpublished and newly available data, the number of wells in which pre-Quaternary igneous material was identified has grown from 71 (Van Bergen & Sissingh, 2007) to 101 (this work), while the number of radiometrically dated samples increased from 23 to 33. This update presents a thoroughly revized overview of igneous intrusive material (sills, dykes, larger bodies) and extrusive deposits (lavas, ash and other pyroclastic rocks) reported from onshore and offshore exploration wells in publicly available sources, ranging from hand-written notes in internal company documents with core descriptions to peer-reviewed publications. Indirect geophysical evidence for the subsurface presence of igneous rocks is included as well.

In comparison to the preceding overviews (Sissingh, 2004; Van Bergen & Sissingh, 2007) several adjustments have been made. The most conspicuous change concerns the re-evaluation of ages assigned to individual occurrences in the sources consulted. This issue is particularly relevant, given the difficulty of reliably dating magmatic rock without information on the mode of emplacement and the local geological context, a typical drawback in studies of drill-core samples. Since the large majority of radiometric ages is based on conventional K-Ar dating of whole-rock samples, and virtually all of this material underwent significant post-emplacement alteration, the reported ages are of limited value and mostly significantly too young. The restricted number of ages obtained by Ar-Ar methods, generally considered more accurate, should be considered with caution as well, as only a few meet an acceptable quality standard. Furthermore, (bio)stratigraphic age constraints for host sedimentary rocks have little relevance in cases where petrography is inadequate to determine if an interval of solid igneous rock represents effusive material (lava) or a subvolcanic equivalent (sill or dyke). This uncertainty applies to a fair number of cases.

Taking these limitations into account, the available information has been scrutinized and re-interpreted, resulting in an improved subdivision into distinct episodes for Paleozoic, Mesozoic and Cenozoic magmatic activity in the Netherlands. Supporting evidence comes from geochemical signatures of Dutch igneous rocks including an extensive set of new data compiled and discussed in this work. Additional petrographic evidence is illustrated by optical microscope images, representative for the distinct rock types. Coherence from inferred chronology, compositional properties and geographic distribution yields new time frames of recurrent igneous activity, which match the general pattern of magmatism in neighbouring parts of northwest Europe and can be linked to a common history of episodic large-scale rift tectonics.

Finally, more attention is devoted to Cenozoic magmatic activity, including Paleocene manifestations related to the opening of the North-East Atlantic Ocean and the distribution of pyroclastic material in the Netherlands emitted by Quaternary explosive volcanism abroad.

Rock names mentioned throughout this work are not always based on a rigorous application of petrographic or geochemical classifications because appropriate information is sometimes lacking. Instead, the terminology of the original sources is maintained, except for a few cases of obviously incorrect labelling. Qualifications of intrusive or extrusive modes of emplacement should also be taken with care, as interpretations sometimes hinge on poor or conflicting evidence.

Crystalline basement

The oldest igneous rocks in the Netherlands belong to the crystalline basement and were encountered only in offshore well A17-01 on the Elbow Spit High (Fig. 11.1).

According to Frost et al. (1981), the rocks can be classified as biotite monzogranite containing heavily altered biotite and oligoclase (Fig. 11.2). The authors reported a $^{40}Ar/^{39}Ar$ age of 346±7 Ma, obtained from micas, but this should be regarded as a minimum in view of the degree of alteration. The considerably older U-Pb zircon age of 410±7 Ma (A. Gerdes, pers. comm. 2022) is probably a better approximation of the intrusion age. The granite is covered by Devonian sediments and was presumably emplaced during or shortly after the Caledonian Orogeny.

The A17-01 granite is one of 22 occurrences of igneous rocks in the North Sea Basin that can be assigned to the Caledonian basement complex, which further contains a variety of metamorphic rocks (Frost et al., 1981). It is one of the few locations where basement has been encountered in the far eastern Avalonia terrain, close to the Thor Suture. The latter represents the structural border with Precambrian crust of the Baltica paleo-continent (see Vis et al., 2025, this volume) and geophysical modelling suggests that the suture originated from the south-westward underthrusting of Baltica lower crust below the Avalonian margin prior to collision of the continental blocks (Pharaoh et al., 2006; Lyngsie & Thybo, 2007). The A17-01 well is situated in a 50-100-km-wide band running parallel to this boundary, marking a crustal domain characterized by abnormally low seismic velocity and interpreted as remnants of a collapsed Caledonian accretionary complex (Smit et al., 2016).

Available $^{40}Ar/^{39}Ar$ ages of these metamorphic basement rocks cluster around 450 to 440 Ma (latest Ordovician or earliest Silurian) and fall within the Caledonian radiometric dates of Britain and Scandinavia (Frost et al., 1981, and references therein). Many of the obtained ages likely represent overprints of earlier phases of metamorphism or deformation related to the Caledonian Orogeny or older, Precambrian orogenies. Post Caledonian overprints show less consistency and can be attributed to local thermal or tectonic events. One such event around 350 Ma may explain the younger $^{40}Ar/^{39}Ar$ age of the A17-01 monzogranite relative to its intrusion age.

Devonian

The A17-01 well (Fig. 11.3; Table 11.1) also contained Devonian igneous rocks consisting of altered rhyolitic volcanics or quartz porphyry. These rocks are intercalated in non-metamorphic Old Red Sandstone, which covers the basement and was dated at 341±30 Ma with unknown method and reliability (see Sissingh, 2004). However, if the extrusive mode of emplacement and stratigraphic position are correct, this early Carboniferous radiometric age is too young. In the southern end of the Norwegian sector of the North Sea (Fig. 11.3), highly altered quartz porphyries in the Embla oil field have been dated at 374±3 Ma (zircon U-Pb age). They are thought to represent multiple early Famennian alkali rhyolite eruptions with an intraplate compositional signature that form a bimodal suite together with transitional basalts (Lundmark et al., 2012, 2018). These isolated examples of volcanic activity in the North Sea area accompanied the tensional tectonics characteristic for the Devonian development of northwest and central Europe. Devonian bimodal alkaline volcanics also occur in the Cornwall and Rhenish basins, as well as in the more southerly Central Armorican-Saxothuringian Basin. In contrast, calcalkaline volcanism and emplacement of post-orogenic granites accompanied the development of Old Red basins in the northern British Isles (Ziegler, 1990).

Carboniferous and Permian

There is ample evidence for Carboniferous and Permian magmatic activity in the form of igneous intrusive and effusive rocks in ca. 30 wells in the Netherlands subsurface, both onshore and offshore (Fig 11.1). The majority of these occurrences were found in the eastern part of the country. Two igneous episodes have been distinguished but it is worth emphasizing that radiometric age constraints are poor, making a chronological subdivision tenuous. Rocks here denoted as (late) Carboniferous are dominated by mafic intrusions (dolerite, gabbro), while the extrusive nature of subordinate rocks referred to as 'basalts' is not always certain. On the other hand, 'Rotliegend volcanics' of latest Carboniferous-early Permian age are mostly effusive. Both rhyolitic and basaltic varieties occur but compositional information is often lacking. The allocation of igneous rock intervals from individual wells to one of these igneous episodes in the description below and Table 11.1 should be taken with care, particularly for the intrusions that lack independent stratigraphic age control.

Carboniferous

Igneous rocks with a radiometrically determined Carboniferous age are restricted to onshore wells around the eastern Texel-IJsselmeer High (Fig. 11.1). A basaltic lava from Nagele-1 (NAG-01) has been K-Ar dated at 327±8 Ma, which is consistent with its occurrence in the Epen Formation of the Limburg Group (Sissingh, 2004), i.e. near the lower and upper Carboniferous transition. An extrusive basaltic rock in Westphalian sediments in Steenwijkerwold-1 (SWD-01), however, was K-Ar dated as early Permian, in obvious conflict with its alleged extrusive nature (Sissingh, 2004; core photo in Huis in 't Veld & Den Hartog Jager, 2025, this volume). Gabbroic intrusive rocks

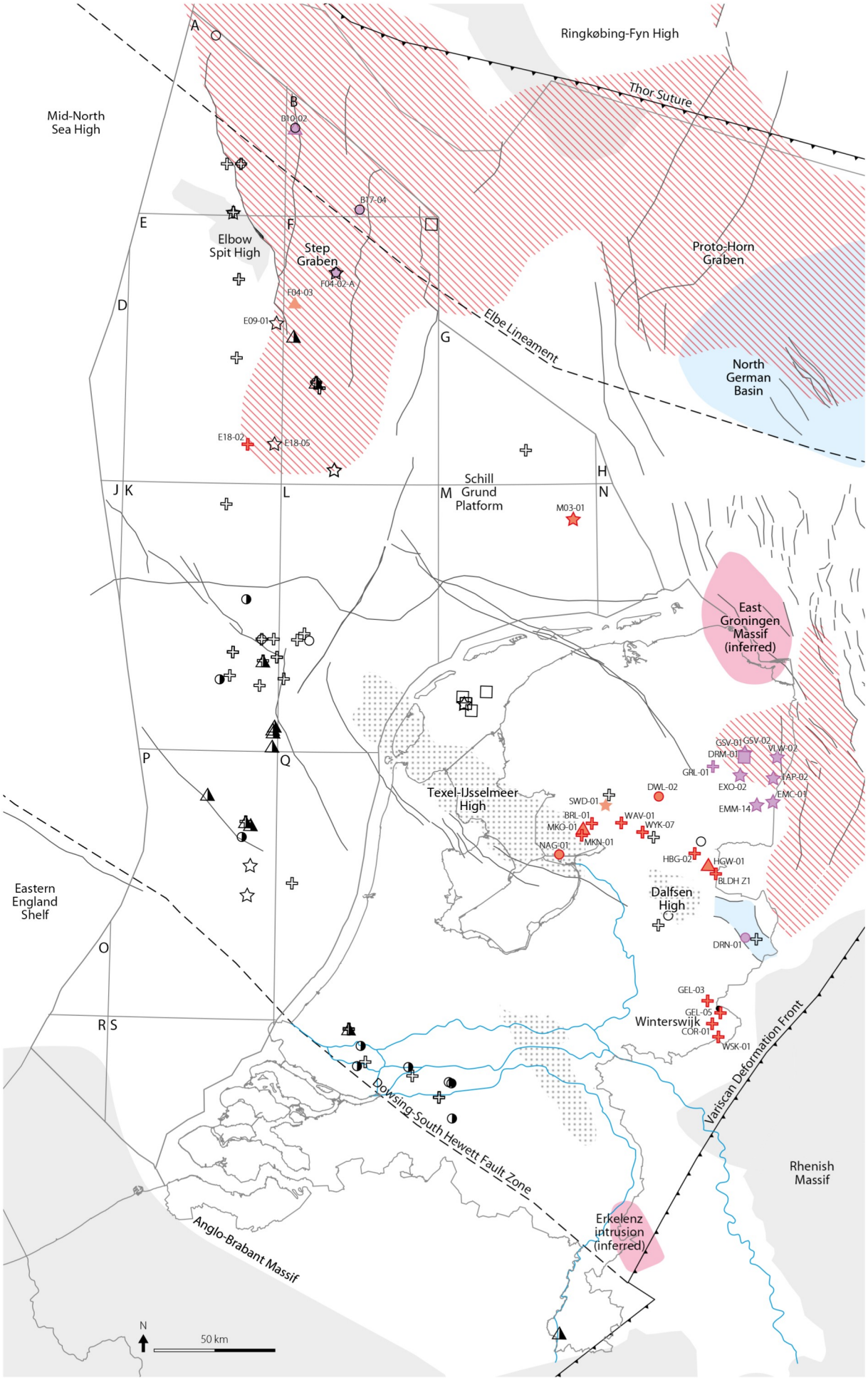
Ringkøbing-Fyn High
Thor Suture
Mid-North Sea High
Elbow Spit High
Step Graben
Proto-Horn Graben
Elbe Lineament
North German Basin
Schill Grund Platform
East Groningen Massif (inferred)
Texel-IJsselmeer High
Dalfsen High
Winterswijk
Eastern England Shelf
Dowsing-South Hewett Fault Zone
Variscan Deformation Front
Rhenish Massif
Anglo-Brabant Massif
Erkelenz intrusion (inferred)
B10-02
B17-04
F04-02-A
F04-03
E09-01
E18-02
E18-05
M03-01
GSV-01
GSV-02
DRM-01
VLW-02
GRL-01
TAP-02
EXO-02
EMC-01
EMM-14
DWL-02
SWD-01
BRL-01
WAV-01
MKO-01
WYK-07
MKN-01
NAG-01
HBG-02
HGW-01
BLDH Z1
DRN-01
GEL-03
GEL-05
COR-01
WSK-01
A
B
D
E
F
G
H
J K
L
M
N
O
P
Q
R S
N
50 km

← ***Figure 11.1.*** *Well locations in the Netherlands where igneous rocks, attributed to the Carboniferous and latest Carboniferous-early Permian ('lower Rotliegend') episodes of magmatic activity, have been found. Wells with igneous material from other or unknown periods are shown for comparison. Structural elements and faults from early Permian times are based on Gast et al. (2010) and Pharaoh et al. (2010). Details on the rocks encountered in the wells are listed in Table 11.1.*

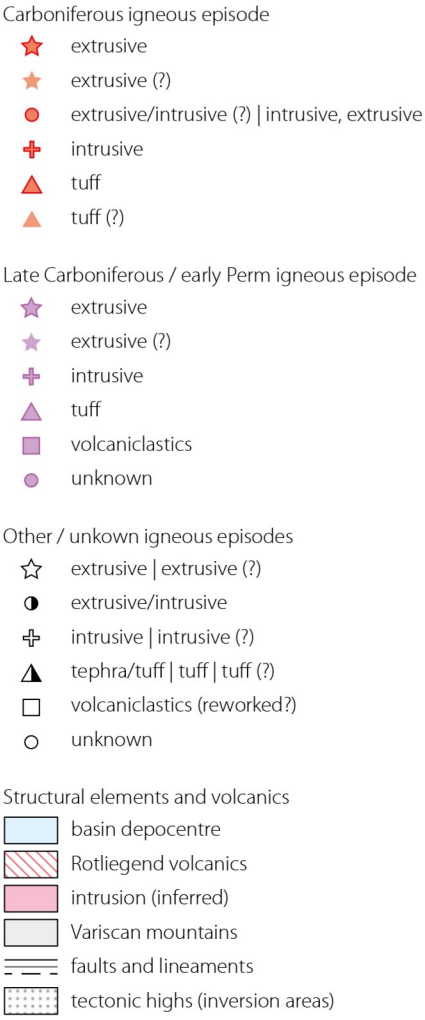

in Dwingelo-2 (DWL-02) (Thiadens, 1963; Eigenfeld & Eigenfeld-Mende, 1986) form a sill-like body of several kilometres in length according to seismic data. K-Ar dating yielded an age of 322±15 Ma. Based on the consistent mafic (gabbroic) character and geographic clustering of these intrusions, it is reasonable to suppose that all of the rocks in the east of the Texel-IJsselmeer High and Dalfsen High are manifestations of this Carboniferous igneous episode despite their generally much younger K-Ar ages.

A similar affinity is probably also valid for some 15 igneous bodies in well Wanneperveen-1 (WAV-01, Fig. 11.1), which were originally interpreted as basalts, dolerites and olivine-dolerites intruded into lower Permian (British Autunian stage) shales and siltstones (Kimpe, 1953). However, in a later revision of the biostratigraphy, Van Amerom (1972) assigned an upper Carboniferous age (Westphalian-A) to these sedimentary rocks. On the basis of petrographic similarity, Dixon et al. (1981) proposed that most, if not all of the igneous rocks in Wanneperveen-1 represent Permian flows equivalent to those present in North Sea wells in the German, Danish and UK sectors around the Ringkøbing-Fyn High. K-Ar dating of a sample from 2035-2030.5 m depth yielded an age of 217±20 Ma (Sissingh, 2004), but this is inconsistent with Rotliegend (or older) volcanics and thus reflects the inaccuracy of the method for these rocks. Hence, if (at least some of) the igneous intervals in Wanneperveen-1 are extrusive, the biostratigraphic age of the intercalated sediments favours a late Carboniferous rather than a 'Rotliegend' magmatic episode. Available compositional evidence is inconclusive as will be discussed below.

Doleritic intrusions in wells around Winterswijk (Fig. 11.1) have not been dated except for an olivine dolerite in Winterswijk-1 (WSK-01; Figs 11.4d, 11.5a), which yielded an (erroneous) K-Ar age of 218±6 Ma. They include the nearby Corle 'melaphyre' and Gelria-3 (GEL-03) 'leucophyre' intrusives, originally referred to as 'dolerites' (Tomkeieff & Tesch, 1931; Tesch & Van Voorthuysen, 1944), and the Gelria-5 (GEL-05) 'dolerite', and are presumably representatives of the same (late) Carboniferous magmatic episode as that of the igneous intervals on the eastern Texel-IJsselmeer High.

Eigenfeld & Eigenfeld-Mende (1986) used petrographic criteria to infer that 'Permo-Carboniferous' mafic intrusive rocks in the eastern Netherlands, including those in Wanneperveen-1, Dwingelo-2, De Wijk-7 (WYK-07) (Fig. 11.6a), the undated intrusions in the wells around Winterswijk (Gelria-3, Corle-1 (COR-01)), and (equally altered) equivalents encountered in wells across the border in Germany all belong to a single magmatic province. An olivine-gabbroic dyke in Balderhaar-Z1 (see Table 11.1b) may well be an example that would fit into this group. These authors proposed that these events could be genetically related to a laccolithic intrusion ('Bramsche Massif') in the southwestern part of the Lower Saxony Basin, inferred from a sizeable gravity and magnetic anomaly coinciding with high thermal maturity of sedimentary organic matter. However, since the maturation process may have been related to the Mesozoic basin evolution instead, a magmatic intrusion as explanation for the anomaly is questionable (Senglaub et al., 2006). In view of the poor absolute age constraints, a Carboniferous rather than Permian affinity is favoured.

Table 11.1. *Pre-Cenozoic igneous rocks encountered in wells in the subsurface of the Netherlands: a) Radiometrically dated igneous rocks (33 ages, 25 wells); b) Igneous rocks without radiometric age dates, but with interpretation of igneous episode (42 wells); c) Igneous rocks without reliable age (41 wells). A more elaborate version of this table, including remarks is available as online supplementary material. Igneous episode is interpreted from geochronological and stratigraphic evidence (letter code with question mark indicates an expected but unconfirmed episode): C = Carboniferous; D = Devonian; J = Jurassic; LC-EP = late Carboniferous-early Permian. Emplacement is based on petrographic and stratigraphic evidence; note that original information is not always conclusive (letter code with question mark indicates uncertainty): ? = undefined; E/E? = extrusive (possibly); E/I? = extrusive or intrusive; I,E = intrusive and extrusive; I/I? = intrusive (possibly); T/T? = tuff (possibly); V/V (rew.?) = volcaniclastic/ possibly reworked volcaniclastic. Rock type/composition is based on the original report where possible; note that the compositions listed here do not follow a rigid classification scheme and must be used with care. NCP = Netherlands Continental Platform; MD = metres along hole; T.D. = Total Depth; CWL = Composite Well Log. A more elaborate online version is available at: DOI: 10.5117/ aup.27114895.*

Table 11.1. *(a)*

Location	Short name	Well name	Igneous interval(s) (MD)	Dated interval (MD)/ Sample depth	Age (Ma)
NCP	A17-01	A17-01	2157.0-2295.0	?	341±30
NCP	A17-01	A17-01	3013.0-3044.0 (=T.D.)	~3043.0	Min. 346±7
NCP	A17-01	A17-01	3013.0-3044.0 (=T.D.)	unknown	410±7
Andel-4	AND-04	Andel-4	1651-1657	1651.4-1652.1 or 1657.1-1658.0	133±2
Baarlo-1-S1	BRL-01-S1	Baarlo-1-S1	1772.5-1775.0; 1780.0-1782.0; 1792.0-1794.0	1775.6	266±18
Berkel-1-S1	BRK-01-S1	Berkel-1-S1	2952-2970	~2964.66	214±25?
De Wijk-7	WYK-07	De Wijk-7	2443-2486	2456.1	155±4
De Wijk-7	WYK-07	De Wijk-7	2684.0-2691.0	2690.5	289±7
Drouwenermond-1-S1	DRM-01-S1	Drouwenermond-1-S1	3920.5-3953.5	3921.0	258±6
Dwingelo-2	DWL-02	Dwingelo-2	3719.0-3799.7 (=T.D.)	3788.8	322±15
NCP	E06-01	E06-01	2405-2428	2415	161±4
NCP	E06-01	E06-01	2405-2428	2420	183±4
NCP	E12-03	E12-03	3653-3682; 3788-3875 (=T.D.)	3678	221±23
NCP	E18-02	E18-02	4432-4460	4439	274±7
NCP	F03-07	F03-07	?	~2928.05	236±6
NCP	F04-02-A	F04-02-A	4630-4656 (=T.D.)	4650-4656	165±2
NCP	F10-01	F10-01	3426-3460 (=T.D.)	3450.25	99±5
NCP	F10-01	F10-01	3426-3460 (=T.D.)	~3449-3460	>127
NCP	F10-01	F10-01	3426-3460 (=T.D.)	~3449-3460	151±2
Giessendam-1	GSD-01	Giessendam-1	1190-1218; 1350-1380	~1220	125±25
Hardenberg-2-S1	HBG-02-S1	Hardenberg-2-S1	3376.5-3441.0	3410.6	290±16
NCP	K12-05-S1	K12-05-S1	3057-3292	~3121-3133	152±7
NCP	L13-03	L13-03	877-909, 1604-1645; 1808-1821; 1931-1943	~1820	101±1
Loon-op-Zand-1	LOZ-01	Loon-op-Zand-1	2454-2457.5; 2572-2610; 2682-2694	?	132±3
NCP	M03-01	M03-01	4038-4055	4036-4055	188.5±8.4
Nagele-1	NAG-01	Nagele-1	2772.0-2776.0	2774.0	327±8
NCP	Q07-02	Q07-02	3405-3440	~3450 (?)	95±2 to 106±2
Steenwijkerwold-1	SWD-01	Steenwijkerwold-1	1937.0-1944.5	1940.5	291±8
Wanneperveen-1	WAV-01	Wanneperveen-1	2017-2019; 2028-2028.5; 2064-2069.5	2034.0	217±20?
Winterswijk-1	WSK-01	Winterswijk-1	4078-4149	4150.0	218±6
Zuidwal-1	ZDW-01	Zuidwal-1	1944-3002	?	144±1
Zuidwal-1	ZDW-01	Zuidwal-1	1944-3002	?	145
Zuidwal-1	ZDW-01	Zuidwal-1	1944-3002	?	152±3

Method	Igneous episode (interpreted)	Stratigraphy of host/ intruded interval	Emplacement	Rock type/composition as reported	Reference(s)
?	D	Buchan Fm	E	Rhyolite-Rhyodacite	Sissingh (2004)
$^{40}Ar/^{39}Ar$	D	'Basement'	I	Biotite monzo-granite	Frost et al. (1981)
U-Pb	D	'Basement'	I	Biotite monzo-granite	Axel Gerdes, pers. com. (2022)
$^{40}Ar/^{39}Ar$	J	Werkendam Fm	E/I?	Nephelinite, basanite	Dixon et al. (1981)
K-Ar	C	Ruurlo Fm	I	Dolerite ('diabase')	Sissingh (2004)
K-Ar	J	Werkendam Fm	I	Essexite or theralite	Sissingh (2004); Dixon et al. (1981); Van der Sijp (1953)
K-Ar	C	Maurits Fm	I	Olivine gabbro	Sissingh (2004); Eigenfeld & Eigenfeld-Mende (1986)
K-Ar	C	Maurits Fm	I	Gabbro	Sissingh (2004)
K-Ar	LC-EP?	Emmen Volcanic Fm	V	Mixed clastic and igneous	Sissingh (2004)
K-Ar	C	Baarlo Fm	I,E	Olivine gabbro	Sissingh (2004); Eigenfeld & Eigenfeld-Mende (1986)
K-Ar	?	Elleboog Fm	I	No data	Sissingh (2004)
K-Ar	?	Elleboog Fm	I	No data	Sissingh (2004)
K-Ar	?	Millstone Grit Fm	I	Dolerite or microgabbro	CWL on NLOG.nl; Peniguel et al. (1992)
K-Ar	C	Klaverbank Fm	I	Gabbro	Sissingh (2004)
K-Ar	?	Lower Graben Fm	V (rew.?)	No data	Sissingh (2004); Herngreen (1985)
K-Ar	LC-EP	Step Graben Fm	E?	Porphyritic rhyolite lava/ micro-granodiorite	Slater (1980); Kuijper (1991)
K-Ar	J	Zechstein Gp	I	Lamprophyre	Kuijper (1991); Sissingh (2004)
$^{40}Ar/^{39}Ar$ whole-rock	J	Zechstein Gp	I	Potassic alkaline lamprophyre	Latin (1990)
$^{40}Ar/^{39}Ar$ kaersutite	J	Zechstein Gp	I	Potassic alkaline lamprophyre	Latin (1990)
K-Ar	J	Nieuwerkerk Fm	E/I?	'Basalt'	Rieffe & Van Lil (1992); Sissingh (2004)
K-Ar	C	Ruurlo Fm	I	Olivine gabbro	Sissingh (2004)
K-Ar	J	Zechstein Gp	I	Alkali-rich lamprohyre	Well K12-05-S1 on NLOG.nl
$^{40}Ar/^{39}Ar$	J	Zechstein Gp	I	Resembling South Holland olivine nephelinites	CWL on NLOG.nl; Dixon et al. (1981)
$^{40}Ar/^{39}Ar$	J	Aalburg Fm	E/I?	Nephelinite, basanite	Dixon et al. (1981)
K-Ar	C	Ruurlo Fm	E	Pyroxene basalt with trachytic texture	Meadows & Hrycyszyn (1992)
K-Ar	C	Epen Fm	E/I?	Thin dolerite-like intrusive bodies (?)	RGD (1993); Sissingh (2004)
$^{40}Ar/^{39}Ar$	J	Solling Fm	I	Undersaturated basalt	Dixon et al. (1981)
K-Ar	C	Ruurlo Fm	E?	'Basalt'	Sissingh (2004)
K-Ar	C	Limburg Gp	I	Dolerite, (olivine-) gabbro	Sissingh (2004); Kimpe (1953)
K-Ar	C	Epen Fm	I	Olivine dolerite	Sissingh (2004); NITG (1998)
$^{40}Ar/^{39}Ar$	J	Zuidwal Volcanic Fm	E	(Mafic) phonolite, phonolitic basanite	Dixon et al. (1981)
K-Ar	J	Zuidwal Volcanic Fm	E	Trachyte	Harrison et al. (1979)
$^{40}Ar/^{36}Ar$-$^{40}K/^{36}Ar$	J	Zuidwal Volcanic Fm	E	Trachyte, phonolite, leucitite	Perrot & Van der Poel (1987)

Table 11.1. (b)

Location	Short name	Well name	Igneous interval(s) (MD)	Igneous episode (interpreted)
Andel-2	AND-02	Andel-2	1355-1421	J?
NCP	B10-02-S1	B10-02-S1	3780-3810	LC-EP
NCP	B17-04	B17-04	4376-4391	LC-EP
Balderhaar Z1 (Germany)	BLDH Z1	Balderhaar Z1 (Germany)	3608.4-3748.3; 3845.0-3847.0; 3863.0-3866.0	C
Berkel-1-S1	BRK-01-S1	Berkel-1-S1	2863-2875; 2933-2984	J
Corle-1	COR-01	Corle-1	970-983	C?
Deurningen-1	DRN-01	Deurningen-1	1468-1471	LC-EP
Emmen-14	EMM-14	Emmen-14	4087-4153	LC-EP
Emmer-Compascuum-1(-S1)	EMC-01(-S1)	Emmer-Compascuum-1(-S1)	3935-4014	LC-EP
Exloo-2-S2	EXO-02-S2	Exloo-2-S2	4190-4200	LC-EP
NCP	F04-03	F04-03	4206-4250; 4262-4288; 4375-4403	C
NCP	F16-02	F16-02	1662-1701	J
Gasselternijveen-1	GSV-01	Gasselternijveen-1	3736-3766	LC-EP
Gasselternijveen-2	GSV-02	Gasselternijveen-2	3909.5-3941.0 (=T.D.)	LC-EP
Gelria-3 (Hupsel)	GEL-03	Gelria-3 (Hupsel)	1320.7-1321.7	C?
Gelria-5 (Meddeho)	GEL-05	Gelria-5 (Meddeho)	957-958; 1070-1070.45	C?
Grollo-1	GRL-01	Grollo-1	3513-3525.5	LC-EP
Heinenoord-1	HEI-01	Heinenoord-1	2213-2261	J
Hoogenweg-1	HGW-01	Hoogenweg-1	3134	C
NCP	K12-G-05-S1	K12-G-05-S1	3917-3971; 4011-4095; 4098-4104	J
NCP	K14-FA-103	K14-FA-103	3215-3240 or 3439-3459 (cored sections)?	J
NCP	K15-13	K15-13	3687-3691	J
NCP	K18-01	K18-01	2184-2436 (interval with tuffs)	J
NCP	K18-02-A	K18-02-A	2170-2190 (interval with tuffs)	J
NCP	K18-03	K18-03	1905-1927 (interval with tuffs)	J
NCP	K18-05	K18-05	2550-2645 (interval with tuffs)	J
Marknesse Oost-1	MKO-01	Marknesse Oost-1	1864-1882	C
Marknesse-1	MKN-01	Marknesse-1	1908-1918	C
NCP	P02-06	P02-06	1366-1560 (interval with tuffs)	J
NCP	P06-01	P06-01	2060-2180 (interval with tuffs)	J
NCP	P06-B-01	P06-B-01	1595-1640 (possible tuff layer)	J
NCP	P09-08-S1	P09-08-S1	3060 (breccia: 3049-3071)	J
NCP	P12-08	P12-08	2665 (breccia: 2659-2702)	J
Slenk-1	SLK-01	Slenk-1	2274.5-2352.5	J
Ter Apel-2-S1	TAP-02-S1	Ter Apel-2-S1	4534.2-4601.5	LC-EP
Vlagtwedde-2	VLW-02	Vlagtwedde-2	4140-4165	LC-EP
Zuidwal-2	ZDW-02	Zuidwal-2	2167-2189	J
Zuidwal-3	ZDW-03	Zuidwal-3	2055-2080	J
Zuidwal-A-01(-S1)	ZDW-A-01(-S1)	Zuidwal-A-01(-S1)	1950-2060; 1950-2130 (S1)	J
Zuidwal-A-02	ZDW-A-02	Zuidwal-A-02	2048-2245	J
Zuidwal-A-04	ZDW-A-04	Zuidwal-A-04	2662-2835	J
Zuidwal-A-05	ZDW-A-05	Zuidwal-A-05	2060-2260	J

Stratigraphy of host/ intruded interval	Emplacement	Rock type/composition as reported	Reference(s)
Werkendam Fm	E/I?	Olivine nephelinite, basanite	Kuijper (1991)
Lower Rotliegend Gp	T	Volcanic tuff	Sissingh (2004)
Lower Rotliegend Gp	E?	?	CWL on NLOG.nl
Westphalian A	I	Dolerite (gabbroic rock containing abundant olivine and feldspar laths, as well as magnetite, glass and biotite)	Sissingh (2004); Anonymous (1992)
Werkendam Fm	T	No data	Sissingh (2004)
Ruurlo Fm	I	Dolerite	Tomkeieff & Tesch (1931)
Emmen Volcanic Fm	?	?	CWL on NLOG.nl
Emmen Volcanic Fm	E	No data	Sissingh (2004)
Emmen Volcanic Fm	E	Basalt and tephra	Sissingh (2004); NITG (2000)
Emmen Volcanic Fm	E	No data	Sissingh (2004)
Maurits Fm	T?	No data	CWL on NLOG.nl; De Bruin et al. (2015)
New Fm; Mulciber	E	Tuff grading into "basalt" and tuffaceous siltstone; porphyritic (basaltic-) andesitic extrusive rock	Lester (1985)
Emmen Volcanic Fm	E	No data	Sissingh (2004)
Emmen Volcanic Fm	E	No data	Sissingh (2004)
Ruurlo Fm	I	Dolerite ("diabase")	Tesch & Van Voorthuysen (1944)
Ruurlo Fm	I	Dolerite ("diabase")	Tesch & Van Voorthuysen (1944)
Emmen Volcanic Fm	I	Dolerite ("diabase")	Sissingh (2004)
Nieuwerkerk Fm	E/I?	Alkali basalt	Helmers (1991)
Maurits Fm	T	Sanidine-containing ash	Van Buggenum & Den Hartog Jager (2007)
Zechstein Gp	I	No data	Neptune Energy
Slochteren Fm	E/I?	Trachybasalt	Dixon et al. (1981)
Slochteren Fm	I	No data	CWL on NLOG.nl
Breeveertien Fm	T	No data	Sissingh (2004)
Breeveertien Fm	T	No data	CWL on NLOG.nl
Breeveertien Fm	T	No data	Sissingh (2004)
Breeveertien Fm	T	No data	Sissingh (2004)
Limburg Gp	T	Tuff with augite	Rieffe & Van Lil (1992)
Ruurlo Fm	I	Extrusive rock according to CWL	Sissingh (2004)
Nieuwerkerk Fm	T	No data	Sissingh (2004)
Nieuwerkerk Fm.	T	No data	Sissingh (2004)
Vlieland Sandstone Fm	T?	No data	King et al. (1985)
Breeveertien Fm	E?	Olivine basalt	Sissingh (2004); Galavazi (1999); NLOG.nl
Vlieland Sandstone Fm	E?	Lamprophyric	Sissingh (2004); Galavazi (1999); NLOG.nl
Wadden Volcaniclastic Mbr	V	Volcanic breccia (CWL)	Herngreen et al. (1991)
Emmen Volcanic Fm	E	No data	Sissingh (2004)
Emmen Volcanic Fm	E	No data	Sissingh (2004)
Wadden Volcaniclastic Mbr	V	Volcanic tuff (CWL)	Herngreen et al. (1991)
Wadden Volcaniclastic Mbr	V	Volcanic breccia (CWL)	Herngreen et al. (1991)
Wadden Volcaniclastic Mbr	V	Volcanic breccia (CWL)	CWL on NLOG.nl
Wadden Volcaniclastic Mbr	V	Volcanic breccia (CWL)	CWL on NLOG.nl
Wadden Volcaniclastic Mbr	V	Volcanic breccia (CWL)	CWL on NLOG.nl
Wadden Volcaniclastic Mbr	V	Volcanic breccia (CWL)	CWL on NLOG.nl

Table 11.1. (c)

Location	Short name	Well name	Igneous interval(s) (MD)
NCP	A05-01	A05-01	3930-3971.8 (=T.D.)
NCP	A14-01	A14-01	2718-2775
NCP	A15-01	A15-01	3591-3753
NCP	A15-01	A15-01	3753-3773; 3790-3883
NCP	B10-02-S1	B10-02-S1	3810-3972 (=T.D.)
NCP	B17-04	B17-04	4300-4376
Barendrecht-Ziedewij-1	BRTZ-01	Barendrecht-Ziedewij-1	3092-3096
Berkel-2	BRK-02	Berkel-2	1758-1784
Coevorden-17-S1	COV-17-S1	Coevorden-17-S1	?
De Blesse-1-S1	BLS-01-S1	De Blesse-1-S1	2014-2070
De Wijk-15-S1	WYK-15-S1	De Wijk-15-S1	?
NCP	E09-01	E09-01	3290-3345
NCP	E18-05	E18-05	~4318-4328
NCP	F04-02-A	F04-02-A	4400-4425; 4490-4515
NCP	F04-02-A	F04-02-A	4425-4533.5
NCP	F07-02	F07-02	3783-3927
NCP	F10-02	F10-02	2010-3441 (interval with tuffs)
NCP	F10-02	F10-02	4055-4061
NCP	F10-02	F10-02	4061-4090
NCP	F16-02	F16-02	1738-1872 (interval with tuffs)
NCP	F16-02	F16-02	1872-1985
NCP	G17-02	G17-02	4295-4310
Haarle-1	HLE-01	Haarle-1	1480-1497
Hellendoorn-1	HLD-01	Hellendoorn-1	1455-1493 (=T.D.)
Heugem-1	HEU-01	Heugem-1	397
IJsselmonde-64(-S1)	IJS-64(-S1)	IJsselmonde-64(-S1)	2242-2263; 2260-2268 (S1)
NCP	K02-02	K02-02	4556-4588
NCP	K09-01	K09-01	3567-3571
NCP	K12-05	K12-05	2897-2902
NCP	K12-05-S1	K12-05-S1	2919-2923
NCP	K12-B-04	K12-B-04	4103.5-4110.5 (tuff band in this interval)
NCP	K12-B-06	K12-B-06	3875-3888 (within cored interval?)
NCP	K12-D-01	K12-D-01	3760-3765, 3854-3862, 3989-3997
NCP	K12-D-03	K12-D-03	3880-3890
NCP	K12-G-08	K12-G-08	3804-3810; 3881-3906, 4082-4248
NCP	K12-K-01	K12-K-01	3795-3917 (three intercalated salt layers)
NCP	K15-04-S2	K15-04-S2	3230, 3237, 3344, 3338, 3350, 3242, 3248, 3250, 3217, 3226, 3414, 3436, 3568
NCP	L10-06	L10-06	3835-3870
NCP	L10-31	L10-31	3610-3638
NCP	L10-L-05-S1(?)	L10-L-05-S1(?)	5164, 5176, 5194
Oldenzaal-2	OLZ-02	Oldenzaal-2	269-274
Overkamp	B34G1431	Overkamp	142.0-142.5
NCP	P06-10	P06-10	3200-3227
NCP	P06-B-01	P06-B-01	?
Sprang-Capelle-1	SPC-01	Sprang-Capelle-1	2219-2223
Sprang-Capelle-1	SPC-01	Sprang-Capelle-1	2357-2377
Sprang-Capelle-1	SPC-01	Sprang-Capelle-1	2598-2606.5
Werkendam-1	WED-01	Werkendam-1	1553.5-1554.5

Stratigraphy of host/intruded interval	Emplacement	Rock type/composition as reported	Reference(s)
Lower Rotliegend Gp	?	Volcanics in claystone	CWL on NLOG.nl
Epen Fm	I	Porphyry?	Sissingh (2004)
Lower Rotliegend Gp	?	?	CWL on NLOG.nl
Lower Rotliegend Gp & Millstone Grit Fm	I	Gabbro, micro-granodiorite	Kuijper (1991)
Lower Rotliegend Gp	?	?	CWL on NLOG.nl
Lower Rotliegend Gp	?	?	CWL on NLOG.nl
Strijen Fm	I	Dolerite	Van Buggenum & Den Hartog Jager (2007)
Nieuwerkerk Fm	I	No data	Sissingh (2004)
?	?	Uncertain; no public data	Sissingh (2004)
Ruurlo Fm	I	Gabbroic (plagioclase, pyroxene, olivine in groundmass of chloritic serpentinitic clays with local magnetite and calcite)	Sissingh (2004); NLOG.nl
?	I	No data	Sissingh (2004)
Millstone Grit Fm	E?	Porphyry?	Sissingh (2004)
Limburg Gp	E?	Basaltic	Kuijper (2003)
Lower Rotliegend Gp	E?	Claystone with volcanic fragments	CWL on NLOG.nl
Lower Rotliegend Gp	?	Volcanics (?) in siltstone/sandstone	CWL on NLOG.nl
Lower Rotliegend Gp	T?	Tuff (?) in claystone/siltstone/sandstone	CWL on NLOG.nl
Lower Zechstein salt	T?	No data	CWL on NLOG.nl
Lower Rotliegend Gp	I?	Leucocratic, equigranular, quartz, amphibole, feldspar	CWL on NLOG.nl; De Bruin et al. (2015)
Lower Rotliegend Gp	?	?	CWL on NLOG.nl
Zechstein Gp	E	Anhydrite with tuff layers	Lester (1985)
Zechstein Gp	E	Acidic porphyritic volcanic rock containing augite, biotite, apatite; volcaniclastic sediment	Lester (1985)
Limburg Gp	I	Dolerite	Kuijper (1991)
Maurits Fm	I	Dolerite (diabase')	Sissingh (2004)
Ruurlo Fm	?	No data	Sissingh (2004)
Zeeland Fm	T	No data	Bless et al. (1981)
Werkendam Fm	E/I?	Basanitic	Sissingh (2004)
Klaverbank Fm	I?	No data	CWL on NLOG.nl
Z3 Salt Mbr	E/I?	Olivine basalt	CWL on NLOG.nl
Zechstein Gp	I	Lamprophyre	Kuijper (1991)
Zechstein Gp	I	Alkali-rich lamprohyre	Neptune Energy
Zechstein Gp	T	No data	Neptune Energy
Silverpit Fm	I	No data	Neptune Energy
Slochteren Fm	I	Andesite, olivine dolerite	Neptune Energy
Slochteren Fm	?	No data	Neptune Energy
Zechstein Gp	I	Lamprophyre	Neptune Energy
Zechstein Gp	I	Lamprophyre	Neptune Energy
Lower and Upper Germanic Trias gps	I?	No data	Sissingh (2004)
Slochteren Fm	I	Lamprophyre-type (?)	Neptune Energy
Slochteren Fm	I	Lamprophyre-type (cutting thin section 3630 mMD)	Neptune Energy
Limburg Groep	?	High plagioclase content (14-60 wt.%)	Neptune Energy
Coevorden Fm	I	Dolerite (hornblende 'diabase')	Van Voorthuysen (1944)
Volpriehausen Fm (?)	T	Tephra?	water well (pers. com. M. van den Bosch, 2022)
Detfurth Fm	E/I?	Mafic rock	Sissingh (2004)
?	I	Lamprophyre	Kuijper (1991)
Werkendam Fm	I	Contains nepheline and biotite	CWL on NLOG.nl
Sleen Fm	I	Contains nepheline and biotite	CWL on NLOG.nl
Hardegsen Fm	I	Contains nepheline and biotite	CWL on NLOG.nl
Brabant Fm	I	Dolerite	Sissingh (2004)

Widespread kaolinite-coal-tonstein beds in the Limburg Group represent altered tuffaceous horizons in the former coal-mining district of the south-eastern Netherlands, providing evidence for explosive volcanism during the late Carboniferous (Lippolt et al., 1984). A 5-cm-thick ash layer at 3134 m depth in well Hoogenweg-1 (HGW-01) (Huis in 't Veld & Den Hartog Jager, 2025, this volume) may be a northern equivalent.

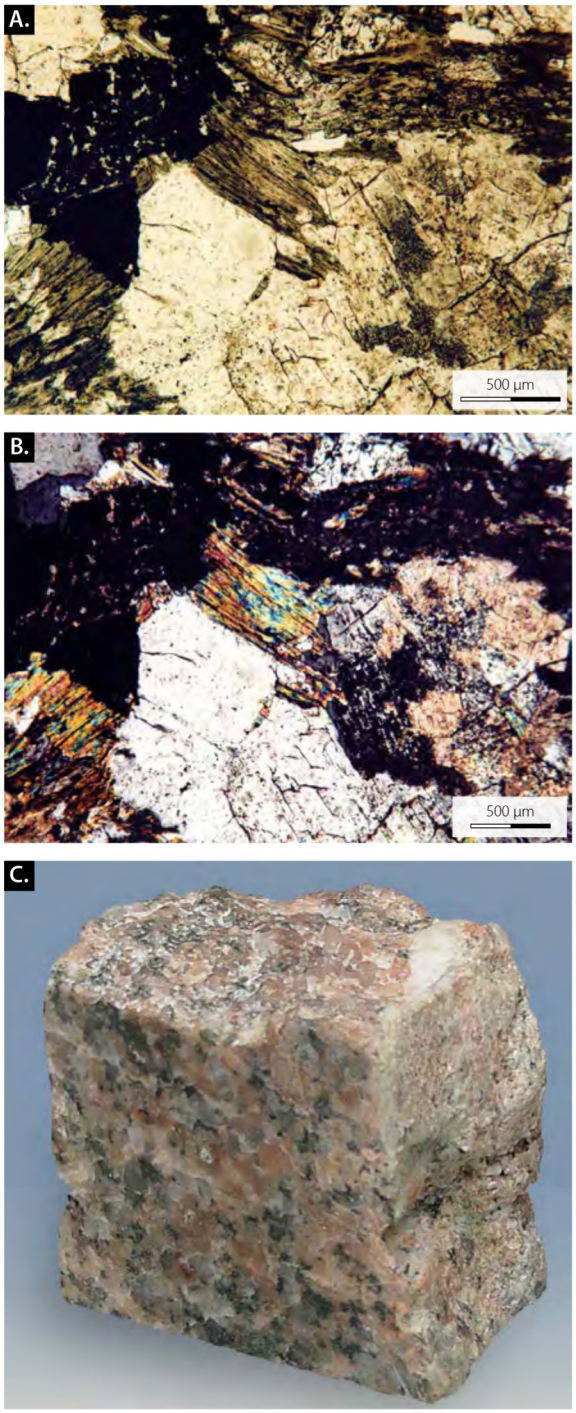

Figure 11.2. *Microphotographs and the single available core sample of the oldest igneous rock encountered in the Dutch subsurface (well A17-01): a) Altered biotite granite (PPL) (depth 2985 m); b) Same in XPL; c) Core sample of the same rock of ~5 cm wide. (estimated depth 2985 m). Images (a-b) are taken from De Vos et al. (2010) and were originally supplied by Frost (Conoco) and Miller (University of Cambridge).*

In the offshore, dated and undated igneous intervals in Carboniferous sediments have been encountered mostly in the Step Graben area and the Schill Grund Platform (quadrants A, E, F and M; see Fig. 11.1). Putative extrusive lavas and ash/tuff layers would be consistent with emplacement during the Carboniferous episode (wells E09-01, E18-05, F04-02A), whereas a K-Ar age of 188.5±8.4 Ma for a basaltic rock in the Ruurlo Formation (well M03-01; Meadows & Hrycyszyn, 1992) is too young.

Considering the stratigraphic relationships of the extrusive products, most of the magmatic bodies encountered in wells in the Netherlands would appear to have a late Carboniferous age. Given the similar compositional character and foreland position (just north of the Variscan front), they likely correspond to manifestations of Namurian-Westphalian magmatism cropping out in the British Isles, in particular with alkaline and locally subalkaline basaltic flows, sills and dykes in the English Midlands and Derbyshire (Timmerman, 2004; Wilson et al., 2004). Probably, there also is a temporal and compositional overlap with the long-lived magmatism in the Midland Valley of Scotland where mostly mildly alkaline magmas were produced during intermitted pulses throughout Carboniferous times (Monaghan & Pringle, 2004; Upton et al., 2004; Monaghan & Parrish, 2006).

Latest Carboniferous – early Permian

Igneous rocks representing 'Rotliegend volcanics' with reliable, radiometrically determined ages around the Carboniferous-Permian boundary (299 Ma; Gradstein et al., 2004) are lacking in the database documented here (Table 11.1). This is in spite of the widespread occurrence of 'Rotliegend volcanics' and intrusives in the Southern Permian Basin (Fig. 11.7) (cf. Glennie, 1997, and references therein; cf. Scheck & Bayer, 1999), which extend over some 1700 km from England across the North Sea through northern Germany into Poland (Ziegler, 1990; Gast et al., 2010).

According to zircon U-Pb and whole-rock Ar-Ar ages of igneous intervals in wells in the neighbouring northeast German Basin system, North Sea Central Graben and Danish North Sea, 'Rotliegend volcanics' were emplaced in a narrow time window between 303±10 and 293±2 Ma (Heeremans et al., 2004; Breitkreuz et al., 2007). The thickest occurrences of these volcanics may have been associated with caldera subsidence (Benek et al., 1996). In North Sea wells, volcanic intervals from the lower Permian have been referred to as the Inge Volcanics Formation in the UK Central Graben and as the Karl Formation in the Danish Central Graben and Norwegian-Danish Basin.

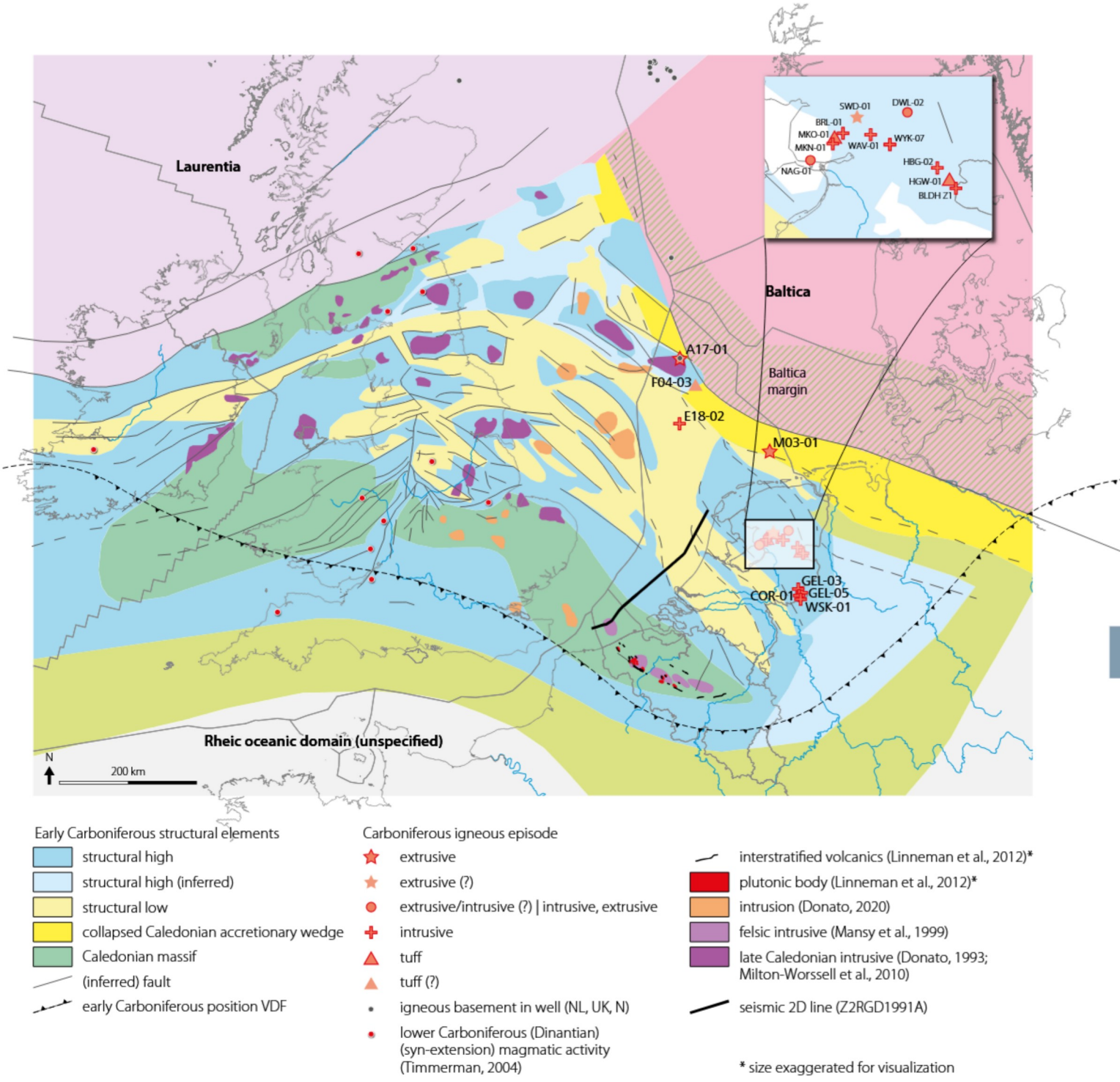

Figure 11.3. Onshore and offshore locations where the oldest igneous rocks in the Netherlands were recovered from drill cores. In well A17-01, a pre-Devonian basement granite and a presumably late Devonian extrusive felsic rock were encountered. In other labelled wells, intrusive or extrusive igneous rocks with an assumed (late) Carboniferous age were found. Red dots indicate locations of Carboniferous magmatism in Britain and Ireland (Timmerman, 2004) and black dots indicate wells where igneous basement rock was found in the northern North Sea (Frost et al., 1981; Slagstad et al., 2011; Lundmark et al., 2012; Riber et al., 2015). The horst-graben type structural framework at the end of the early Carboniferous and the approximate margin of the Variscan Deformation Front (VDF) are after Smit et al. (2018). Late Caledonian, mostly granitic intrusions, inferred from gravity anomalies after Donato (1993, 2020), Mansy et al. (1999), Linneman et al. (2012) and Milton-Worssell et al. (2010).

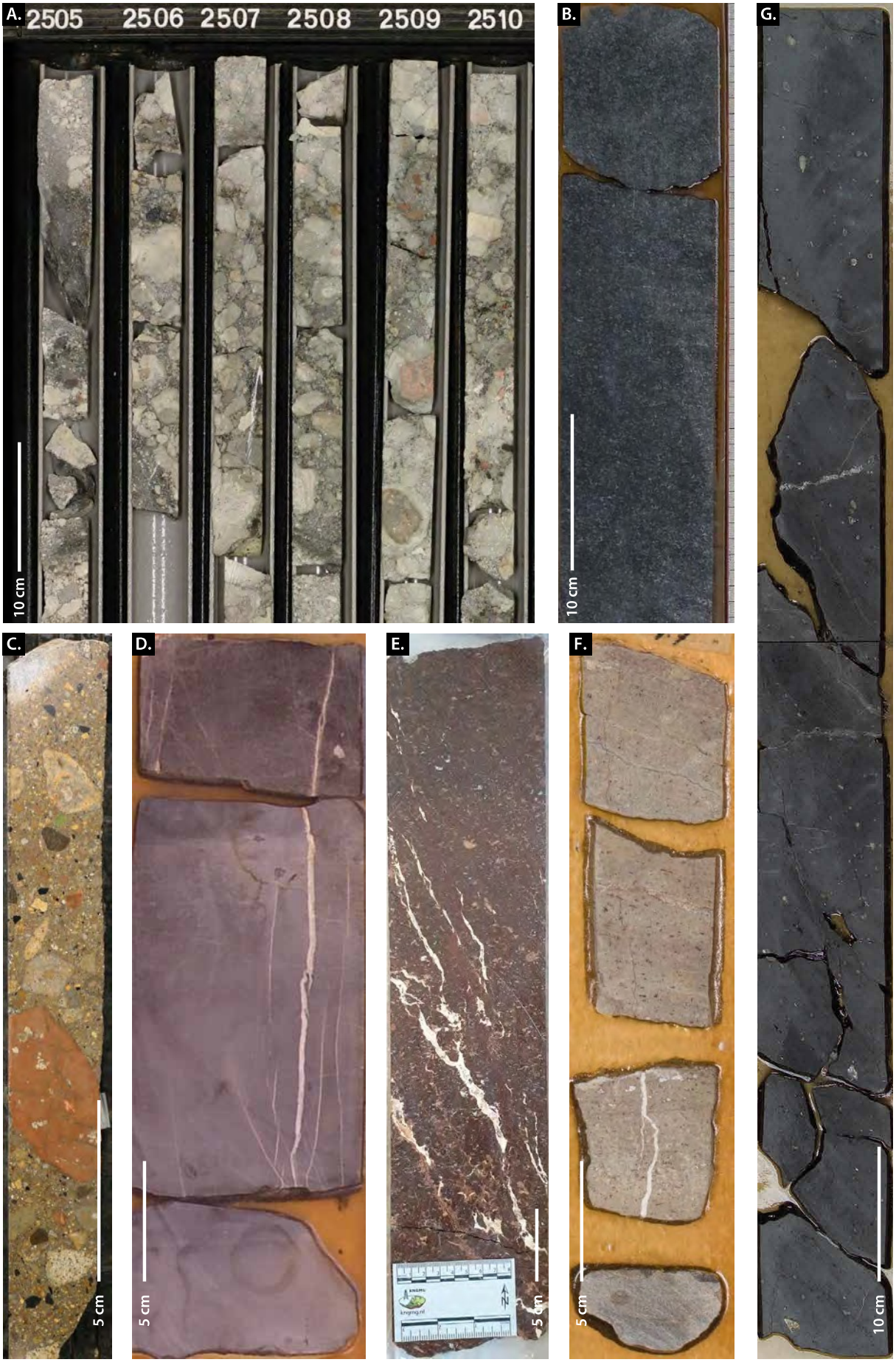
A.
2505
2506
2507
2508
2509
2510
10 cm
B.
10 cm
G.
10 cm
C.
5 cm
D.
5 cm
E.
5 cm
F.
5 cm

Corresponding deposits in the Dutch subsurface onshore are represented by undated rocks of the Emmen Volcanic Formation (Fig. 11.7), which consist of basaltic lava flows and pyroclastic rocks, usually intercalated between clastic sedimentary rocks of the Limburg Group (below) and basal layers of the Zechstein Group (above). Reaching a maximum thickness of 66 m (TNO-GDN, 2022), they can be considered as a westerly extension of 'Rotliegend volcanics' in the adjacent German Ems Graben (Figs 11.1 & 11.7), which have been described as spilitized, mildly alkaline andesites with subordinate basaltic and rhyolitic rocks (Eckhardt, 1979; cf. Plein, 1995, and references therein). Volcaniclastics in the sidetrack of Drouwenermond-1 (DRM-01-S1) with a K-Ar age of 258±6 Ma may also belong to this suite. Near the Dutch Central Graben, a porphyritic rhyolite in well F04-02A (Figs 11.1 & 11.4e) and rocks in wells within and near the A and B quadrants (Figs 11.1 & 11.7) represent time-equivalent magmatic rocks. These volcanics are almost 150 m thick and consist of pyroclastic rocks and lavas up to tens of metres thick (Geluk, 1997).

Dixon et al. (1981) reported the presence of a bimodal association of lower Permian volcanics along the northern and western flanks of the Ringkøbing-Fyn High and from within the Horn Graben, west of Denmark. Strongly altered basalts contain primary biotite and, on the basis of immobile trace elements, have been classified as transitional between olivine tholeiites and mildly alkaline basalts. The silicic rocks may represent silicified trachytes, although their original chemical composition is unclear. Stemmerik et al. (2000) suggested that Permian volcanism in the Danish part of the North Sea took place during two separate events dated 276-281 Ma and 261-269 Ma, thus postdating the early Permian volcanism in the Southern Permian Basin (Fig. 11.8). However, Heeremans et al. (2004) argued that these K-Ar ages might be too young, based on an Ar-Ar age of 299±3 Ma, which the authors obtained on a basalt sample from well 39/2-4 (Fig. 11.7) on the adjacent western flank of the UK Central Graben. Thin intervals of (strongly altered) alkaline intra-plate basalts have also been reported from the Norwegian Embla oil field (well 2/7-23S, Fig. 11.3), and potentially correlative basalts from the nearby Argyll and Auk oil fields in the UK sector of the Central North Sea (Lundmark et al., 2012, 2018, and references therein). A sample from the Danish offshore well C-1 in the eastern North Sea near the Jylland Peninsula (Fig. 11.7), yielded a high-resolution ion microprobe U-Pb zircon age of 303±10 Ma (Breitkreuz et al., 2007).

Different periods of extensive intrusive and extrusive magmatism accompanied the development of the Oslo Rift (Fig. 11.7; Neumann et al., 1992, 2004). According to U-Pb dating (zircon, perovskite, titanite), initial mainly mafic magmatism at ca. 300 Ma was followed by a ca. 40 Myr long interval of mafic and felsic intrusive and extrusive activity (Pedersen et al., 1995; Dahlgren et al., 1996; Corfu & Dahlgren, 2008; Corfu & Larsen, 2020). The rocks vary in composition between basaltic and granitic, all having a strongly alkaline character.

A comprehensive study of the widespread late Carboniferous-Permian magmatism in the northeast German Basin showed that thick rhyolitic rocks and ignimbrites volumetrically dominate over intermediate and basaltic varieties in this part of the Southern Permian Basin (Benek et al., 1996). Zircon U-Pb dating yielded ages between 302±3 and 297±3 Ma for the volcanic activity in this area, thus straddling the Carboniferous-Permian boundary (Breitkreuz & Kennedy, 1999). The authors also reported that these rocks included populations of inherited zircons with ages reflecting reworked Cadomian (650-550 Ma) and older Gondwanan elements. Manifestations of corresponding latest Carboniferous-earliest Permian volcanism and dyke and sill emplacements on the British Isles include the voluminous Whin Sill Complex (mostly high-Fe subalkaline basalts) of northeast England and the extensive dyke swarm and sill in the Midland Valley of Scotland (tholeiitic quartz dolerites). Coeval intrusive rocks in southwest England have a granitic composition and their emplacement was probably accompanied by extrusion of rhyolitic lavas (Timmerman, 2004).

In summary, although many of the Carboniferous and Permian igneous rocks discovered in the Netherlands subsurface lack unequivocal constraints on their composition, timing and mode of emplacement, they tend to fit well into the distribution and setting of equivalent intervals in onshore and offshore wells across northwestern Europe.

← ***Figure 11.4.*** *Core photographs showing examples of igneous rocks from the Dutch subsurface: a) Volcanic agglomerate from the Upper Jurassic Zuidwal volcano (well Zuidwal-1, upper 0.4 m of interval 2505-2511 m); b) Olivine gabbro in the upper Carboniferous Ruurlo Formation (well Hardenberg-2-S1, 3408.2-3408.6 m), photo: NAM; c) Volcanic agglomerate from the Upper Jurassic-Lower Cretaceous Zuidwal volcano (well Zuidwal-1, 3001.0-3001.2 m); d) Olivine dolerite in the upper Carboniferous Epen Formation (well Winterswijk-1, 4149.0-4149.3 m), photo: NAM; e) Porphyritic trachyte lava in the upper Carboniferous Step Graben Formation (well F04-02-A, 4652.27-4652.77 m); f) Dolerite sill or dyke in the Middle Jurassic Brabant Formation (well Werkendam-1, 1554.70-1554.97 m); g) Alkali basaltic rock in the Upper Jurassic Nieuwerkerk Formation (well Heinenoord-1, 2239.31-2240.20 m), photo: NAM.*

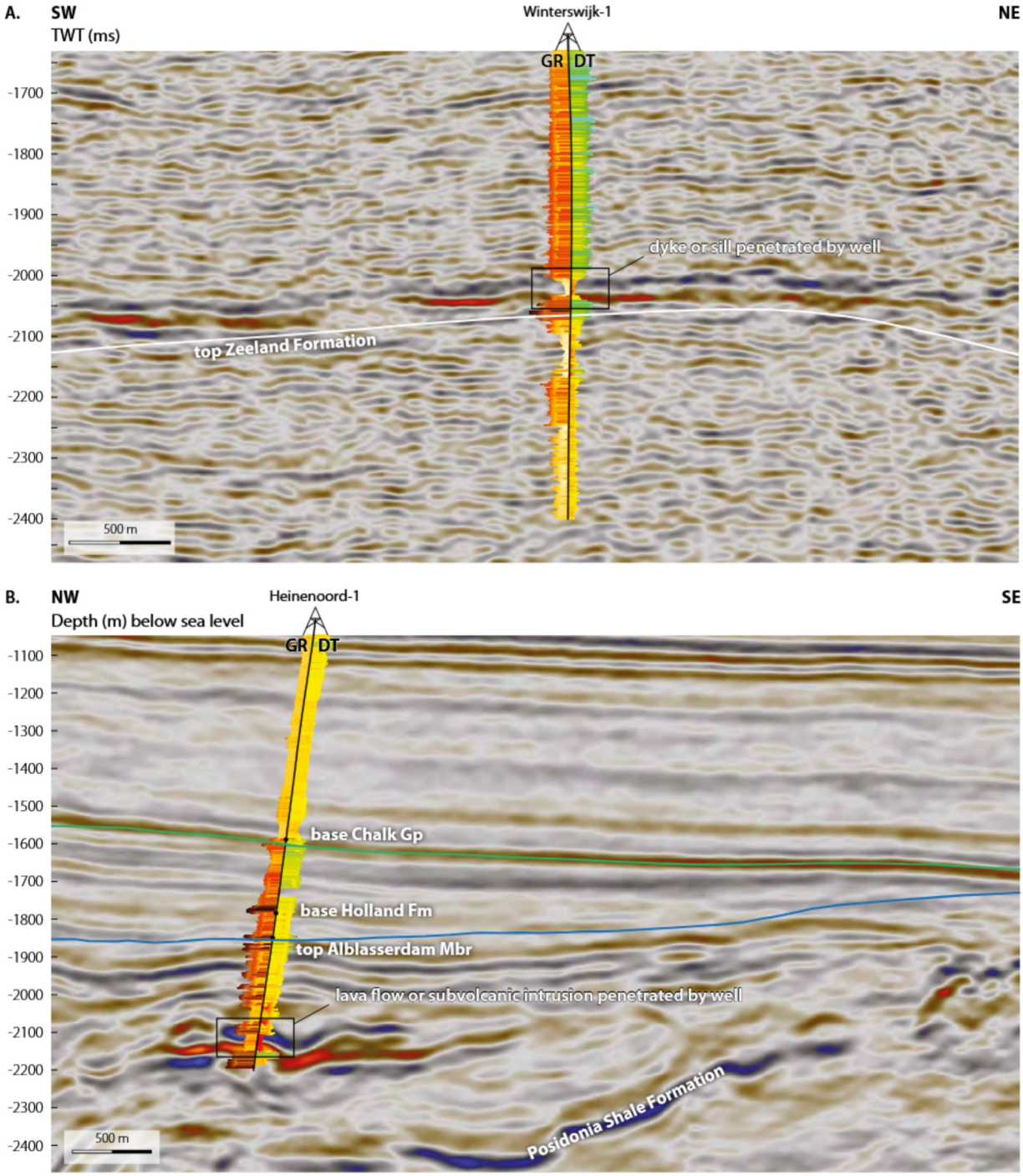

Figure 11.5. *Seismic profiles in which direct observations confirm the presence of intrusive magmatic rock (sill or dyke) as high-amplitude reflectors in seismic data: a) Well Winterswijk-1 where the upper Carboniferous Epen Formation hosts an interval of olivine dolerite (see Fig. 11.4d); seismic survey L2NAM1975L, line 1011; b) Well Heinenoord-1 where the Upper Jurassic Nieuwerkerk Formation contains an interval of alkali basaltic rock (see Fig. 11.4g); seismic image from a depth-migrated merged 3D seismic dataset for the West Netherlands Basin (TNO). GR = gamma-ray log, DT = sonic log.*

Jurassic

In the Dutch subsurface, igneous rocks with a Late Jurassic age have been found offshore in wells along the rim of the Dutch Central graben (Fig. 11.9), in the Broad Fourteens Basin (K, L, P, Q-quadrants) and in the Vlieland Basin (Zuidwal volcano), but also in onshore wells in the West Netherlands Basin (near Andel, Berkel, Giessendam, Heinenoord and Loon op Zand). They represent the southernmost expression of Jurassic magmatism in and around the

North Sea Central Graben System (Fig. 11.9). Details on the rifting history are given in De Jager et al. (2025, this volume).

The igneous intervals encountered in wells in the West Netherlands Basin are mostly relatively mafic rocks with a silica-undersaturated affinity, referred to as nephelinites, basanites, theralites/essexites and alkali basalts in original descriptions (Table 11.1).

Fine-grained rocks in the Andel-2 and Andel-4 and Loon op Zand-1 wells (AND-02 and LOZ-01 shown in Fig. 11.6e,f) have been described as intrusions in the middle and lower Jurassic, respectively. A sample from Andel-4 (AND-04) has been $^{40}Ar/^{39}Ar$ dated at 133±2 Ma and one from Loon op Zand-1 at 132±3 (Dixon et al., 1981). Because of a partial overprint at <120 Ma the emplacement ages are likely older. The Loon op Zand-1 and Andel-4 rocks are highly altered glassy olivine nephelinites, containing pseudomorphed olivine and clinopyroxene phenocrysts in a groundmass with the same mineral phases, as well as kaersutitic hornblende, biotite and apatite. The Andel-2 samples are probably basanites with pseudomorphed olivine, plagioclase and possibly nepheline. Several observations cast doubt on the alleged intrusive nature as dykes or sills in the Andel and Loon op Zand wells. The strongly porphyritic texture and abundance of vesicles, as well as the presence of a thin layer of baked sediment at bottom sides only, as core descriptions suggest, are consistent with an origin as lava flows. As the true emplacement ages may well fall in the late Jurassic band (Fig 11.8), an extrusive emplacement cannot be excluded at least for the rocks in the Andel wells.

The Ar-Ar ages correspond reasonably well with a K-Ar age of 125±25 Ma obtained on a body of (biotite-bearing?) olivine basalt in the Tithonian-Berriasian sandstone-shale succession of the Alblasserdam Member, which was sampled in Giessendam-1 (GSD-01) (Sissingh, 2004). The thin basaltic layers found in this well may have had an extrusive origin but the K-Ar age is not sufficiently reliable to confirm this. Dixon et al. (1981) suggested that the Berkel-1 (BRK-01) hornblende basalt intruded in Jurassic sediments (Van der Sijp, 1953) may be a fine-grained essexite or theralite, and is possibly also similar in age to the Andel and Loon op Zand rocks.

A nearly 40 m thick interval of relatively fresh olivine-rich alkali basalt in well Heinenoord-1 (HEI-01, Fig. 11.5b) has been studied in some detail (Helmers, 1991; Frezzotti, 1992; this work). The porphyritic rock (Figs 11.4g, 11.6d), carrying abundant clinopyroxene and olivine phenocrysts, shows petrographic similarities with the olivine nephelinites in Loon op Zand-1 (Fig. 11.6f). Although the basaltic rock is considered to represent a near-surface sill, emplacement as a lava flow cannot be excluded, given its stratigraphic position in the upper Jurassic-lower Cretaceous Nieuwerkerk Formation, its textural appearance (Fig. 11.4g) and the absence of a radiometric age date. Based on the whole-rock composition, the basalt classifies as tephrite or basanite. Helmers (1991) reported the presence of accessory rhönite, a rare high-Ti aluminosilicate, which is usually only present in silica-undersaturated mafic to intermediate igneous rocks.

In summary, the available information suggests that the intervals of igneous rocks in the onshore wells of the West Netherlands Basin were emplaced in a Jurassic shallow-marine succession of predominantly fine-grained mudstones and minor silt- and sandstones, either as near-surface subvolcanic intrusions or as lava flows.

Igneous rocks from wells in the offshore F, K, L, P and Q quadrants have been described as strongly silica-undersaturated basaltic intrusions (Dixon et al., 1981; Latin, 1990; Latin et al., 1990b). According to phenocryst assemblages and bulk-rock compositions, the rocks from K12-05-S1, K14-FA-103 (in the border areas of the Broad Fourteens Basin) and F10-01 (near the rim of the Central Graben) share a potassium and volatile-rich character. The first constitutes a ca. 130 m thick lamprophyric intrusion in salt of the Zechstein Group, the second a thin fine-grained trachybasaltic layer in Upper Permian sandstone and the third a >30 m thick potassic alkaline lamprophyre, also intercalated in Zechstein salt. Typical phenocrysts include Ti-rich augite and amphibole (kaersutite), while minor olivine and biotite have been found as well.

The other offshore occurrences (L13-03 and those in the P and Q quadrants further to the south) are mafic intrusions with a more nephelinitic character, compositionally and petrographically comparable to the rocks of the West Netherlands Basin mentioned above. Tuffaceous layers in late Jurassic sediments in the region of the Broad Fourteens Basin may indicate that alkaline magmatism of this episode was also accompanied by explosive eruptive activity.

The large variation in radiometric ages available for this period (Table 11.1, Fig. 11.8) underscores the uncertainties inherent to the dating methods used. The ca. 50 Ma age range obtained by different methods on virtually the same rock sampled in F10-01 is an instructive example. The plateau $^{40}Ar/^{39}Ar$ age of 151±2 Ma, obtained on separated kaersutite, is considered to represent the most robust result (Latin, 1990). A within-errors identical whole-rock K-Ar age of 152±7 Ma, obtained on fresh material from the thick lamprophyre in K12-05-S1 (Krueger, 1982), together with consistent results for the Zuidwal volcanic centre below the Waddenzee and biostratigraphic age constraints for the Mulciber volcanic centre on the rim of the Dutch Central Graben (see below) further limit the timing of Mesozoic magmatism in the Netherlands to a relatively short late Jurassic episode. The other reported ages (Table

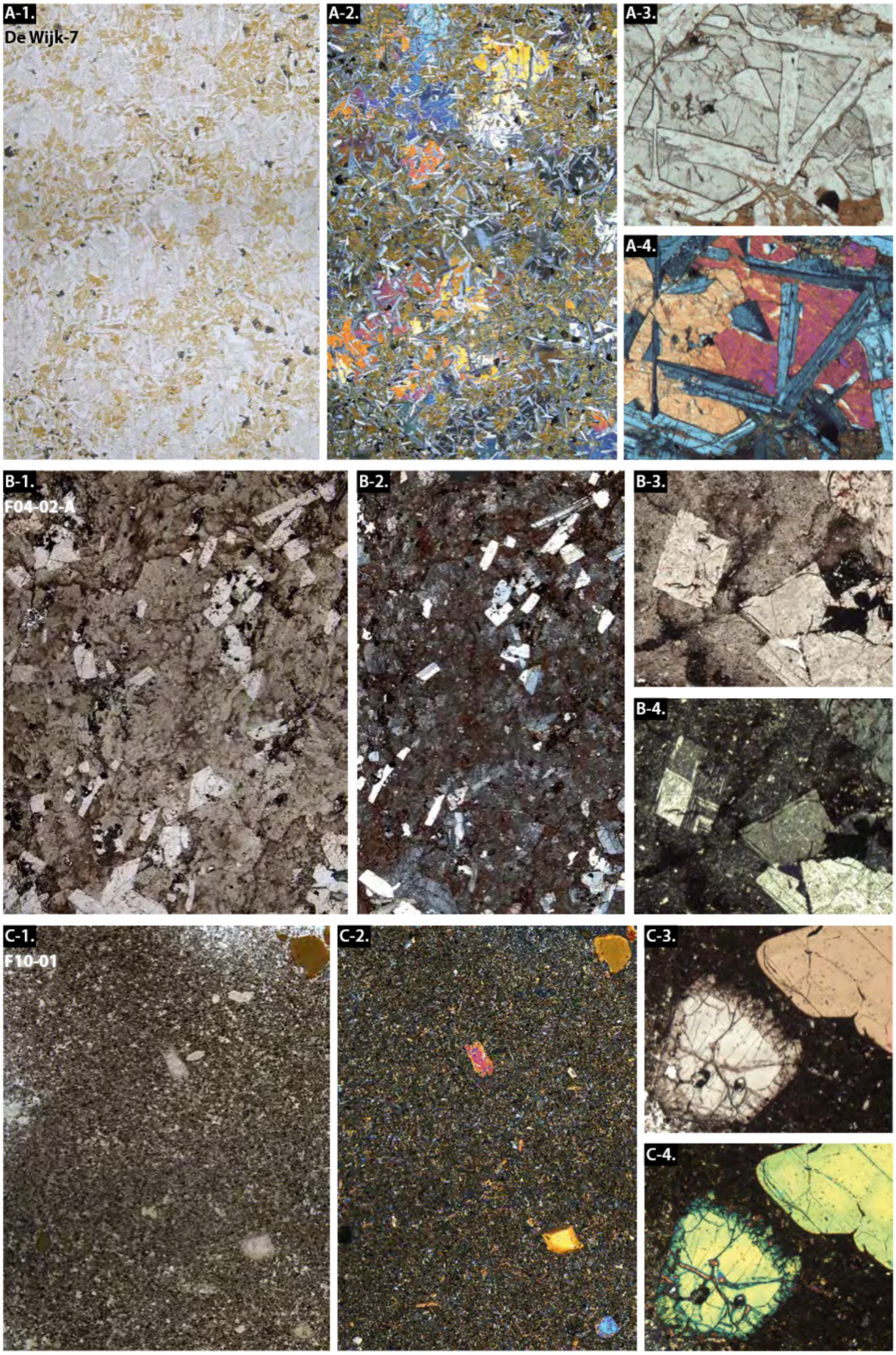
A-1.
De Wijk-7
A-2.
A-3.
A-4.
B-1.
F04-02-A
B-2.
B-3.
B-4.
C-1.
F10-01
C-2.
C-3.
C-4.

11.1), a few older but mostly considerably younger, are ambiguous and may not represent magma emplacement ages.

Buried volcanoes

Two prominent geomorphic structures have been interpreted as buried volcanoes in Mesozoic sedimentary basins offshore: the 'Zuidwal volcano' below the Wadden Sea, southeast of the island of Vlieland, and 'Mulciber volcano' below the North Sea, some 100 km northwest of the island of Terschelling. Their outlines correspond to gravity highs and positive geomagnetic anomalies (Fig. 11.10). Considering the size of the geomagnetic anomalies and their volumes based on 3D seismic reflection data, both systems fall in the category of large (>5km^3), composite shield and caldera volcanoes (cf. Bischoff et al., 2021).

The Zuidwal volcanic centre

The 'Zuidwal volcano', identified during petroleum exploration below the Wadden Sea (Cottençon et al., 1975), is located north of the Texel-IJsselmeer High in the Vlieland Basin (Fig. 11.9). Cores from well Zuidwal-1 (ZDW-01) revealed volcanic agglomerates between 1950 m and the total depth of 3000 m (Fig. 11.4a, c). The volcanics are unconformably overlain by gas-bearing Valanginian sandstone. Details on the geological setting, exploration geophysics, structural evolution and reservoir characteristics are provided in Perrot & Van der Poel (1987) and Herngreen et al. (1991). Magma may have reached the surface along Permo-Carboniferous and Cimmerian faults that were opened during the Late Jurassic. Based on geophysical data the agglomerates represent a neck, which forms part of a dome-like structure. This is illustrated by the isopach map of 'Upper Jurassic' units (Delfland Subgroup and Kimmeridge Clay Formation), which shows a division of the Vlieland Basin into two sub-basins with thinning around the dome (Fig. 11.11a). Perrot & Van der Poel (1987) interpreted local aeromagnetic anomalies in terms of a circular caldera-type body with a central volcanic conduit (Fig. 11.11c). They hypothesized that after a major

← ***Figure 11.6.*** *Microphotographs of thin sections of representative igneous rocks from well cores in the Dutch onshore and offshore, taken in plain polarized light (PPL) and in cross polarized light (XPL). Indicated ages are best estimates and in most cases are not constrained by accurate radiometric dating (see Table 11.1 and Fig. 11.8).* ***De Wijk-7, depth 2445 m:*** *a-1) Gabbroic intrusive rock (dolerite) largely consisting of ophitic intergrowths of plagioclase laths and large pyroxene crystals and containing small opaque grains of Fe-Ti oxide (PPL); a-2) Same in XPL; a-3) Detail showing intergrown clinopyroxene and elongated plagioclase (PPL); a-4) Same in XPL.* ***F04-02-A, depth 4650 m:*** *b-1) Porphyritic trachyte showing euhedral plagioclase phenocrysts set in an altered fine-grained matrix (PPL); b-2) Same in XPL; b-3) Detail showing plagioclase cluster with Fe-Ti oxide (PPL); b-4) Same in XPL; note the complex twinning in the plagioclase on the left.* ***F10-01, depth 3451 m:*** *c-1) Porphyritic basanite (referred to as 'lamprophyre' by Latin, 1990) with phenocrysts of clinopyroxene with brown Ti-rich amphibole (e.g. in the upper right corner) and minor biotite in a crystalline matrix (PPL); c-2) Same in XPL; c-3) Magnified detail showing clinopyroxene phenocryst (left) with somewhat darker outgrowths on its rim, as well as a brownish amphibole megacryst with concentric colour zoning and smoothly curved outlines suggesting resorption (PPL); c-4) Same in XPL.* ***Heinenoord-1, depth 2249.3 m:*** *d-1) Porphyritic rock with an alkali-basaltic composition, containing abundant phenocrysts of olivine and clinopyroxene, chromium spinel and rhönite in a fine crystalline matrix (PPL); d-2) Same in XPL; d-3) Magnified detail (PPL) showing micro-phenocrysts of partly serpentinized olivine (green rims and crack fringes); d-4) Same in XPL.* ***Andel-2, depth 1367.8 m:*** *e-1) Strongly altered porphyritic alkalibasalt with a fine-grained groundmass (PPL); white spots (black in e-2) represent former phenocrysts (probably clinopyroxene and or amphibole), which are now voids sometimes partly filled with carbonate; the F10-01 basanite (see c) may well be a much fresher equivalent; e-2) Same in XPL; e-3) Detail showing the abundance of small feldspar laths in the groundmass and a completely altered microphenocryst (PPL); e-4) Same in XPL.* ***Loon op Zand-1, depth 2589.5 m:*** *f-1) Strongly altered porphyritic alkalibasaltic rock with ghosts of clinopyroxene and olivine phenocrysts set in a fine-grained groundmass (PPL); f-2) Same in XPL; f-3) Detail showing carbonated phenocryst, presumably olivine (PPL); f-4) Same in XPL.* ***Zuidwal-1, depth 1948.5 m:*** *g-1) Altered porphyritic trachyandesite with phenocrysts of elongated plagioclase and euhedral nepheline set in a crystal-rich groundmass made up of the same minerals, (altered) biotite flakes and Fe-Ti oxides (PPL); g-2) Same in XPL; note the low birefringent to nearly isotropic appearance and euhedral outlines of nepheline crystals (XPL);* ***Zuidwal-1, depth 1957.9 m:*** *g-3) Magnified detail with plagioclase phenocrysts (PPL); g-4) Same in XPL; note the strong zoning in the plagioclase (XPL).* ***Zuidwal-1, depths unknown:*** *h-1) Leucitophyre with abundant pseudomorphs after leucite, now consisting of a fine aggregate of brownish carbonate (sample ZU6); h-2) Cluster of brown titaniferous clinopyroxene (salite) and small greenish clinopyroxene (aegirine augite) in the groundmass in leucite basanite (PPL) (sample ZU5); h-3) Phenocryst of brown titaniferous clinopyroxene (salite) rimmed by green clinopyroxene (aegirine augite) (PPL) (sample ZU5). Images h are from Latin (1990). Approximate image widths: 16.5 mm for panels 1 and 2 of a, b, c, d and e; 9.5 mm for panels 1 and 2 of f and g; 3.3 mm for panels 3 and 4 of a, b, c, d, e, f, g; 1.5 mm for panels h-1 and h-3; 3.6 mm for panel h-2.*


D-1.
Heinenoord-1

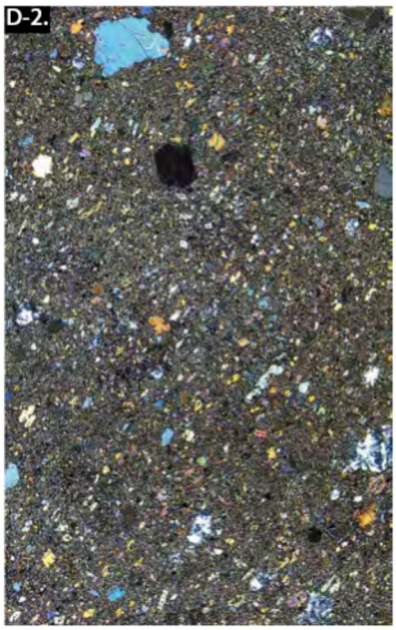
D-2.

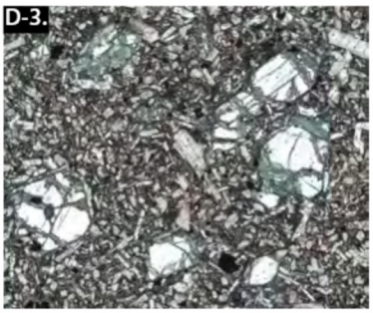
D-3.

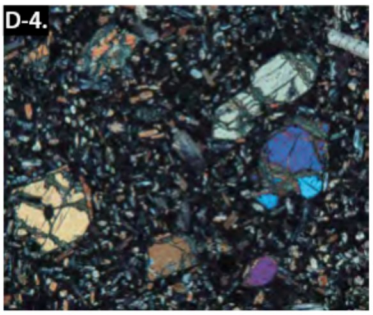
D-4.


E-1.
Andel-2

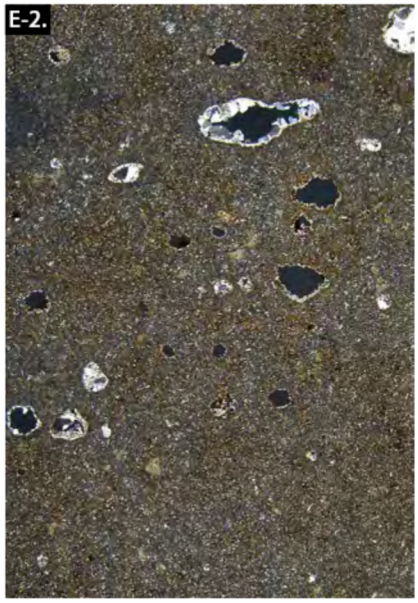
E-2.

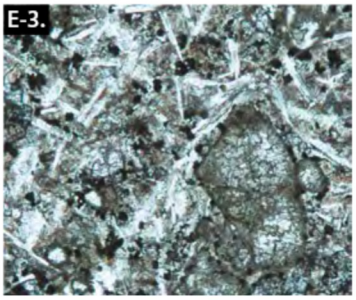
E-3.

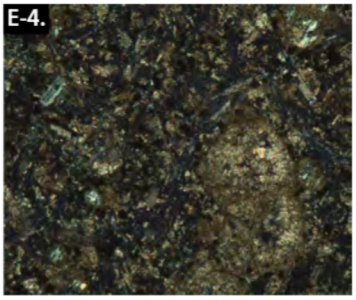
E-4.

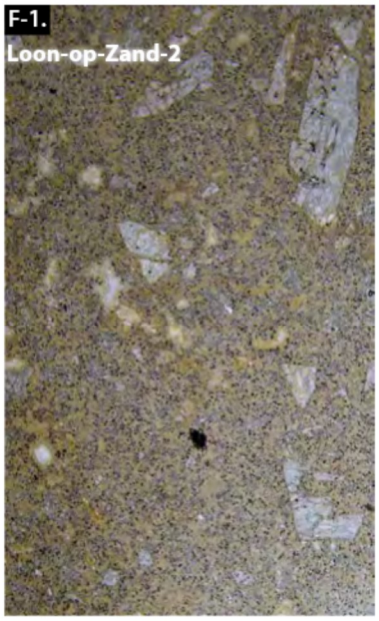
F-1.
Loon-op-Zand-2


F-2.

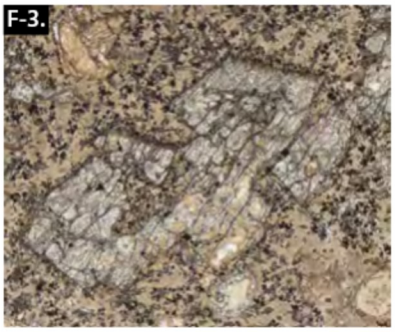
F-3.

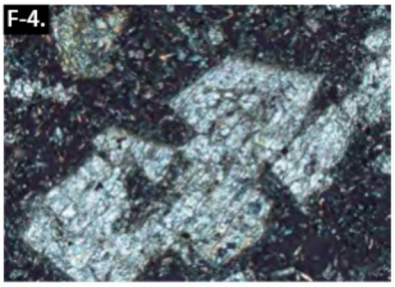
F-4.

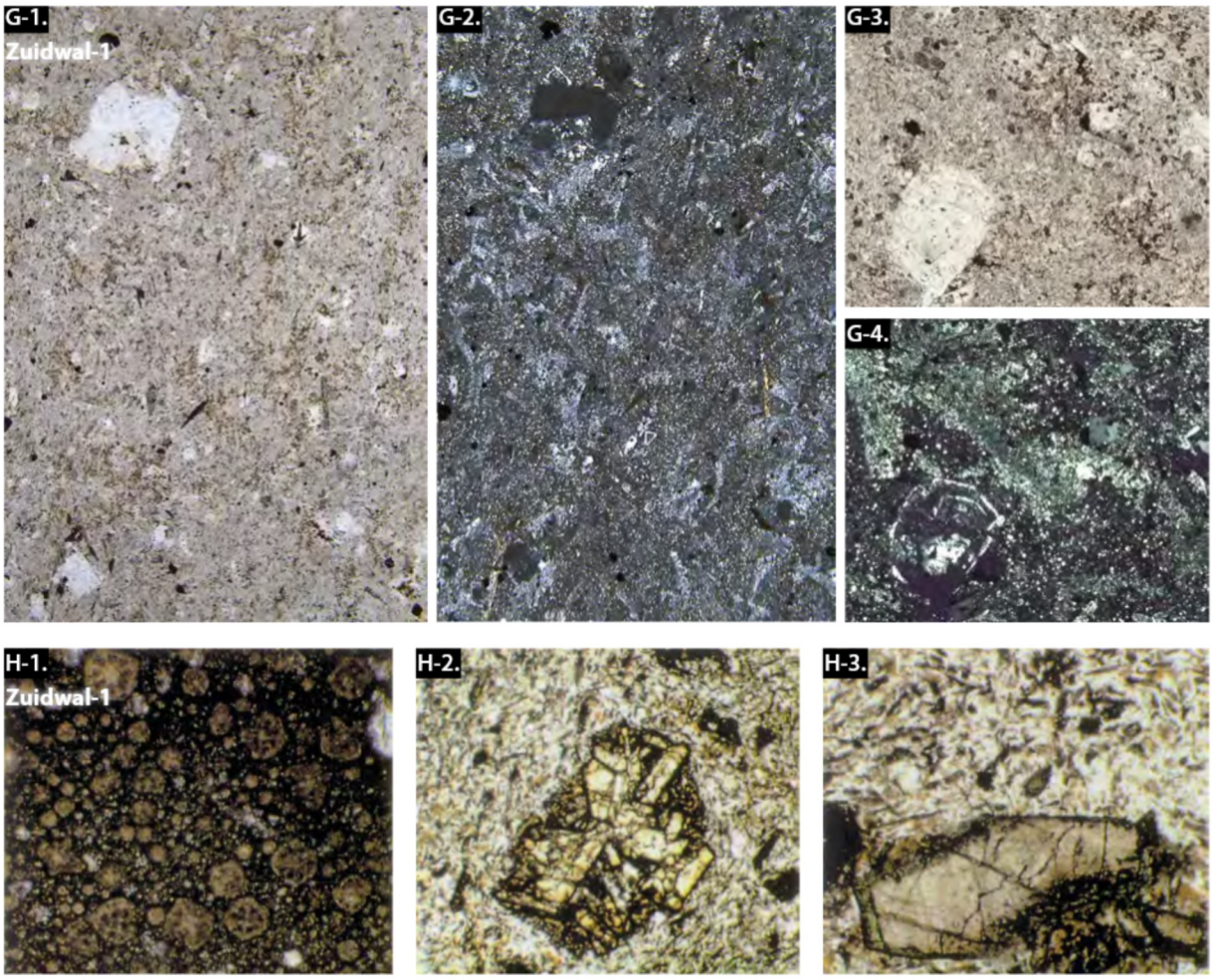

eruption, the magma chamber must have collapsed, and that any volcanic islands were largely removed by Late Jurassic and Cretaceous erosion. The Wadden Volcaniclastic Member of the Delfland Subgroup, 78 m thick in Slenk-1 (SLK-01) and also found in Zuidwal-2 and Zuidwal-3 (ZDW-02, -03), consists of fine- to coarse-grained volcaniclasts in a tuffaceous matrix (Fig. 11.4a, c). Because of the weathered appearance and proximity to the dome, these sediments probably represent erosion products rather than primary volcanic deposits (Herngreen et al., 1991).

Radiometric dating of Zuidwal-1 yielded inconsistent results. Initial K-Ar ages obtained on four samples (3000-1950 m) ranged between 119±2 Ma and 92±2. These are probably only minimum ages, considering the extensive alteration (Jeans et al., 1977; Harrison et al., 1979). An expected true age of >120 Ma was supported by a K-Ar date of 145 Ma obtained on a sample of unknown origin (pers. comm. G. Flacelière, in Jeans et al., 1977). Subsequent $^{40}Ar/^{39}Ar$ dating yielded a virtually identical age of 144±1 Ma with a minor overprint between about 120 and 90 Ma, suggesting that the younger K-Ar ages reflect argon loss (Dixon et al., 1981). Finally, Perrot & Van der Poel (1987) reported an age of 152±3 Ma, based on the $^{40}K/^{36}Ar$-$^{40}K/^{36}Ar$ method. These oldest ages (Late Jurassic) are presumably closest to the true emplacement age.

Documented petrographic descriptions of Zuidwal samples are not uniform. Dixon et al. (1981) inferred that the eight altered rocks they examined originally were phonolite samples, biotite pyroxenites, a phonolitic basanite and a rock rich in pseudomorphed leucite respectively (cf. Fig. 11.6g, h). The agglomerate matrix attached to one of the phonolites contained leucite basanite and leucite tephrite clasts. Rock types referred to as trachytes, phonolites and leucitites from observations on 12 samples (Perrot & Van der Poel, 1987) are consistent with this description. On the other hand, Harrison et al. (1979) described finely crystalline to partly glassy trachyte as the most common rock type, together with less abundant, heavily altered lava of probably basic composition and pieces of originally glassy vesicular pumice and minette. They noted that sphene is relatively abundant and do not record the presence of primary feldspathoids or their pseudomorphs. According to Dixon et al. (1981) it is conceivable that the Zuidwal volcanics represent one or more cycles of trachyte-phonolite eruptions and that they included subordinate amounts of more primitive lavas such as basanites and tephrites.

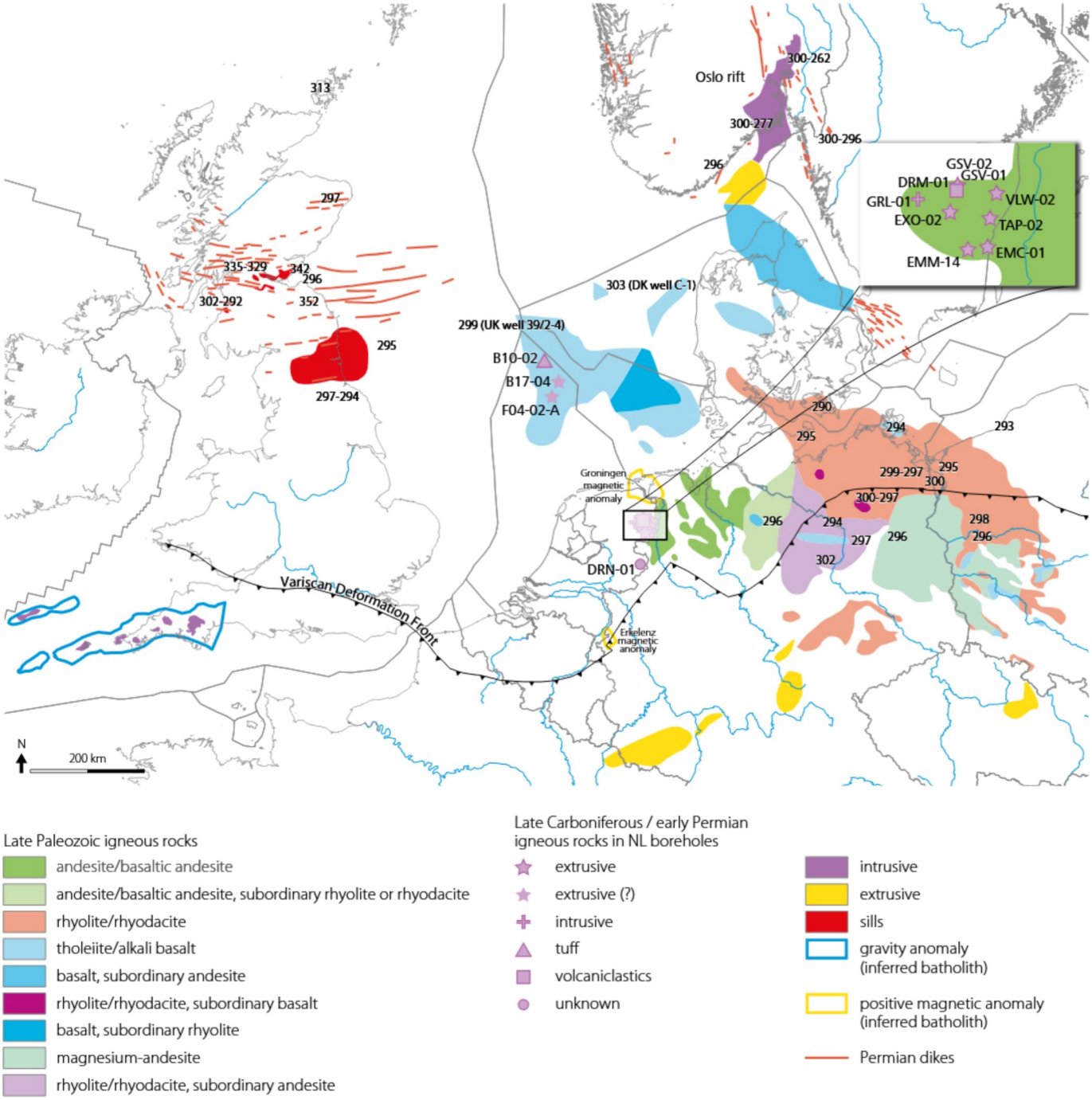

Figure 11.7. Distribution of latest Carboniferous-early Permian ('lower Rotliegend') igneous rocks in northwest Europe and locations of wells in the Netherlands with intrusive and extrusive igneous rocks, volcaniclastics and tuffs from this period. Numbers refer to radiometric ages in Ma obtained by U-Pb zircon, $^{39}Ar/^{40}Ar$ and by other high-quality dating methods. Information on the Whin Sill Complex: Hamilton and Pearson (2011), Timmerman (2004); Midland Valley of Scotland: Monaghan and Pringle (2004); Orkney: Lundmark et al. (2011); Mid North Sea High: Lundmark et al. (2012), Heeremans et al. (2004); Horn Graben: Breitkreuz et al. (2007); northeast German Basin: Breitkreuz and Kennedy (1999); Oslo Rift: Pedersen et al. (1995), Corfu and Dahlgren (2008), Corfu and Larsen (2020); late Paleozoic igneous rocks: Gast et al. (2010; Fig. 7.16); additional Permain igneous rocks: Van Bergen & Sissingh (2007); East Groningen Massif: Bredewout (1989); Cornubian batolith (Cornwall): Searl et al., (2024); Watts et al., (2024).

Taking effects of secondary alteration into account, the available geochemical data (see below) indicate that the Zuidwal volcanics originally represent a typical ultrapotassic, silica-undersaturated rock series, including leucite-bearing phonolitic members (Fig. 11.6g, h), which probably originated during the residence of a more mafic, mantle-derived, clinopyroxene-rich tephritic-basanitic parent magma in a relatively shallow subvolcanic reservoir.

The Mulciber volcanic centre

The existence of a buried igneous centre in the subsurface of the Dutch sector of the North Sea (block F16, Fig. 11.12) had been suspected for some time from the existence of a positive magnetic intensity anomaly around Amoco exploration well F16-02 (Sissingh, 2004) and from the presence of volcanic material in core samples (Lester, 1985). An integrated regional sedimentary and stratigraphic study in the area around the well (Bouroullec et al., 2018) ultimately led to the identification of the Mulciber volcanic centre, made public by the Geological Survey of the Netherlands in 2020. The volcano was named after the Roman god of fire and volcanoes.

Sidewall core samples and borehole logs from well F16-02 (Fig. 11.12a) include tuff and tuffaceous claystone grading into solid volcanic rock in the succession between 1702 and 1662.5 m depth, as well as tuffaceous claystone interbedded with anhydrite, and volcaniclastics between 1983 and 1737 m (Lester, 1985). Petrographic information provides insight into the mode of emplacement and composition. Five pieces of igneous rock sampled between 1672 and 1662.5 m were interpreted as basaltic-andesitic and andesitic lavas. This was based on their porphyritic, vesicular nature and the mineral content, which includes clinopyroxene, plagioclase, Fe-oxide, apatite and a matrix of devitrified glass that hosts the same phases, often together with biotite. Due to strong alteration, most of the original assemblage has been replaced by secondary minerals. The presence of biotite (and locally amphibole) suggests an alkaline affinity of the rock suite. Although it has been proposed that the igneous material of this interval represents a continuation of the Zuidwal volcanics into the Central North Sea Graben (Lester, 1985), it is now clear that the Mulciber volcanic centre was the source.

The magnetic anomaly in block F16 is similar to that of the Zuidwal volcano (Fig. 11.10b). A strongly reflective interval with a high acoustic impedance contrast, mapped on 3D seismic data a few kilometres to the west of well F16-02 (Fig. 11.12b), indicates the presence of layers of solid rock, as can be readily inferred from the sonic log (Fig. 11.12a). Its spatial distribution coincides with that of the magnetic anomaly (Fig. 11.12b), and its reflections can be traced to the well (Fig. 11.12c, d), so it probably represents the same lavas as found in the sidewall cores in F16-02. The morphology of the uppermost seismic reflector resembles that of a smoothed volcano, likely due to subaerial weathering and erosion prior to burial by younger sediments.

Biostratigraphic constraints indicate that the upper interval of igneous rocks (1702-1662.5 m) is latest Jurassic to Early Cretaceous in age, while the overlying claystone (1662.5-1659 m) is Late Hauterivian to Early Barremian (Lester, 1985; Bouroullec et al., 2018). Samples from the sidewall cores were completely used for petrographic analyses and igneous material is no longer available for radiometric age determination.

The position of strong seismic reflectors at a considerably deeper level (3300 m) west of well F16-02 relative to that near the well and the volcanic interval (ca. 1660 m), marks the effect of salt tectonics (Fig. 11.12d). The seismic data suggest that faulting along the Dutch Central Graben was active during magmatic activity and that, rock salt (Zechstein) moved upward along the fault-related weakness zones in the overburden, pushing the succession of igneous rocks to higher levels at the well location (Fig. 11.12c).

Below the igneous rocks of Jurassic age in well F16-02, evaporites of the Zechstein Group host an interval with felsic volcanics between 1985 and 1738 m. Considering the stratigraphic position, these are probably of late Permian age. Strongly altered material at 1975-1965 m represents a porphyritic extrusive rock with clinopyroxene, biotite and glassy matter, presumably originally a dacitic lava.

Jurassic igneous rocks in adjacent areas

The triple junction between the Moray Firth, the Viking Graben and the Central Graben (northern North Sea) has been known as a centre of voluminous volcanism in middle to late Jurassic times since its discovery in 1970 (Fig. 11.13). An over 3000 m thick succession of basaltic lavas ('Forties Volcanics') constitutes a volcanic field that covers an area of about 12000 km^2, extending eastward across the southernmost part of the Viking Graben (Woodhall & Knox, 1979). The volcanics are also known as the Forties Igneous Province and the Rattray Volcanics amongst others. Based on well data and seismic reflection profiles, Smith and Ritchie (1993) proposed that at least three major volcanic centres existed, whereas from a recent re-interpretation using 3D-seismic data Quirie et al. (2019) inferred that the volcanics were sourced in fissure eruptions from linear vents. The rocks were emplaced as subaerial lavas and volcaniclastics, subaqueous basaltic hyaloclastics and reworked material and as subordinate intrusive units (Quirie et al., 2019). The basalts are silica-undersaturated, belong to the alkaline series and contain abundant phenocrysts of olivine and clinopyrox-

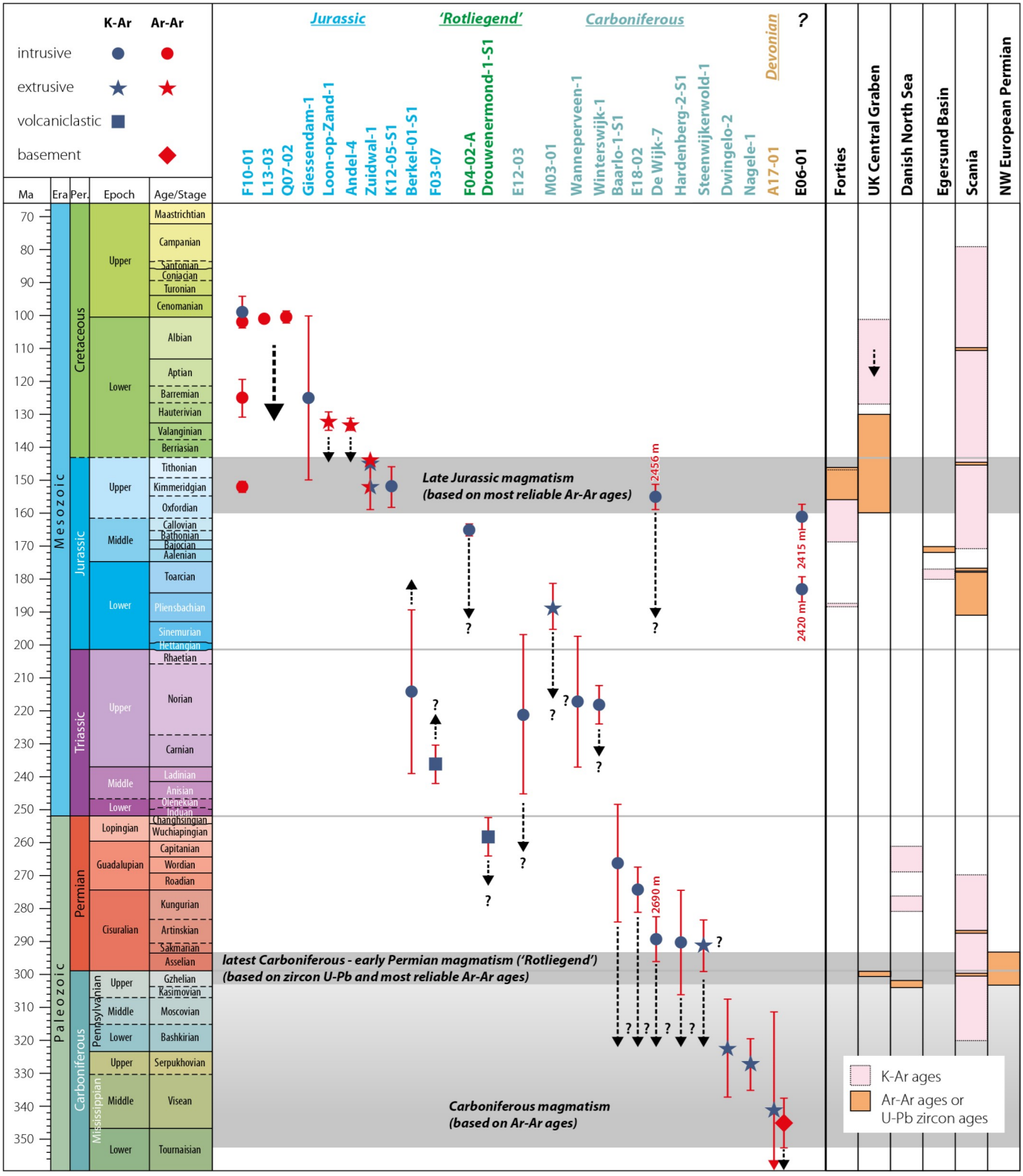

Figure 11.8. *Stratigraphic overview of radiometrically dated igneous and volcaniclastic rocks from wells in the Netherlands, plotted against periods of magmatic activity in surrounding northwest European areas (see Table 11.1 for references). Red bars indicate error margins, black arrows point towards expected more correct ages.*

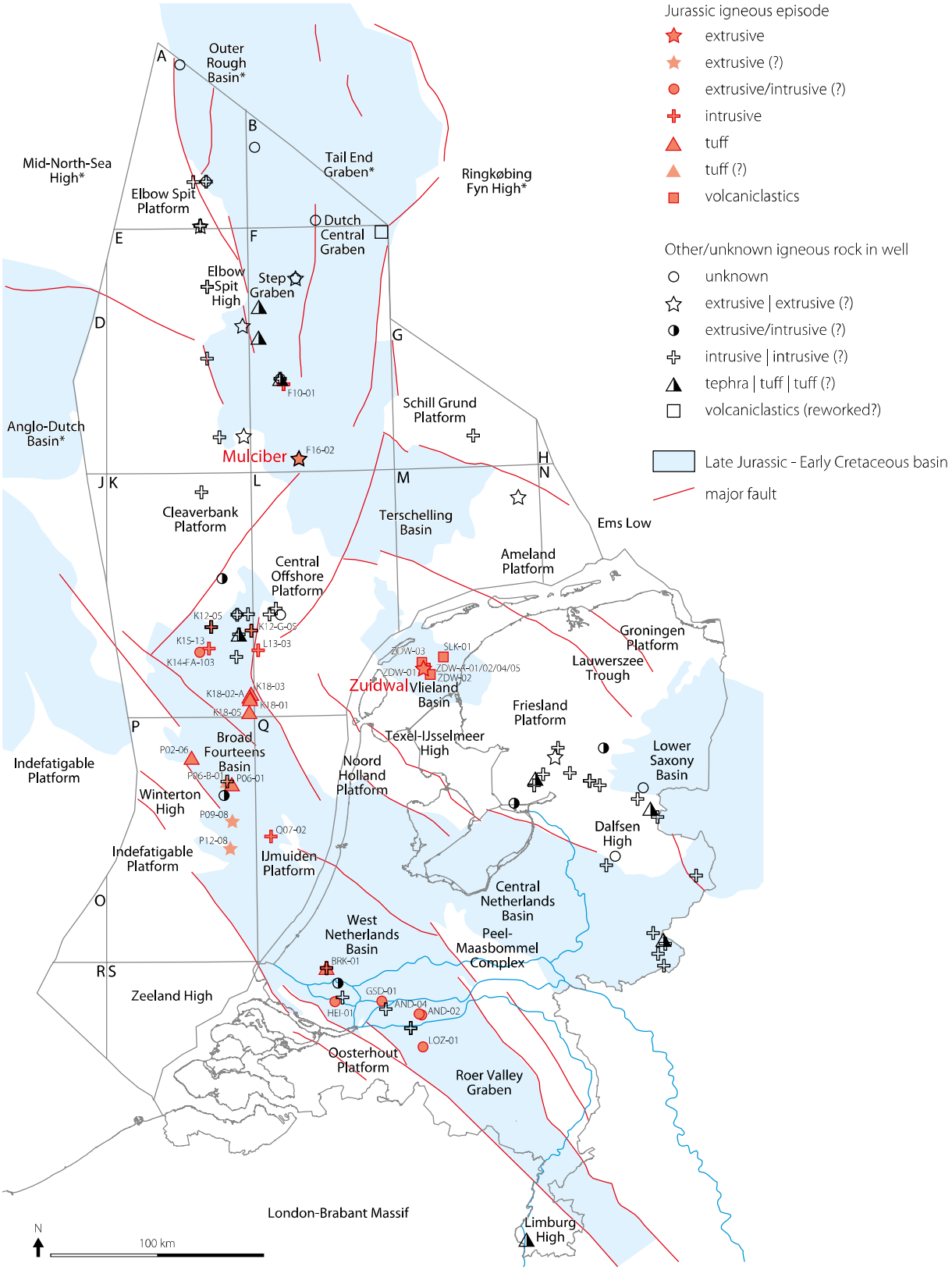

Figure 11.9. *Wells located in the Netherlands in which igneous rocks attributed to the Late Jurassic episode of magmatic activity have been found. Wells with igneous material from other or unknown periods are shown for comparison. Structural elements are those from Late Jurassic-Early Cretaceous times (Pharaoh et al., 2010; Kombrink et al., 2012; Hopper et al., 2014). Details on the rocks in each well are listed in Table 11.1.*

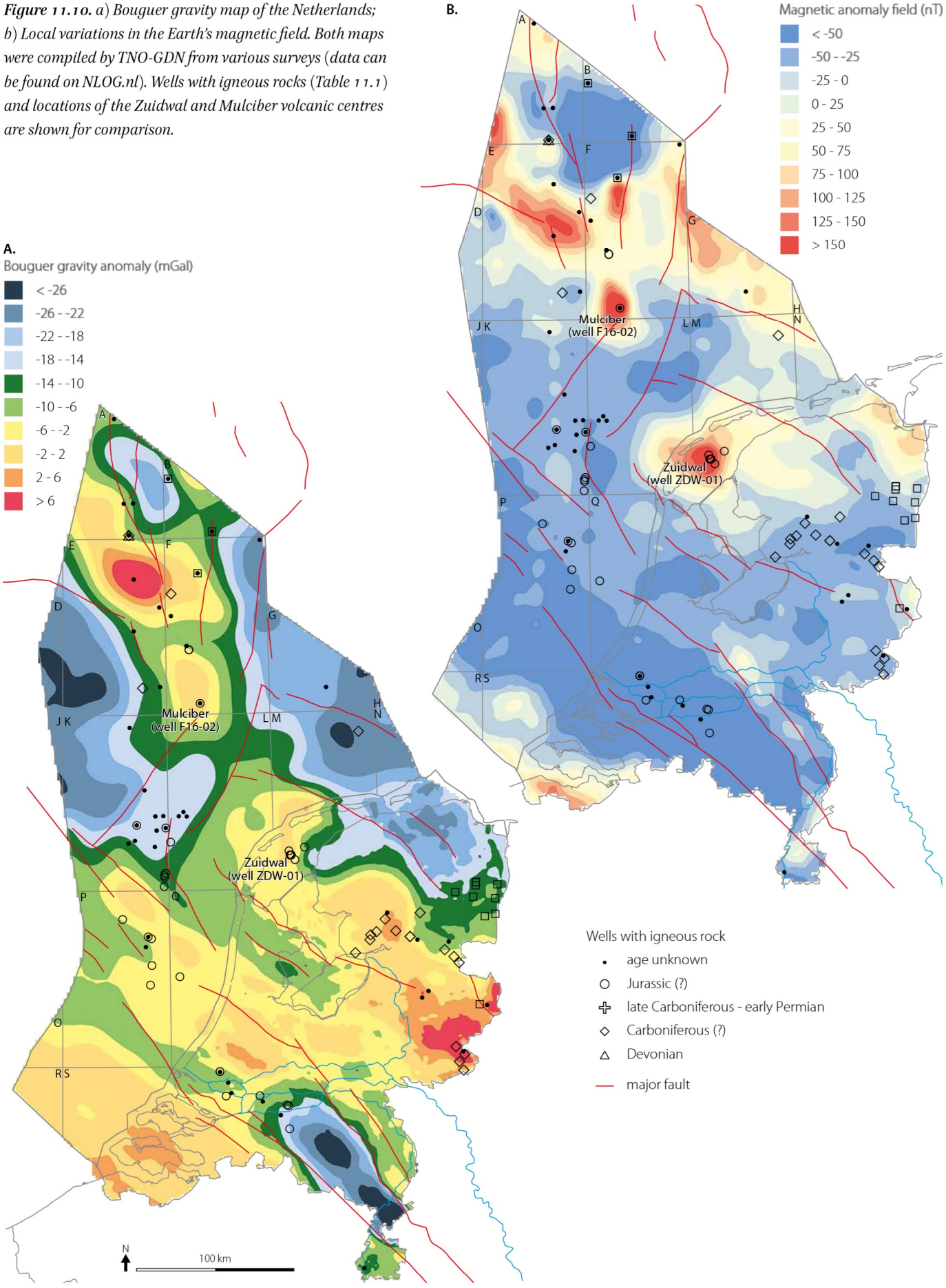

Figure 11.10. a) Bouguer gravity map of the Netherlands; b) Local variations in the Earth's magnetic field. Both maps were compiled by TNO-GDN from various surveys (data can be found on NLOG.nl). Wells with igneous rocks (Table 11.1) and locations of the Zuidwal and Mulciber volcanic centres are shown for comparison.

ene (Gibb & Kanaris-Sotiriou, 1976; Dixon et al., 1981; Latin & Waters, 1992). Most are fairly primitive, whereas more evolved hawaiites and mugearites have been found as well. The precise age and duration of the effusive event is still elusive as there is disagreement between radiometric and biostratigraphic age dates (see discussions in Latin, 1990; Quirie et al., 2020). Stratigraphic evidence based on palynology, suggests a middle Jurassic age (Bajocian-Callovian), while scrutiny of available radiometric dating results (Latin, 1990) favours an upper Jurassic age (Kimmeridgian-Tithonian), based on ages of 153±4 Ma and 148±2 Ma obtained on a $^{40}Ar/^{39}Ar$ stepwise degassing study of samples from well 21/03b-3 (Ritchie et al., 1988).

The Central North Sea igneous province on the western margin of the UK Central Graben (Fig. 11.13) is made up of mostly subaerial lava flows, tuffs and epiclastic rocks, together with several intrusions in the Zechstein interval. The rocks share a silica-undersaturated and potassium-rich character and carry mineral assemblages that include primary biotite and amphibole (Latin et al., 1990b). Fine-grained extrusive rocks in well 30/16-A13Y (sample SH1), labelled as kaersutite leucitite, contain Ti-rich clinopyroxene and amphibole as phenocrysts, whereas severely altered, fine-grained and largely aphyric rocks in well 9/14b-1 (sample AH2) were tentatively classified as basanite (Latin, 1990). Two intervals with intrusive varieties in well 29/25-1, referred to as mafic biotite phonolite (Dixon et al., 1981) or potassic lamprophyre (Latin, 1990), contain phlogopite and pseudomorphs of clinopyroxene and olivine phenocrysts. From an irregular $^{40}Ar/^{39}Ar$ age plateau of a phlogopite sample, the oldest age of 157 Ma is probably closest to that of the emplacement (Latin, 1990). All of these ultrapotassic rocks belong to the same series and share similar settings as those of the Dutch Central Graben and the Zuidwal volcanic centre.

On the western rim of the Egersund Basin in the Norwegian sector of the North Sea, nephelinite lavas have been found interbedded with Jurassic sediments, forming a sequence several hundred metre thick (well 17/9-1; Fig. 11.13). They are porphyritic vesicular rocks with large clinopyroxenes and pseudomorphs after olivine, which are set in a fine-grained or glassy groundmass. High contents of incompatible trace elements confirm the alkaline nature of these rocks (Dixon et al., 1981; Latin & Waters, 1992). A lower succession, cored in the same well, intruded into Lower Jurassic and/or Triassic sediments (Furnes et al., 1982; Latin et al., 1990b). These are strongly undersaturated mafic potassic-alkaline rocks, similar to the lamprophyres of the Central Graben area, with phlogopite-rich mineral assemblages and textures that resemble alnöites (Latin, 1990). Conventional K-Ar ages obtained on phlogopite in the intrusive rocks yielded 180-177 Ma (Furnes et al., 1982) and a $^{40}Ar/^{39}Ar$ plateau age on phlogopite a younger age of 170±2 Ma (Latin, 1990). Together with the Bajocian-Bathonian age of the sedimentary rocks intercalated with the lavas, this would make the Egersund magmatic event somewhat older than the most reliable radiometric ages of Jurassic magmatism in the Netherlands and UK sectors of the North Sea.

Numerous volcanic necks and plugs, associated with minor remnants of lava flows and pyroclastic deposits represent Jurassic mafic alkaline magmatic rocks with nephelinite-basanite composition in central Scania (south Sweden, Fig. 11.13). Whole-rock determinations produced a K-Ar age range between 171 and 79 Ma, and a $^{40}Ar/^{39}Ar$ range in three age groups between 191 and 110 Ma, but the younger results are probably compromized by secondary Ar loss (Tappe et al., 2016, and references therein). However, two $^{40}Ar/^{39}Ar$ plateau ages obtained on anorthoclase feldspar megacrysts yielding a weighted average of 176.7±0.5 Ma (2-sigma), probably provide the current best estimate for Jurassic magmatism along the southwestern margin of the Baltic Shield. A Middle Jurassic olivine-biotite gabbro with a K-Ar age of 166±4 Ma was encountered in a borehole off the west coast of Cornwall (Harrison et al., 1979), while Jurassic smectitic clays in southern and eastern England have been interpreted as alteration products of volcanic air-fall, part of which may originate from volcanic centres in the North Sea (Bradshaw, 1975; Jeans et al., 1977, 2000).

In summary, the extensive database on Mesozoic magmatism in the Netherlands encountered in wells (Table 11.1) discloses clear systematic patterns in the onshore and offshore distribution, timing, composition and mode of emplacement of the igneous rocks. Despite a usually high degree of alteration, the available petrographic and geochemical evidence indicates that all of the rocks sampled have a silica-undersaturated alkaline signature. Most of the occurrences solidified as sills or dykes from mafic mantle-derived magmas, whereas a minority represents lava flows or tuffaceous intervals indicative of explosive eruptive activity. The buried volcanoes of Zuidwal and Mulciber form complex igneous edifices. Petrographically the rocks are often porphyritic, carrying clinopyroxene and olivine (or pseudomorphs) as dominant phenocrysts, while assemblages of primary silicate phases may further include amphibole, biotite, nepheline, leucite and plagioclase. Parental magmas are tephritic/basanitic with a more sodic affinity around the West Netherlands Basin and a more potassic character in the areas of the Vlieland Basin, Broad Fourteens Basin and Dutch Central Graben. Tuff-bearing intervals are mostly reported in logs from wells near the Broad Fourteens Basin. Available results from conventional absolute age dating span a range from Late Triassic to Late Cretaceous but in many cases relia-

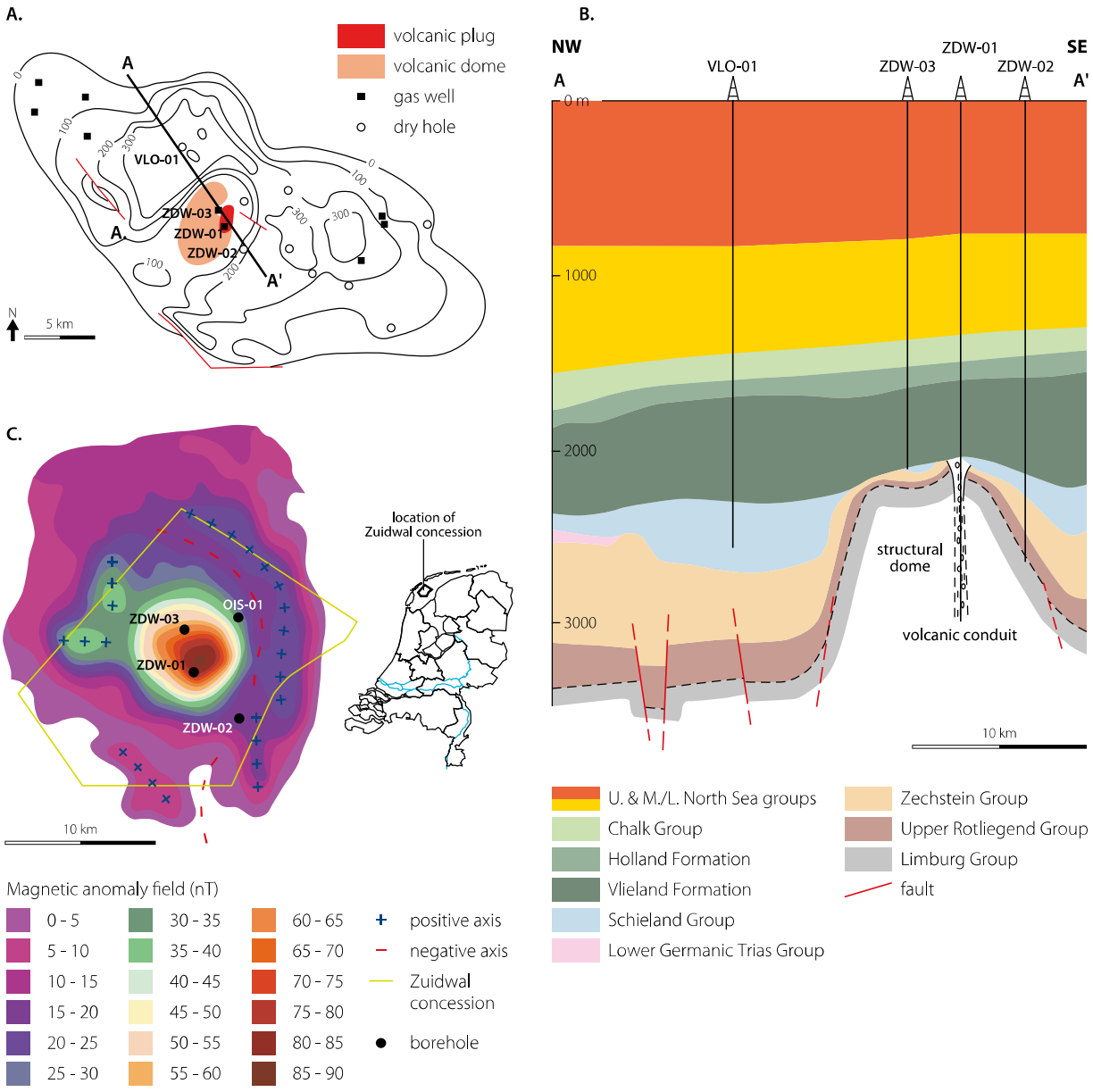
A.
volcanic plug
volcanic dome
gas well
dry hole
VLO-01
ZDW-03
ZDW-01
ZDW-02
A
A'
N
5 km
B.
NW
SE
A
A'
VLO-01
ZDW-03
ZDW-01
ZDW-02
0 m
1000
2000
3000
structural dome
volcanic conduit
10 km
C.
location of Zuidwal concession
OIS-01
ZDW-03
ZDW-01
ZDW-02
10 km
Magnetic anomaly field (nT)
0 - 5
5 - 10
10 - 15
15 - 20
20 - 25
25 - 30
30 - 35
35 - 40
40 - 45
45 - 50
50 - 55
55 - 60
60 - 65
65 - 70
70 - 75
75 - 80
80 - 85
85 - 90
positive axis
negative axis
Zuidwal concession
borehole
U. & M./L. North Sea groups
Chalk Group
Holland Formation
Vlieland Formation
Schieland Group
Lower Germanic Trias Group
Zechstein Group
Upper Rotliegend Group
Limburg Group
fault
D.
temperature
solidus of 'enriched' lithosphere
dry solidus
rising geotherms
E.
30
100
125 km
partial melting of 'enriched' lithosphere
crust
lithosphere
asthenosphere
depth

← ***Figure 11.11.*** *The Zuidwal volcanic centre (for location, see Fig. 11.1): a) Isopach map (metres) of the 'Upper Jurassic' in the southern part of the Vlieland Basin (modified from Herngreen et al., 1991); b) Cross section showing the dome structure of the Zuidwal volcano (modified from Herngreen et al., 1991) c) Aeromagnetic map (modified from Perrot & Van der Poel, 1987; cf. Fig. 11.10b); d) and e) Tentative model for mantle melting below the Zuidwal volcano in response to stretching and thinning of the continental lithosphere, illustrated by connecting a hypothetical temperature-depth (pressure) phase diagram for mantle rock (d) to a simplified cross section through the local crust (modified from Herngreen et al., 1991; see text for details).*

bility is compromized by post-crystallization disturbance. Considering the most robust age dates only, Mesozoic magmatism is probably limited to a Late Jurassic interval.

Paleogene-Neogene

The lower Eocene marine tuffaceous clay of the De Wijk Member (formerly Basal Dongen Tuffite Member) is widely distributed in the subsurface of the Netherlands (Table 11.2). Equivalent tephra deposits are widespread in offshore and onshore stratigraphic records of the UK, Germany and Denmark (Fig. 11.14), where locally tens to hundreds of individual air fall layers have been identified. This early Eocene ash interval has been recognized in large parts of NW Europe and is the expression of an episode of major explosive volcanism (Knox & Morton, 1988; Morton & Knox, 1990; Larsen et al., 2003; Stokke et al., 2020). Given the regional distribution, the interval represents a conspicuous marker in the North Sea Basin, which is well detectible in wire-line logs (Jacqué & Thouvenin, 1975; Knox & Morton, 1988).

The ashfalls were initially bimodal (mixed basaltic to rhyolitic) but subsequent main stage series were predominantly basaltic, as inferred from key sections in northwest Denmark (e.g. Larsen et al., 2003; Stokke et al., 2020). Tephra deposits or their alteration products with largely similar geochemical signatures, have also been described from wells and clay pits in northern Germany (e.g. Obst et al., 2015 and references therein) and from offshore wells in the North Sea area (Morton & Knox, 1990). The ashes probably originated from volcanic centres in the North Atlantic Igneous Province (NAIP), formerly referred to as the 'Thulean igneous province', which comprises intrusive and extrusive rocks encountered in Greenland, Iceland, the Faroe Islands, the UK and Ireland as well as vast submarine areas of the adjacent continental margin (Á Horni et al., 2017). Massive flood basalts and sill intrusions were emplaced between 63 and 52 Ma (maximum activity between 56 and 54 Ma), accompanying the separation of Greenland from Eurasia and the opening of the North-East Atlantic Ocean (Storey et al., 2007). The ash eruptions were particularly explosive and voluminous. The most powerful single event in the succession (dated at 54.04±0.14 Ma; Chambers et al., 2003) ejected ca. 1200 km^3 of ash material with a fall-out distance up to some 1900 km from the source, i.e. as far south as the Austrian Alps (Egger & Brückl, 2006). In the absence of evidence from tephrochronology, it is assumed that the ash particles in the De Wijk Member originate from this eruption (Table 11.2). The magnitude and explosivity of the NAIP eruptions are exceptional for basaltic systems and may have been enhanced by hydromagmatic interaction in a shallow marine environment (Larsen et al., 2003; Stokke et al., 2020). The intrusion of dykes in the North Sea area (see below) may have further contributed to the widespread deposition of tephra in the North Sea Basin through explosive interaction between rising magma and sea water (Wall et al., 2010).

The large-scale igneous activity that marks the NAIP is related to a plume of upwelling hot mantle material arriving at the base of the lithosphere below Greenland, the subsequent continental break-up and the initiation of ocean floor spreading (Morgan, 1971; Saunders et al., 1997; Torsvik et al., 2001). The postulated plume is currently centred below Iceland. Although the mantle plume concept successfully explains the origin of the NAIP, there is ongoing debate as to the shape, size and depth of the mantle source, the location of first impingement, the areal extent of the geological effects, and the stability of its position (see review of Meyer et al., 2007). Alternatives for a classical hot-plume hypothesis have been proposed as well (e.g. Foulger & Anderson, 2005; Hole & Natland, 2020). This episode of intense volcanism had a global environmental impact as it is thought to have triggered the onset of the Paleocene-Eocene Thermal Maximum (PETM) at ca. 56 Ma (e.g. Storey et al., 2007).

The NAIP encompasses the British-Irish Paleogene Igneous Province (BIPIP), which consists of igneous centres and dyke swarms in Scotland, England, (Northern-)Ireland and the Irish Sea (Fig. 11.14; Wright et al., 1971). Dyke swarms also extend into the Southern North Sea (Kirton & Donato, 1985; Brown et al., 1994), as inferred from magnetic anomalies and seismic stratigraphy (see compilation in Fig. 11.14). Since their discovery, several authors have reported evidence for WNW-ESE striking dykes in the Southern North Sea, reaching as far east as the Netherlands offshore (Gauer et al., 2004; Underhill, 2009; Wall et al., 2010; Hernandez Casado & Underhill, 2013; Kortekaas et al., 2018; Carver et al., 2023; Engie/Neptune Energy unpublished internal studies). The dyke swarms appear as

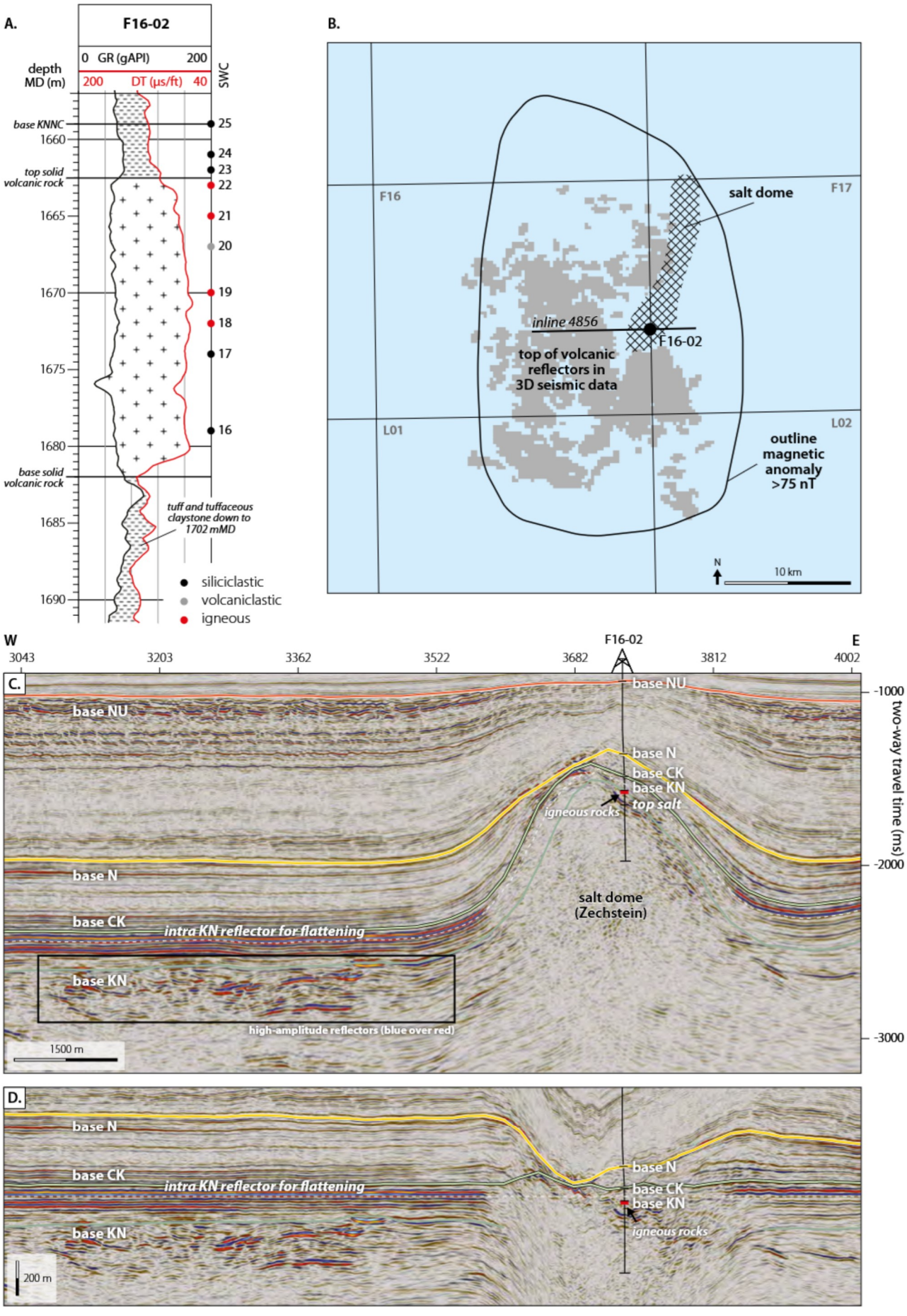
A.
F16-02
0 GR (gAPI) 200
depth MD (m)
200 DT (µs/ft) 40
SWC
base KNNC
top solid volcanic rock
base solid volcanic rock
tuff and tuffaceous claystone down to 1702 mMD
siliciclastic
volcaniclastic
igneous
B.
F16
F17
L01
L02
salt dome
inline 4856
F16-02
top of volcanic reflectors in 3D seismic data
outline magnetic anomaly >75 nT
N
10 km
W
E
3043
3203
3362
3522
3682
3812
4002
C.
base NU
base N
base CK
base KN
top salt
igneous rocks
salt dome (Zechstein)
intra KN reflector for flattening
high-amplitude reflectors (blue over red)
1500 m
two-way travel time (ms)
-1000
-2000
-3000
D.
200 m

← ***Figure 11.12.*** *The Mulciber volcanic centre (for location, see Fig. 11.9): a) Volcanic rock, tuff and tuffaceous claystone in well F16-02, as inferred from geophysical borehole logging and identified in sidewall cores (SWC). GR = gamma-ray log, DT = sonic log, MD = Measured Depth, KNNC = Vlieland Claystone Formation; b) The area around well F16-02 showing the coincidence of the magnetic anomaly (also see Fig. 11.10b) and a seismic reflector representing layers of solid (volcanic) rock with a high acoustic impedance; c) Seismic line across well F16-02, penetrating an underlying salt dome (3D survey Z3WIN2003B, inline 4856); d) Flattened version of the seismic line to illustrate the correlation between the volcanic deposits in well F16-02 and the seismic reflector further to the west. NU = Upper North Sea Group, N = North Sea Supergroup, CK = Chalk Group, KN = Rijnland Group.*

noisy sub-vertical zones on seismic data but the deep roots of the igneous bodies remain elusive.

The age of the dykes in the Southern North Sea is not well established but can be inferred from their onshore equivalents in Scotland and England. Interpretation of conventional K-Ar dates of a large set of samples from the Cleveland Dyke Echelon, which stretches from the Mull intrusive complex in western Scotland to the north-east coast of England, yielded an emplacement age of 59.3±2.0 Ma (Mitchell et al., 1989). Stratigraphic relationships point to a consistent age of 58-54 Ma (Underhill, 2009; Wall et al., 2010) or 59-58 Ma (Carver et al., 2023), i.e. near to the Paleocene-Eocene boundary for the Southern North Sea dykes that form the south-easterly continuation of the Cleveland and associated dykes. Thoroughly screened and recalibrated Ar-Ar and U-Pb dates of various igneous rocks return an age cluster between 63 and 58 Ma for the entire BIPIP (Wilkinson et al., 2017).

Dyke swarms of similar age to those of the BIPIP and Southern North Sea also occur on the north-American side of the spreading zone, i.e. along the east coast of Greenland (Kirton & Donato, 1985; Wilkinson et al., 2017). In the Southern North Sea, the dykes may reflect the regional stress pattern in the Paleogene as they do not coincide with prominent faults at sub-salt level (Underhill, 2009). On the other hand, Wall et al. (2010) noted that dykes have the same trend as regional basement lineaments. The dykes occur preferentially in synclines where Zechstein salt has flowed away (Brown et al., 1994; Underhill, 2009; Wall et al., 2010). Based on seismic interpretation, Hernandez Casado & Underhill (2013) suggested that Paleogene igneous activity triggered mobility of the Zechstein salt in the Southern North Sea, which played a major role in shaping the structural configuration. Carver et al. (2023) tentatively inferred a minimum of at least three intrusive episodes spread over a period of about one million years. Linear channel-like features, visible at the top of the Upper Cretaceous Chalk (Brown et al., 1994; Carver et al., 2023), may reflect catastrophic dewatering, compaction and consequent extensional collapse as a thermal effect of dyke intrusion. Based on 3D seismic imaging, Wall et al. (2010) identified various types of craters at the top of the Chalk.

The dyke intrusions may have influenced petroleum prospectivity in various ways. Some authors (e.g. Kirton & Donato, 1985; Dewey & Windley, 1988) refer to the coincidence of the NW-SE trending dyke systems in Scotland and northern England with a broad zone of 'devolatilized Westphalian coals' that crosses the North Sea and extends to the Netherlands towards the Ruhr Graben. Fracturing around and above the dykes could have permitted gas migration from the Carboniferous source rocks into Triassic reservoirs, thus explaining the linear orientation of Triassic gas fields in the Southern North Sea (Underhill, 2009; Kortekaas et al., 2018). It has also been proposed that intrusion of the Paleogene dykes had an influence on the composition of subsurface gas, such as a rise in CO_2 or N_2 content (Verweij et al., 2016).

Volcanism also affected sediment composition in the North Sea Basin during the early Oligocene (Rupelian), in particular that of the Boom Member ('Boom clay'), a 50 to 75-m-thick marine shelf sediment present over large parts of the Netherlands subsurface (Table 11.2). According to petrographic observations on samples from outcrops in Belgium the sediment contains volcanic heavy minerals and up to 10% of argillized volcaniclasts in a clayey matrix that is thought to be the altered volcanic ash of trachytic and basaltic composition (Zimmerle, 1993). Plausible sources are volcanic centres of the Siebengebirge and Hocheifel that produced basaltic and evolved lavas and pyroclastics with alkaline affinities (Wedepohl et al., 1994; Jung et al., 2006, 2012). They were active from ca. 30-22 and 44-35 Ma, respectively, according to $^{40}Ar/^{39}Ar$ dating (Fekiacova et al., 2007; Przybyla et al., 2018). Direct ash falls and/or reworking of weathered volcanic soils were possible modes of transport to the North Sea area. Admixture of ash from the BIPIP cannot be excluded, as the main sea current along the British uplands at the time was counterclockwise (Vandenberghe et al., 2014).

Several layers containing ash particles have been found intercalated in shallow marine clay of the upper Oligocene to lower Miocene Veldhoven Formation in boreholes in the Winterswijk region (Table 11.2; Burger, 1979, 1992; Van den Bosch, 2015). The presence of 'Eifel titanite' and 'basaltic hornblende' suggests a link with explosive volcanism in the Eifel. This volcanism around the Rhine-Roer-Hessian graben triple junction in the Rhenish Massif started in the Eocene and lasted well into the Quaternary, with episodes of increased activity in the Late Oligocene

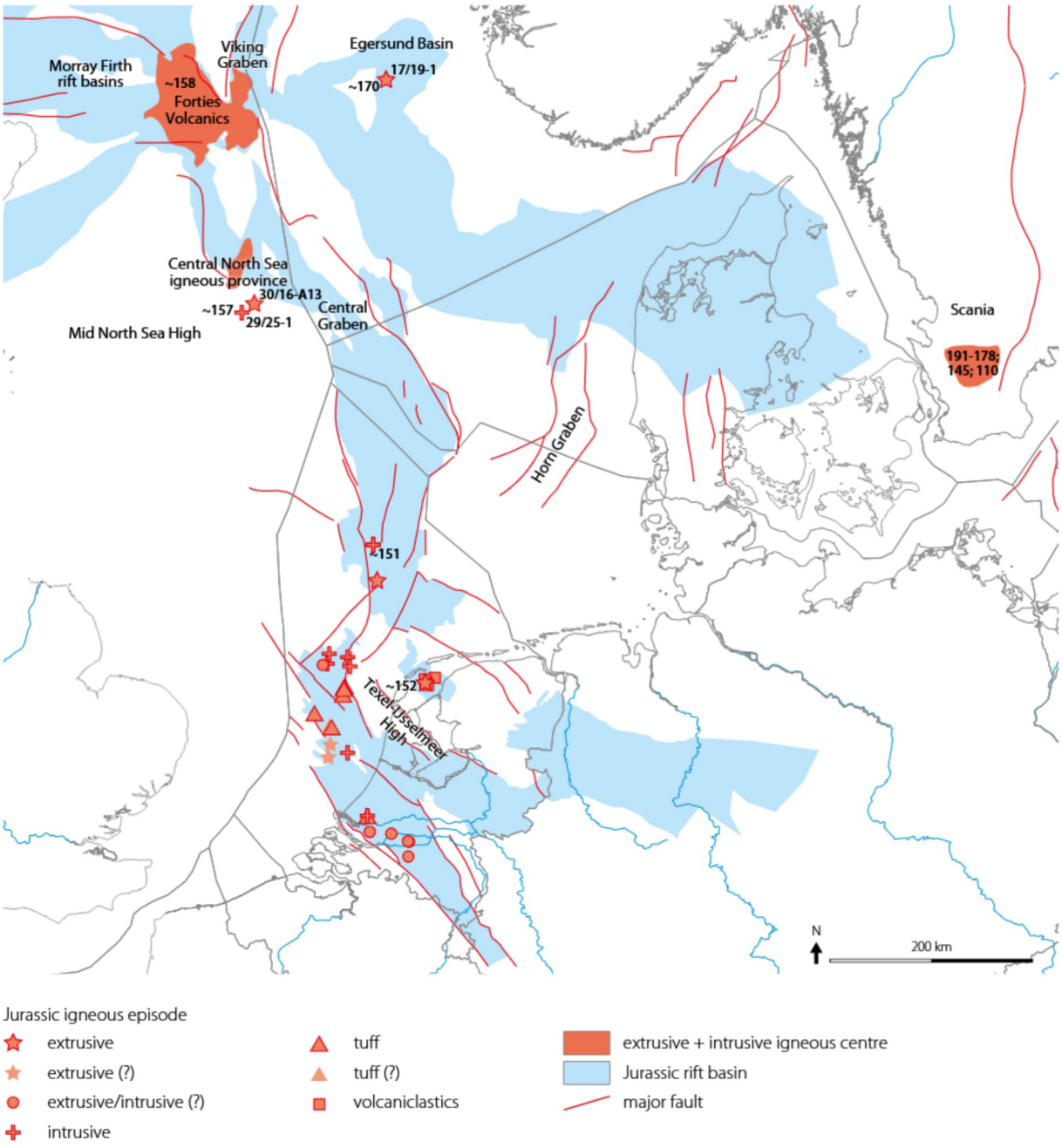

***Figure 11.13.** Distribution of Jurassic igneous rocks in northwest Europe and wells in the Netherlands that penetrated intrusive and extrusive rocks, volcaniclastics and tuffs from this period. Well names can be found in Fig. 11.9.*

and Miocene (Sissingh, 2003; Ziegler & Dèzes, 2005, and references therein). It accompanied the development of the Rhine rift system and has been associated with the rise of a mantle plume and related thermal thinning of the mantle-lithosphere (Ritter et al., 2001).

Quaternary

Tephra layers originating from volcanic centres in the Eifel or Iceland are locally intercalated in Quaternary sedimentary deposits, providing a rare opportunity for tephrostratigraphic correlations in the Netherlands.

Middle Pleistocene fluvial terrace sequences in the Middle and Lower Rhine Basin in Germany record the onset of volcanism in the eastern Eifel about 600 ky ago through the appearance of volcanic heavy minerals that were initially dominated by hornblende and later by clinopyroxene (Boenigk & Frechen, 2006). In the Netherlands, a similar change in the heavy mineral spectrum is used to separate fluviatile deposits of the Sterksel Formation from the overlying Urk Formation (Preusser, 2008), in view of

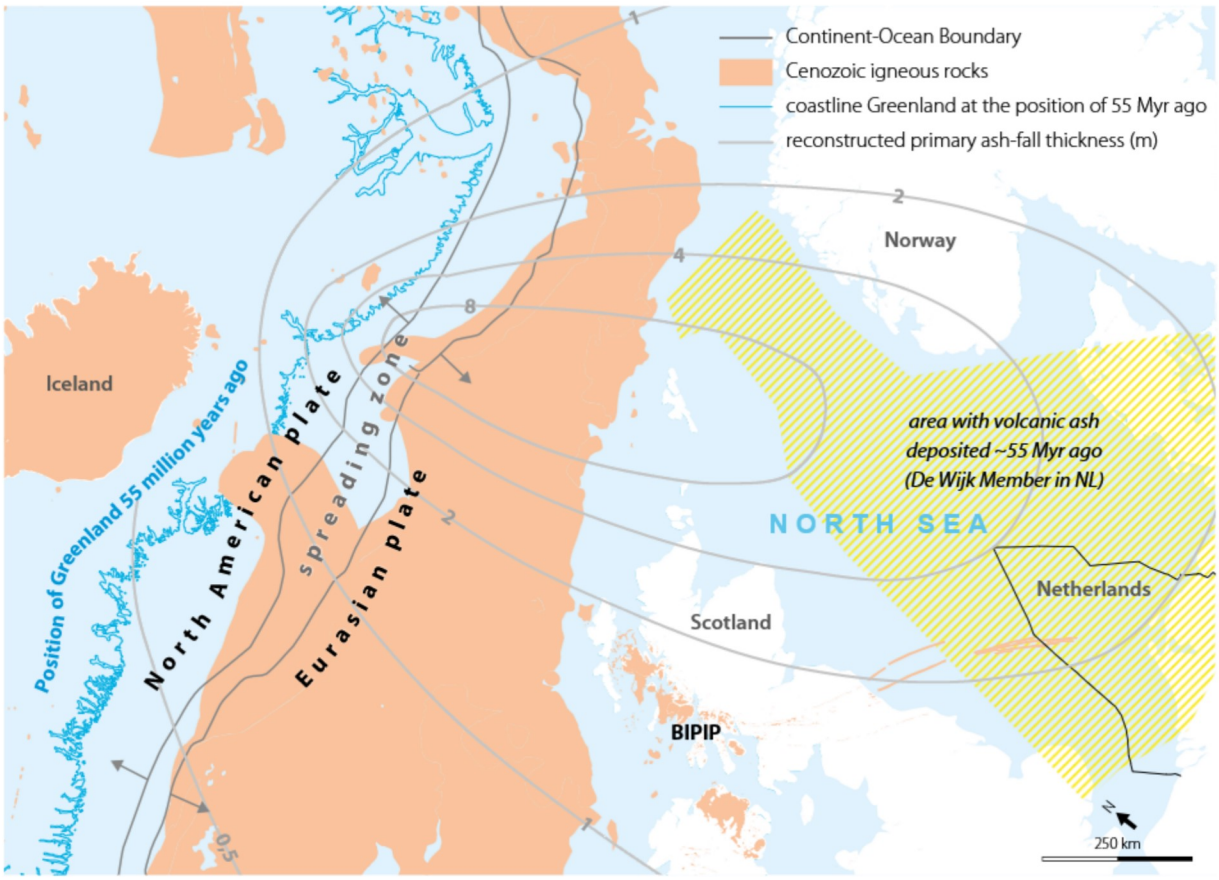

Figure 11.14. The North-East Atlantic Ocean at the onset of breakup (ca. 55 Ma, after Gaina et al., 2014) and the distribution of associated basaltic rocks (after Á Horni et al., 2017). Also shown are reconstructed isopach contours for primary ash fall produced by explosive volcanism that accompanied the rifting process (based on Knox & Morton, 1988; Knox, 1997). In the Netherlands, these ashes form a constituent of the De Wijk Member of the Dongen Formation. Geophysical evidence suggests that rifting-related dykes extend as far as the Dutch offshore (see text). Compilation of dikes in the North Sea is based on: Underhill (2009), Kirton & Donato (1985), Kortekaas et al. (2018), Youri Poslawski/Neptune Energy. BIPIP = British and Irish Paleogene Igneous Province.

the fact that the Lingsfort Member, the lowermost member of the Urk Formation, is thought to correlate with the oldest Middle Terrace sediments (MT I) in the Lower Rhine area (Zagwijn, 1985), where the increased influx of volcanic material is also recorded (Boenigk & Frechen, 2006). This is a rare example of the use of magmatic products for stratigraphic purposes in the Netherlands.

The loess succession of the Middle Pleistocene-Lower Holocene Boxtel Formation in South Limburg contains several tephras with an origin in the Eifel region, taking observations at locations in the immediate vicinity into account: the Rocourt Tephra, the Eltville Tephra and the Laacher See Tephra (Fig. 11.15, Table 11.2).

The Rocourt Tephra (Fig. 11.15b) was produced by a basaltic alkaline volcano with an unknown location presumably in the West Eifel. The tephra is marked by a blocky shape of altered glass shards, suggesting a phreatomagmatic character of the eruption, with a mineral assemblage comprising clinopyroxene, brown amphibole, orthopyroxene (enstatite) and Cr-spinel in decreasing order of abundance (Pouclet et al., 2008). The combination of high- to middle-pressure enstatite and aluminous clinopyroxene with low-pressure fassaitic clinopyroxene is rather unique and makes the tephra easy to recognize. Stratigraphic dating points to an age between 90.3 and 74 ka (Pouclet et al., 2008). Rocourt tephra has been found across large parts of eastern Belgium, including in loess sections near Kesselt, Vroenhoven en Veldwezelt, just west of Maastricht (Mees & Meijs, 1984; Pouclet et al., 2008; Meijs, 2011).

The Weichselian Eltville Tephra (Fig. 11.15c) erupted from an unidentified volcanic centre in the West or East Eifel and has been recognized in loess regions of western and central Germany, southern Netherlands and eastern Belgium, where two to five individual ash layers are part of an interval with a total thickness ranging between a few mm to 20 cm (Meijs et al., 1983; Pouclet & Juvigne, 2009; Zens et al., 2017). The assemblage of mafic vol-

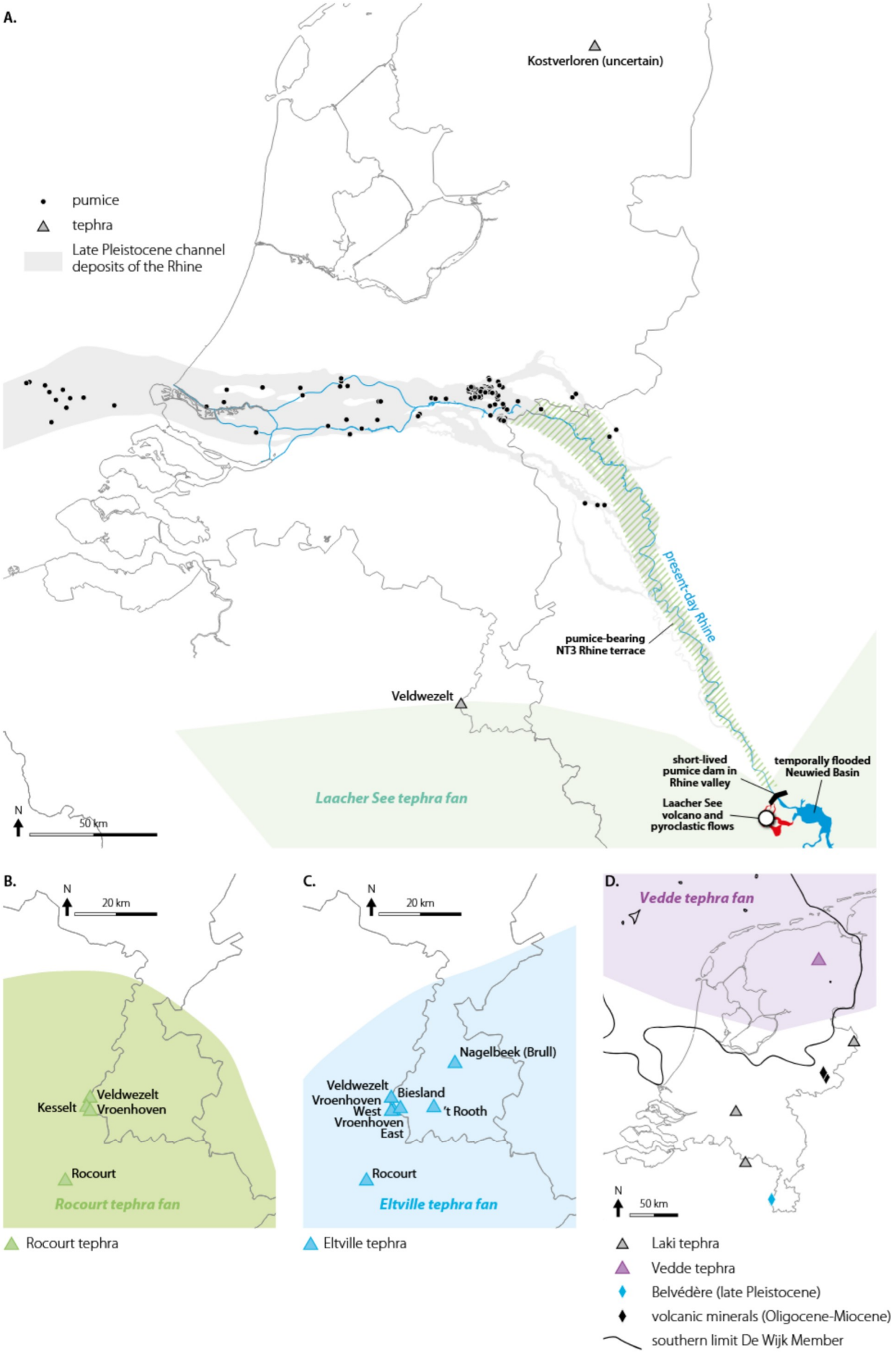
A.
Kostverloren (uncertain)
pumice
tephra
Late Pleistocene channel deposits of the Rhine
present-day Rhine
pumice-bearing NT3 Rhine terrace
Veldwezelt
short-lived pumice dam in Rhine valley
temporally flooded Neuwied Basin
Laacher See volcano and pyroclastic flows
Laacher See tephra fan
N
50 km
B.
N
20 km
Veldwezelt
Kesselt
Vroenhoven
Rocourt
Rocourt tephra fan
Rocourt tephra
C.
N
20 km
Nagelbeek (Brull)
Veldwezelt
Vroenhoven West
Biesland
't Rooth
Vroenhoven East
Rocourt
Eltville tephra fan
Eltville tephra
D.
Vedde tephra fan
N
50 km
Laki tephra
Vedde tephra
Belvédère (late Pleistocene)
volcanic minerals (Oligocene-Miocene)
southern limit De Wijk Member

← ***Figure 11.15.*** *Cenozoic volcanic material in the Netherlands: a) Reworked Laacher See pumice dispersed along the (Late Pleistocene) Rhine River and schematic distribution of air-fall tephra ejected from the Laacher See eruption centre (pumice compilation: K.M. Cohen (2015, 2022: various databases TNO-GDN, UU, literature); tephra and details: Schmincke et al. (1999), Park & Schmincke (2009); Late Pleistocene channel modified from Cohen et al. (2012); b) Approximate distribution of air-fall tephra from the Rocourt event (between 90.3 and 74 ka) and locations where it has been found in sediments (tephra: Pouclet & Juvigne (2009); locations are from: Mees & Meijs (1984), Meijs (2011), Juvigné (1999)); c) Approximate distribution of air-fall tephra from the 25.6-23.2 ka Eltville event and locations where it has been found in sediments (see also Fig. 11.16a) (tephra: Zens et al. (2017); locations are from: Meijs (1980), Juvigné & Semmel (1981), Meijs et al. (1983), Meijs (2011), Juvigné & Semmel (1981)); d) Approximate distribution of crypto-tephra from the 12.1 ka BP Vedde eruption and locations where crypto-tephra from the Vedde and 1783-84 AD Laki eruptions has been found in sediments. The distribution of the De Wijk Member containing Paleocene-Eocene tephra or tuff is indicated based on TNO-GDN (2023). (tephra: Davies et al. (2005); volcanic minerals: Burger (1979, 1992); Laki: Cremer et al. (2010), Andronikov et al. (2016); Belvédère: Meijs (1985)).*

canic minerals is dominated by clinopyroxene, olivine and brown amphibole, whereas titanite, apatite and traces of phlogopite, prehnite, haüyne, tridimite, nepheline and K-feldspars have been identified as well (Juvigné & Semmel, 1981; Meijs et al., 1983; Pouclet & Juvigne, 2009). The tephra is a prominent stratigraphic marker with an age of 25.6-23.2 ka obtained from luminescence dating (Zens et al., 2017). Meijs (1980, 2011), Meijs et al. (1983) and Pouclet & Juvigné (2009) reported its presence in quarries and sections around Maastricht (Nagelbeek, 't Rooth (Fig. 11.16a), Biesland, Lixhe, Veldwezelt, wall of the Albert Canal near Vroenhove).

The Late Pleistocene Laacher See Tephra (Fig. 11.15a) is a prominent stratigraphic marker in large parts of Central Europe. Three main events of violent explosive activity from a centre in the East Eifel Volcanic Field produced ash clouds fanning in different directions and fall-out up to more than 1000 km from the source (Wörner & Schmincke, 1984; Van den Bogaard & Schmincke, 1990). Owing to the phonolitic composition of glass shards, the dominance of clinopyroxene, amphibole and sphene (titanite) as heavy minerals and sanidine and plagioclase as light phases, the Laacher See Tephra is easily distinguishable from ashes with a similar age. The chemical and mineralogical composition changed in the course of time from highly differentiated to mafic phonolite. Recent high-precision dendrochronological and ^{14}C dating yielded an eruption age of 13,006 ± 9 calibrated years before present (Reinig et al., 2021).

Blockage of the Rhine River by abundant pyroclastic flows and rapid deposition of tephra fall near the crater, followed by breaching of the pumice dam and catastrophic flooding, discharged large amounts of tephra into the lower Middle Rhine Valley (Schmincke et al., 1999). Further reworking explains why Rhine sediments in the Netherlands contain Laacher See pumice granules from the Late Allerød onwards (Busschers et al., 2007; Autin, 2008; Fig. 11.16b). Layers with glassy pumice fragments containing phenocrysts of augite and 'basaltic hornblende' were encountered in river sediments from several locations near Arnhem (Crommelin, 1963; Erkens, 2009).

Airborne Laacher See tephra has been identified in the form of volcanic heavy minerals (clinopyroxene and brown amphibole) in the loess succession of the Veldwezelt section that also contains the Rocourt and Eltville tephras (Meijs, 2011). Trace-element signatures of Late Pleistocene eolian cover sands (Lutterzand in the easternmost part of the Netherlands and sites near Lommel in NE Belgium) point to the presence of a volcanic component that may also be derived from the Laacher See Tephra (Andronikov et al., 2016).

Layers with distal (crypto-)tephra have also been identified in a Late Pleistocene peat and gyttja infill of a pingo-remnant at Kostverloren, in the province of Drenthe (Fig 11.15d; Davies et al., 2005). Geochemical fingerprinting identified glass shards of one horizon as the rhyolitic component of the bimodal (basaltic-rhyolitic) Vedde Ash (mid-Younger Dryas), an important regional stratigraphic marker in the North Atlantic, the Norwegian Sea, and the adjacent land area, dated at 12 ka (e.g. Lohne et al., 2013). These Vedde Ash particles are fall-out from an ash cloud thought to have originated from a major explosive eruption in southern Iceland (probably from Katla Volcano), which drifted in south-easterly directions over northern Britain, southern Scandinavia and western Russia. Two other tephras in the Kostverloren succession could not be geochemically characterized but one has tentatively been attributed to the Laacher See Tephra (Davies et al., 2005).

A Holocene micro-tephra has been preserved in the form of glass shards in a sedimentary succession dominated by gyttja, filling in a historic scour-hole lake near Haarsteeg (Fig. 11.15d; Noord Brabant). From chronostratigraphic evidence the tephra corresponds to the large 1783-1784 AD volcanic eruption of the Laki volcano in Iceland (Cremer et al., 2010). This event produced a dry sulphuric fog across large parts of Europe (Thordarson & Self, 1993) with a severe environmental impact. Brugmans (1784) provided a remarkably detailed historic account on

Table 11.2. Cenozoic tephra in the Dutch subsurface with sources and dated eruption events. Note that ages are mostly based on dating of equivalent deposits outside the Netherlands (see references). Emplacement is based on available evidence.

Eruptive event/marker	Location	Well/sample depth (m)	Age	Dating method
Laki eruption	Haarsteegse Wiel (scour lake)	Northern basin (HA-07-05)/ 2.60-2.70	1783-1784 CE	Age-depth relationships and interpolation between various historic events recorded in lake sediments
Vedde Tephra – probably from Katla Volcano	Kostverloren Veen (peat bog)	N/A	12,066±42 cal yr BP	Tephrochronology (Kostverloren Veen) and bayesian age-depth modelling of AMS ^{14}C dates from Icelandic lake sediments hosting Vedde-ash
Laacher See eruption	Rhine-Meuse delta	N/A	13,006±9 cal yr BP	^{14}C and dendrochronology
Eltville Tephra	South Limburg loess	N/A	25.6-23.2 ka	Bayesian age-depth modelling of luminescence ages of minerals above and below the tephra in loess-paleosol sequences between eastern Belgium and central Germany
Rocourt Tephra	South Limburg loess	N/A	90.3-74 ka	Stratigraphic bracketing with thermoluminescence dating of underlying limestone clasts and ^{14}C dating of an overlying peat layer
Tephra in Veldhoven Formation	Subsuface Winterswijk region (East Netherlands)	Beltrum ('100') B34D0232/ 131.5-136.5	28-16 Ma (?)	Age estimate based on formation age
		Lievelde ('101') B41B0073/ 92.5-93.5	28-16 Ma (?)	Age estimate based on formation age
Tephra in Boom Member of Rupel Formation	Onshore and offshore subsurface Netherlands	Holostratoype (B51D0127, Veldhoven-01) and other wells	44-35, 30-22 Ma	Inferred from ^{40}Ar/^{39}Ar ages of possible centres in Siebengebirge and Hocheifel (Germany)
North East Atlantic Province tephra	Onshore and offshore subsurface north Netherlands	Holostratotype (BL020070, L02-04) and other wells	54.04 ± 0.14 Ma	^{40}Ar/^{39}Ar age of '+19 ash' from the Fur Formation (Denmark), presumably equivalent to De Wijk ash

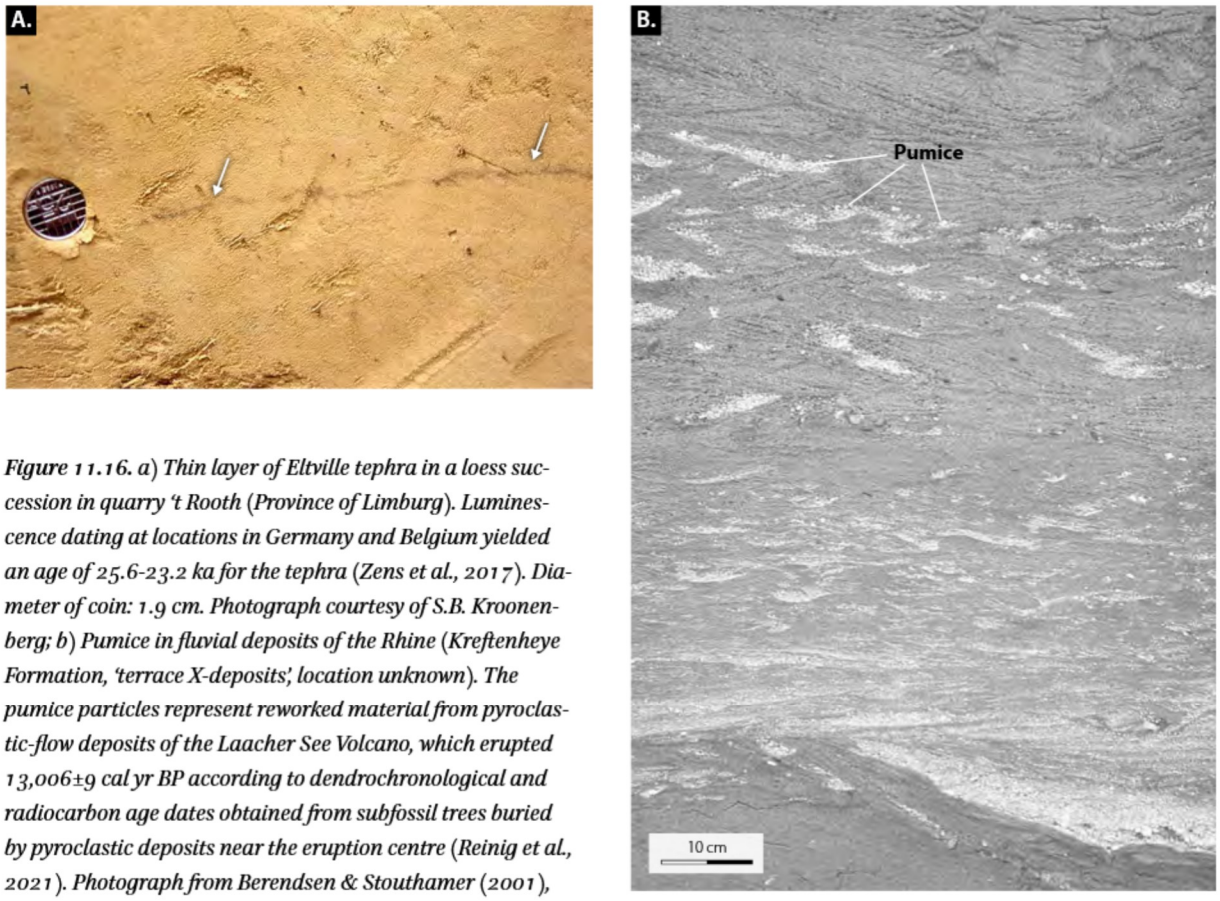

Figure 11.16. a) Thin layer of Eltville tephra in a loess succession in quarry 't Rooth (Province of Limburg). Luminescence dating at locations in Germany and Belgium yielded an age of 25.6-23.2 ka for the tephra (Zens et al., 2017). Diameter of coin: 1.9 cm. Photograph courtesy of S.B. Kroonenberg; b) Pumice in fluvial deposits of the Rhine (Kreftenheye Formation, 'terrace X-deposits', location unknown). The pumice particles represent reworked material from pyroclastic-flow deposits of the Laacher See Volcano, which erupted 13,006±9 cal yr BP according to dendrochronological and radiocarbon age dates obtained from subfossil trees buried by pyroclastic deposits near the eruption centre (Reinig et al., 2021). Photograph from Berendsen & Stouthamer (2001), lacquer-peel made by J. van der Staay (Geological Survey of the Netherlands). Frame size: ~100 x 60 cm.

Source region	Host formation	Chronostratigraphy of host interval	Emplacement	Deposit type/composition	Reference(s)
Iceland	Echteld Formation	Holocene	Airfall	Micro-tephra (glass shards)	Cremer et al. (2010)
Iceland	Nieuwkoop Formation	Pleistocene	Airfall	Cryptotephra (rhyolitic glass shards)	Davies et al. (2005); Lohne et al. (2013)
East Eifel	Kreftenheye Formation	Pleistocene	Reworked airfall	Reworked felsic pumice particles	Verbraeck (1984); Autin (2008); Meijs (2011); Reinig et al. (2021)
West or East Eifel volcanic field	Boxtel Formation	Pleistocene	Airfall	Tephra layer containing mafic volcanic minerals	Meijs et al. (1983); Zens et al. (2017)
Eifel (location unknown)	Boxtel Formation	Pleistocene	Airfall	Reworked tephra containing altered glass shards and a mineral assemblage including orthopyroxene	Mees & Meijs (1984); Pouclet et al. (2008); Meijs (2011)
Eifel (?)	Veldhoven Formation	Oligocene-Miocene	Airfall?	Igneous minerals	Burger (1992); Van den Bosch (2015)
Eifel (?)	Veldhoven Formation	Oligocene-Miocene	Airfall?	Igneous minerals	Burger (1979); Van den Bosch (2015)
Siebengebirge and/or Hocheifel (?)	Rupel Formation	Rupelian	Airfall or reworked airfall	Volcanic heavy minerals and altered trachytic-basaltic volcanic ash	Zimmerle (1993); Fekiacova et al. (2007); Przybyla et al. (2018)
NE Atlantic	Dongen Formation (De Wijk Member)	Eocene	Airfall	Distal ash	Chambers et al. (2003)

an array of adverse effects in the Netherlands. The 2010 eruption of Eyjafjallajökull volcano illustrates that explosive eruptions on Iceland occasionally have produced fallout from ash clouds in the Netherlands in recent times.

Indirect evidence for other magmatic intrusions

Apart from igneous rocks encountered in hydrocarbon wells and seismic data and the evidence for Paleogene dykes extending in the southern North Sea, the presence of intrusive magmatic rocks in the Dutch subsurface has also been inferred from geophysical anomalies and localized heating effects on organic matter. The presence of two sizeable intrusive bodies has been postulated along the border with Germany (Fig. 11.1). A coalification anomaly in upper Carboniferous sediments from wells in the Ems estuary (northeastern Groningen) and the adjacent part of Germany defines the East Groningen Massif (Kettel, 1983). A positive magnetic anomaly and structural contours of the top of the Rotliegend, inferred for Jurassic times, outline the shape of this anomaly (Fig. 11.7, also visible in Fig. 11.10b). This, in combination with the timing of the Zuidwal, Andel and Loon op Zand igneous activity, led Kettel (1983) to assume that the East Groningen Massif represents an intrusive body emplaced around the Jurassic-Cretaceous transition. It cannot be excluded, however, that the inferred intrusion is older and could have an early Permian age (Van Wijhe et al., 1980).

The Erkelenz intrusion near the Peel Boundary Fault Zone of the Roer Valley Graben in the province of Limburg and neighbouring Germany has been identified from geophysical surveys (Fig. 11.7). A pronounced positive magnetic anomaly, in combination with a minor residual gravity anomaly, favours a granitic body as interpretation (Bredewout, 1989). The initial intrusion temperature was 800 ± 100 °C, based on cooling modelling and vitrinite reflection data collected from local coal seams (Erren & Bredewout, 1991). The timing of the intrusion is unknown, but fission-track data and the degree of coalification in overlying sediments point to a heat pulse between late Carboniferous and mid-Cretaceous times (Teichmüller & Teichmüller, 1971; Bredewout, 1989). Assuming a granitic composition, a Permian age of the intrusion is plausible, given the widespread manifestations of 'Rotliegend' acidic magmatism in northwest Europe, particularly near the Variscan front. In the Campine Basin, across the southwestern boundary fault of the Roer Valley Graben, a magnetic anomaly near Bilzen (Dusar & Langenaeker, 1992), and a gravimetric anomaly near the city of Maastricht (see Textbox) also hint at the possible presence of intrusive bodies. A continuous positive pre-Permian residual gravity anomaly largely follows the Dutch onshore and offshore rift pattern and could signal the presence of high-density magmatic intrusions in the crust, but Moho shallowing cannot be ruled out as an alternative explanation (Dirkzwager et al., 2000).

Indirect geophysical evidence points to the presence of buried, mainly granitic intrusions in the domain of the

Anglo-Brabant Massif below the Southern North Sea Basin (e.g. Rijkers & Duin, 1994). They must be pre-Devonian and are probably equivalent to igneous rocks encountered in onshore drill holes and outcrops in east England and Belgium (e.g. Pharaoh et al., 1993; De Vos et al., 2010). Similar geophysical interpretations in areas around the Mid North Sea high (Donato et al., 1983; Kimbell & Williamson, 2015) also suggest that buried granites within the Paleozoic basement may be more widespread than the single occurrence in the A17-01 well. Structural highs such as the Dogger High may well have a granite core. It is of interest to note that the decay of uranium, thorium and potassium isotopes in granitic rocks produces radioactive heat that may drive hydrothermal circulation long after

A granite intrusion below Maastricht?

Nearly a hundred years ago, the front page of a newspaper from The Hague reported on a surprising discovery in a 330 m deep borehole in the city of Maastricht (De Avondpost, 1 February 1930). In a search for new drinking water resources, subsurface water with a temperature of 18°C was sampled, about eight degrees higher than expected. According to a laboratory in Berlin it had medicinal qualities and could be bottled similarly to what was then already practiced in the nearby town of Spa. The well (Kastanjelaan-1) produced the local Trega mineral water until 1960.

In the 1980s two new boreholes were drilled in an attempt to identify a successor to this well: Kastanjelaan-2 and Heugem-1. They were cored over great lengths and investigated in detail under supervision of Martin Bless of the Natural History Museum of Maastricht (Bless et al., 1981). Borehole Heugem-1 drew particular attention, as a temperature of 20-21°C was recorded at 500 m depth. Even more striking was the high degree of coalification in samples of the Dinantian limestone host rock. Measured vitrinite reflectance of 5-7% (and a >10% outlier) fall in the (meta-)anthracite range, suggesting temperatures up to 300°C and burial down to 10 km. A sequence of strong tectonic burial, followed by uplift, could have generated such a high coalification but does not fit with the regional geodynamic history.

It is also conceivable that a granitic intrusion is responsible for the heat. A gravity low beneath Maastricht suggests its presence (Mansy et al., 1999). Interestingly, a magnetic anomaly around Bilzen just west of the city across the Belgian border (Dusar & Langenaeker, 1992) has characteristics similar to the Erkelenz anomaly, which has been linked to a hidden granitic body (Bredewout, 1989), possibly related to a Permo-Carboniferous intrusion *(see main text)*. Unfortunately, drilling could not conclusively confirm this for Bilzen, as borehole Martenslinde ended in Cambrian quartzite at only 300 m depth (Dusar & Langenaeker, 1992).

If a magma body intruded underneath Maastricht in, say, Permo-Carboniferous times, it will have cooled down and solidified long ago. This could explain the anomalous coalification, but seemingly not the elevated temperature of the subsurface water. However, ancient granitic rock bodies often continue to produce heat today, as they are rich in the radioactive isotopes ^{235}U, ^{238}U, ^{232}Th and ^{40}K with half-lives between 700 and 14,000 million years. Upward flowing fluids could transfer this heat to the surface through steep faults. Since fault locations are poorly known in the Maastricht region, could the warm water hint at a hidden fault? On the other hand, how certain is the presence of a granite body? Anomalous coalification ranks have also been recorded in Dinantian shales and carbonates from the Thermae-2000 and Thermae-2002 wells (Wolf & Bless, 1987).

Obvously, further research is needed to test the validity of a Trega water-granite connection.

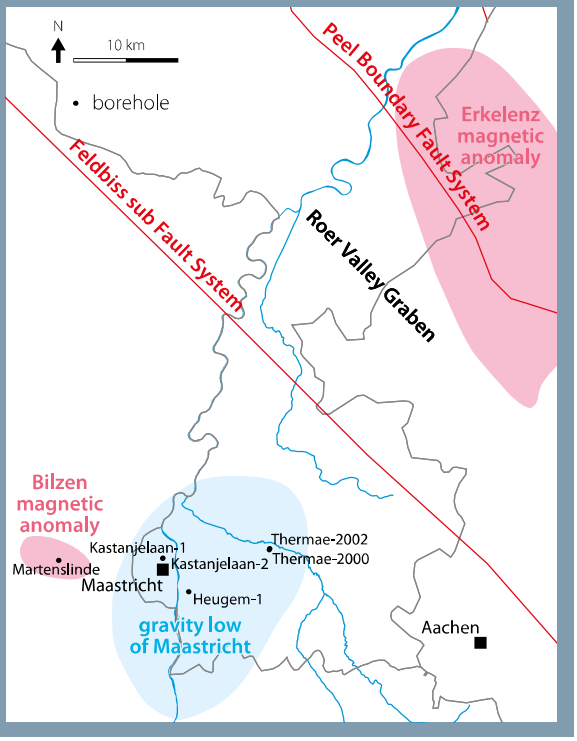

the intrusion event. This may be sufficient to generate local areas of anomalously high organic maturity, or remobilization of Zechstein salts and carbonates (Parnell, 1988).

Geochemical signatures

The petrographic observations show that secondary alteration is a ubiquitous feature in all the Paleozoic and Mesozoic igneous rocks listed in Table 11.1. Hence, many of the reported geochemical compositions of bulk-rock samples are expected to reflect modifications of original signatures to a certain extent (Fig. 11.17). Alteration usually affects mobile elements such as Si, Mg, Ca, K, Na, Sr, Rb, Ba, which may either be added or removed. Standard classifications and petrogenetic interpretations based on these elements will therefore not always be unambiguous. Instead, inferences from relatively immobile minor and trace elements such as Ti, P, Zr, Nb, Y and the rare-earth elements (REE) may be more trustworthy, as these are least sensitive to alteration processes. Compositions of the igneous rocks in the Dutch subsurface are compiled in Table 11.3. The available data show a clear geochemical distinction between Paleozoic and Mesozoic occurrences, as is illustrated in Figs 11.18 and 11.21.

Carboniferous-early Permian

Carboniferous-early Permian magmatic rocks (in Wanneperveen-1, De Wijk-7, Dwingelo-2, Corle-1, Gelria-3, F04-02-A) are subalkaline to mildly alkaline, showing compositional variability, both between different locations and among samples from individual wells. In a TAS classification diagram (wt.% SiO_2 vs Na_2O+K_2O; Fig. 11.18a) they tend to concentrate in the basalt and trachybasalt fields. It should be noted that at least part of the scatter in this diagram is attributable to effects of secondary alteration. The few analysed samples with more evolved compositions (trachyte-trachydacite) are from offshore well F04-02-A (rim of the Dutch Central Graben) and onshore well De Wijk-7 (east of Texel-IJsselmeer High). The additional presence of predominantly basaltic rocks in the latter well signals a bimodal distribution, which is also seen in the Horn Graben (Danish offshore) and in Carboniferous-early Permian sills and dykes in Scotland and southern Sweden (Kirstein et al., 2006). Immobile elements further constrain the geochemical affinity of the Dutch Permo-carboniferous rocks. In a Nb/Y vs. Zr/Ti discrimination diagram (Fig. 11.18c) the mafic rocks straddle the basalt-alkali basalt boundary, whereas the more felsic rocks plot close to the trachyte-trachyandesite-rhyolite+dacite junction. Samples from offshore wells in other sectors of the North Sea show a similar distribution. In contrast, the available data also indicate that the Dutch onshore

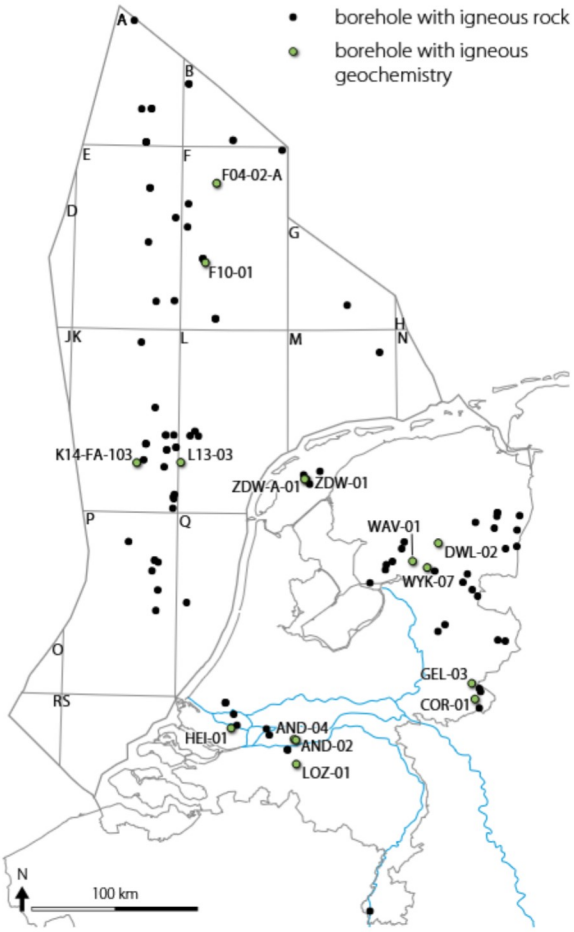

Figure 11.17. Locations of wells with geochemical analyses on core samples of igneous rocks (see Table 11.3).

occurrences are distinct, as they tend to have lower concentrations in TiO_2 and P_2O_5 (Fig. 11.19c), as well as in Zr, Nb, Y, LREE (light rare-earth elements) than Rotliegend rocks from neighbouring North Sea areas if only the relatively mafic samples (>4 wt.% MgO) are considered. Rare-earth-element patterns display a modest LREE enrichment and a relatively flat HREE (heavy rare-earth elements) (Fig. 11.20a). These trends are comparable to those of the subalkaline basalts in Central Graben UK well 39/2-4, but LREE/HREE ratios and total REE concentrations tend to be lower than in the majority of equivalent igneous rocks of northwestern Europe. A final point to note is the significant variation in major and trace element contents of the intrusive rocks from Wanneperveen-1 (Table 11.3a). Several Wanneperveen-1 samples, as well as the Dwingelo-2 rock, are marked by very high MgO (>15 wt.%), presumably due to accumulation of olivine phenocrysts under magmatic conditions.

Abundant geochemical data on Carboniferous-early Permian igneous occurrences encountered in drill cores and outcrops in northwest Europe and available for com-

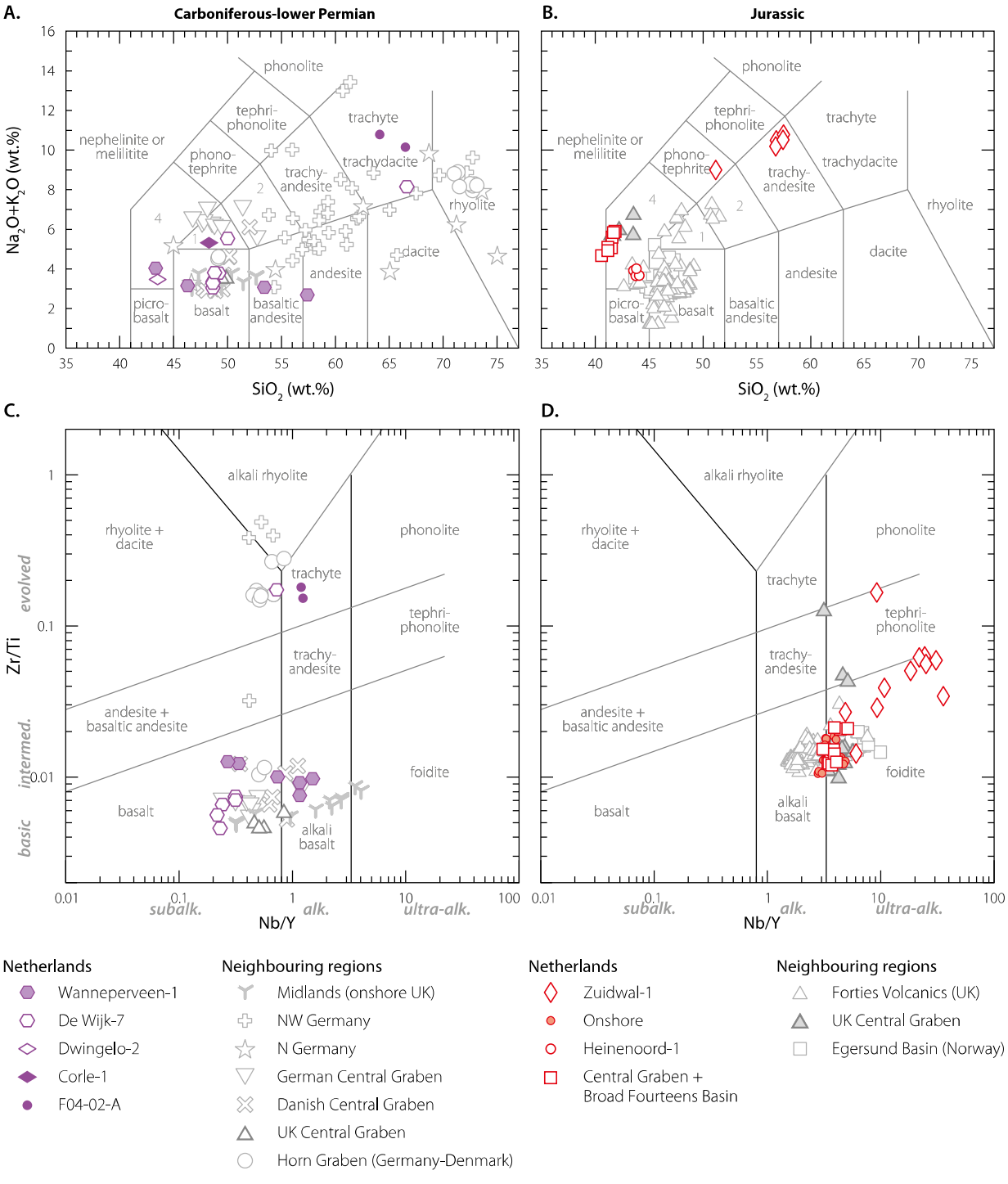

Figure 11.18. *Major and trace-element classification diagrams showing Carboniferous-lower Permian and Jurassic igneous rocks from Dutch exploration wells onshore and offshore, in comparison to rocks from neighbouring regions in northwestern Europe. See Table 11.3 for data sources of the Dutch rocks. Data for neighbouring regions are from Latin (1990), Eckhardt (1979), Aghabawa (1993), Kirstein et al. (2006). (a) and (b) TAS classification diagrams (Le Maitre et al., 2002) for relatively fresh (LOI<6 wt.%) Carboniferous-lower Permian and Jurassic rocks, respectively; (c) and (d) Nb/Y-Zr/Ti classification diagrams (Pearce, 1996); note the subalkaline to mildly alkaline character and the bimodal distribution of the Carboniferous-lower Permian rocks and the (ultra-)alkaline signatures of the Jurassic rocks. 1 = trachybasalt, 2 = basaltic trachyandesite, 3 = tephrite or basanite.*

parison have been obtained from intrusive and extrusive rocks from mainland England and Scotland, the region around the Mid North Sea High, Denmark and offshore surroundings, northern Germany, the Kattegat area, the Oslo Graben and Scania in southern Sweden (Dixon et al., 1981; Latin, 1990; Aghabawa, 1993; Benek et al., 1996;

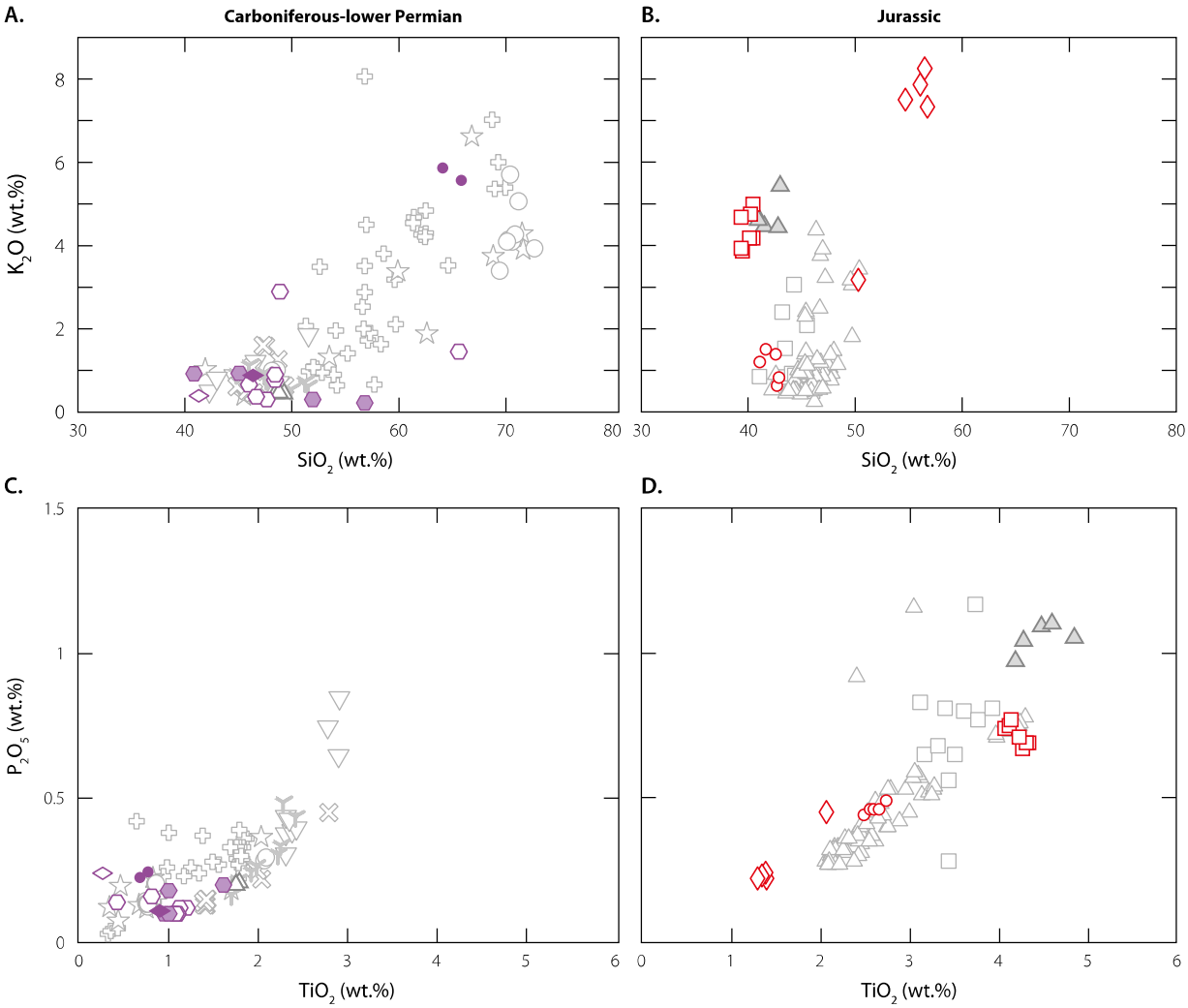

Figure 11.19. *Major and minor element variation diagrams showing compositional differences between Carboniferous-lower Permian and Jurassic igneous rocks from Dutch exploration wells onshore and offshore, in comparison with rocks from neighbouring regions in northwestern Europe: a) and b) SiO_2-K_2O diagram for Carboniferous-lower Permian and Jurassic rocks, respectively; c) and d) TiO_2-P_2O_5 diagrams illustrating variations of minor oxides relatively insensitive to the effects of secondary alteration. For legend and data sources, see Fig. 11.18.*

Heeremans et al., 2004; Obst et al., 2004; Kirstein et al., 2006). They are thus representative for the foreland of the Variscan orogeny.

Mafic rocks from different geographic locations in the North Sea area show significant compositional variation, while diversity in geochemical affinity may also be seen in lava flows, sills or dykes sampled in individual wells. The Central Graben area is illustrative, as most of the lavas are mildly alkaline trachybasalts-tephrites/basanites that are associated with subordinate amounts of subalkaline and highly alkaline basalts or transitional varieties. The ca. 299 Ma old samples from well 39/2-4 on the western flank of the UK Central Graben are an example of subalkaline (tholeiitic) basalts with low abundances of incompatible trace elements, including the light rare-earth elements (REE). They deviate from normal mid-ocean-ridge basalts (N-MORB) in being more enriched in light REE and more depleted in heavy REE (Heeremans et al., 2004).

Immobile-trace-element signatures confirm a 'within-plate' tectonic affinity for virtually all the Carboniferous-early Permian magmatic rocks in the Variscan foreland region (Fig. 11.21). Basalts in the northeast German Basin are an exception, as they show a wide diversity in tectonic discrimination diagrams (Benek et al., 1996).

The trachytic lava in F04-02-A (Fig. 11.1) is most likely the only 'Rotliegend' igneous rock analysed from the Dutch subsurface, since compositional data on rocks from the Emmen Volcanic Formation in onshore wells are lacking and the studied intrusions in the eastern part of the Netherlands presumably have a Carboniferous age. It is reasonable to assume that the igneous rocks of the Emmen Volcanic Formation are similar to (sub-)volcanics in

Table 11.3. *Geochemical compositions of igneous rocks in onshore and offshore wells in the Netherlands: a) Inventory of major and trace element compositions; b) Rare-earth-element concentrations. Source of data and analytical techniques applied: 1 = Latin (1990), major elements by XRF on glass disks, trace elements by XRF on pressed powder pellets, LOI represents weight loss after ignition at 1100°C, all XRF results reported on anhydrous basis, REEs determined by ICP-AES (results reported on hydrous basis); 2 = Helmers (1991, internal report), major elements by XRF on glass disks, trace elements by XRF (no further information); 3 = Eigenfeld & Eigenfeld-Mende (1986), analytical method not reported; 4 = this work (VU Amsterdam), major elements by XRF on glass disks, trace elements by XRF on pressed powder pellets, REEs determined by solution ICP-MS (Klaver et al., 2018), major element totals based on subtracted LOI. [1)] All Fe is expressed as FeO or Fe_2O_3, except when data for both oxides are given; n.a. = not available; <d.l. = below detection limit. Well names for Carboniferous samples from Latin (1990) are inferred from Aghabawa (1993); Latin (1990) listed these samples as 'Permian'. Sample codes and rock types taken from the references.*

Igneous episode	**LATE JURASSIC**												
Well name	**F10-01**							**K14-FA-103**			**L13-03**		
Depth (m)	n.a.	n.a.	n.a.	n.a.	n.a.	3451	3458	n.a.	n.a.	n.a.	n.a.	n.a.	n.a.
Sample code	**PL1/5**	**PL1/6**	**PL1/10**	**PL1/11**	**PL1/12**	**F10-6**	**F10-7**	**DL1**	**DL2**	**DL2A**	**001-1A**	**001-1B**	**001-1C**
Rock type	Lamprophyre	Lamprophyre	Lamprophyre	Lamprophyre	Lamprophyre	Foïdite	Foïdite	Hawaiite-Basanite(?)	Basanite(?)	Basanite(?)	?-	?-	?-
Reference	**1**	**1**	**1**	**1**	**1**	**4**	**4**	**1**	**1**	**1**	**1**	**1**	**1**
Major elements (wt.%)													
SiO_2	39.47	40.47	40.44	40.22	40.13	39.37	39.34	32.56	42.78	51.11	39.95	39.88	39.05
Al_2O_3	14.41	14.13	14.59	14.76	14.45	13.90	14.11	18.73	18.28	19.78	15.15	14.82	15.33
Fe_2O_3 [1)]	14.04	13.92	14.65	14.50	14.64	13.89	13.85	36.90	27.23	16.46	13.22	12.61	12.50
FeO [1)]	-	-	-	-	-	-	-	-	-	-	-	-	-
MgO	11.80	10.80	10.51	10.67	10.74	11.28	10.58	1.87	1.78	1.26	17.78	18.15	20.30
CaO	9.11	9.44	7.20	7.55	8.78	8.67	7.23	1.61	1.65	0.90	3.83	4.33	1.28
Na_2O	0.67	0.76	0.71	0.67	0.78	0.77	0.83	0.34	0.49	0.43	1.09	1.16	0.65
K_2O	3.87	4.18	4.99	4.75	4.18	3.93	4.68	0.38	1.27	2.28	2.60	2.73	3.26
TiO_2	4.33	4.26	4.06	4.11	4.30	4.22	4.13	3.49	3.48	3.64	3.80	3.69	3.93
MnO	0.28	0.27	0.24	0.24	0.24	0.28	0.22	1.35	0.96	0.64	0.12	0.12	0.12
P_2O_5	0.69	0.67	0.74	0.75	0.69	0.71	0.77	0.87	0.87	1.36	0.79	1.00	1.61
TOTAL	98.66	98.89	98.12	98.22	98.93	97.02	95.74	98.10	98.79	97.85	98.34	98.50	98.01
LOI	3.7	3.4	4.2	3.9	3.2	3.75	4.05	20.4	16.8	7.8	8.5	8.8	9.1
H_2O^+	-	-	-	-	-	-	-	-	-	-	-	-	-
CO_2	-	-	-	-	-	-	-	-	-	-	-	-	-
Trace elements (ppm)													
Ni	43	44	34	39	46	38	31	39	56	36	139	138	123
Cr	27	23	19	22	32	24	17	270	264	252	378	361	379
V	484	476	459	461	501	411	387	398	346	267	397	381	392
Sc	35	34	26	24	36	37	32	22	17	9	35	32	34
Cu	52	66	90	81	69	84	55	9	7	8	20	18	24
Zn	119	112	80	114	94	117	80	47	23	10	84	79	39
Sr	651	796	1174	895	883	613	880	1432	1180	6114	589	577	156
Rb	62	57	61	68	63	60	63	19	54	84	25	26	56
Zr	325	320	321	323	318	303	312	434	443	456	345	338	335
Nb	98	96	103	102	94	95	103	154	156	164	115	111	117
Ba	530	614	814	808	760	443	669	142	265	387	724	685	845
Pb	5	3	4	4	2	1.7	1.3	3	7	1	12	21	426
Th	7	6	5	7	6	13	15	6	11	-	8	8	15
La	87	81	81	83	67	102	101	117	108	333	113	99	96
Ce	177	176	182	173	160	154	162	217	198	674	201	180	160
Nd	67	71	69	70	67	67	69	76	65	260	76	69	55
Y	28	28	27	28	27	26	25	35	40	32	30	36	30

Table 11.3 a) Continued

LATE JURASSIC																			
Zuidwal-1 (ZDW-01)										ZDW-A1	Loon-op-Zand-1 (LOZ-01)								
n.a.	n.a.	n.a.	n.a.	n.a.	n.a.	n.a.	n.a.	1958	2180	1950	n.a.	n.a.	n.a.	n.a.	n.a.	n.a.	n.a.	2590	2590
ZU1	ZU2	ZU3	ZU4	ZU5	ZU6	ZU7	ZU8	ZDW-2	ZDW-4	ZDW-5	NAM 2/2	NAM 2/3	NAM 2/7	NAM 2/8	DL3	DL4	DL5	LOZ-11	LOZ-12
Phonolite	Phonolite	Phonolite	Phonolite	Phonolite-Basanite	Phonolite	Lamprophyre(?)	Lamprophyre(?)	Trachyandesite	Altered andesite	Trachyte	Basanite	Basanite	Basanite	Basanite	Basanite	Basanite	Basanite	Altered basaltic andesite	Altered basaltic andesite
1	1	1	1	1	1	1	1	4	4	4	1	1	1	1	1	1	1	4	4
52.78	56.08	56.50	56.74	50.30	55.75	28.51	28.75	54.69	55.95	44.10	39.04	40.71	40.60	35.43	38.05	37.42	43.44	37.44	36.31
26.71	25.45	25.56	24.33	17.71	18.94	15.73	16.76	23.85	13.41	22.02	17.13	18.14	18.32	16.34	16.35	17.16	18.68	16.03	16.27
7.77	4.39	4.77	4.49	8.38	4.14	18.02	17.54	4.20	7.72	10.53	12.40	12.58	13.26	14.18	12.14	14.18	14.06	12.56	12.23
-	-	-	-	-	-	-	-	-	-	-	-	-	-	-	-	-	-	-	-
0.67	0.66	0.80	0.78	4.78	5.72	9.61	9.74	0.90	5.57	1.08	6.05	6.16	6.60	7.18	6.41	7.03	7.74	6.26	5.81
0.65	0.63	0.62	0.62	6.43	1.69	16.37	16.49	0.46	3.65	1.51	15.29	12.36	11.75	17.24	17.36	14.34	9.27	10.24	10.75
1.14	2.49	1.89	3.31	5.67	4.99	0.62	0.41	2.51	1.32	0.75	1.70	2.19	1.70	1.40	1.73	1.57	1.83	1.81	1.59
7.14	7.86	8.25	7.33	3.17	7.28	3.69	3.84	7.50	4.30	5.81	0.93	0.75	0.77	0.74	0.71	0.68	0.81	0.75	0.71
1.52	1.39	1.38	1.34	2.06	0.33	3.15	3.15	1.29	1.28	1.89	3.61	3.94	4.04	3.48	3.48	3.62	3.91	3.31	3.56
0.37	0.02	0.03	0.02	0.17	0.12	0.49	0.47	0.03	0.12	0.55	0.20	0.17	0.16	0.22	0.21	0.18	0.12	0.14	0.15
0.27	0.22	0.24	0.23	0.45	0.03	0.37	0.41	0.22	0.24	0.42	0.96	1.01	1.02	0.88	0.89	0.92	1.00	0.87	0.92
99.03	99.18	100.04	99.18	99.14	99.00	96.56	97.56	95.65	93.56	88.66	97.30	98.02	98.21	97.10	97.32	97.11	100.88	89.41	88.30
8.5	5.0	4.7	4.7	4.0	6.0	21.5	21.4	4.92	6.35	10.80	14.6	13.0	12.5	15.4	15.4	13.0	9.8	10.86	12.22
-	-	-	-	-	-	-	-	-	-	-	-	-	-	-	-	-	-	-	-
-	-	-	-	-	-	-	-	-	-	-	-	-	-	-	-	-	-	-	-
21	50	44	59	40	39	267	254	50	112	34	142	147	148	188	181	181	151	161	119
4	3	5	4	9	120	1881	2098	5.8	313	50	274	303	303	271	294	302	312	211	238
157	218	203	200	135	238	480	484	166	159	236	377	406	421	363	375	396	439	290	341
-	-	-	-	-	13	30	28	0.4	18	5.4	27	36	37	35	29	31	38	34	38
802	11	294	12	143	5	182	446	11	14	26	53	56	55	46	49	54	58	47	56
137	145	175	164	137	92	213	200	165	131	841	112	79	85	103	64	119	79	94	74
2634	3086	2995	3043	2501	1992	650	377	2934	621	533	895	1027	930	826	949	852	823	704	727
201	176	191	165	150	64	170	176	167	161	186	27	20	21	19	20	19	24	23	21
459	522	511	450	423	329	282	287	457	206	440	293	316	323	265	293	291	311	249	256
331	319	307	302	464	157	63	63	302	83	248	113	116	117	99	103	109	109	98	96
1630	1982	1862	2162	3616	1469	3215	1488	2253	933	851	976	1013	1033	952	854	905	1064	871	727
11	12	12	12	4	9	3	4	12	14	64	9	6	6	8	3	5	4	4.0	2.8
26	21	20	18	13	15	-	-	41	15	36	6	6	7	3	5	5	8	13	14
90	72	64	93	137	109	59	34	131	77	236	94	88	89	88	89	94	92	102	93
180	152	135	175	190	178	62	53	160	99	304	177	166	181	190	168	180	157	141	145
53	43	32	42	30	45	20	19	44	38	95	74	60	57	72	64	70	57	53	57
18	13	14	12	13	17	18	19	10	17	23	33	27	27	31	30	31	24	20	20

Table 11.3 a) Continued

Igneous episode	LATE JURASSIC									
Well name	Andel-2 (AND-02)			Andel-4 (AND-04)		Heinenoord-1 (HEI-01)				
Depth (m)	n.a.	n.a.	1368	n.a.	n.a.	2236,5	2238,5	2237	2242	2249
Sample code	DL6	DL7	AND-19	DL8	DL9	HEI-1	HEI-1	HEI-16	HEI-17	HEI-18
Rock type	Alkali basalt-Basanite	Alkali basalt-Basanite	Trachy-basalt	Basanite	Basanite	Alkali basalt	Alkali basalt	Basanite	Basanite	Basanite
Reference	1	1	4	1	1	2	2	4	4	4
Major elements (wt.%)										
SiO_2	42.23	39.63	39.27	41.07	40.17	41.18	41.74	42.67	42.78	42.97
Al_2O_3	19.85	20.70	15.50	19.73	17.82	12.34	12.79	12.69	12.86	13.29
Fe_2O_3 [1])	13.64	14.34	11.17	12.01	14.15	10.84	11.00	11.17	11.36	11.32
FeO [1])	-	-	-	-	-	-	-	-	-	-
MgO	5.66	5.40	5.40	4.43	7.14	12.57	12.22	12.94	12.15	12.32
CaO	7.99	9.01	7.12	11.43	9.02	11.59	12.12	12.24	12.06	11.85
Na_2O	2.28	1.43	2.35	1.62	1.80	2.34	2.23	2.16	2.91	3.08
K_2O	2.38	2.45	2.11	1.70	1.71	1.18	1.48	1.36	0.61	0.81
TiO_2	3.61	3.74	2.84	4.77	4.28	2.48	2.55	2.59	2.65	2.73
MnO	0.21	0.23	0.17	0.18	0.17	0.17	0.17	0.17	0.18	0.17
P_2O_5	0.77	0.81	0.63	0.99	0.89	0.44	0.46	0.46	0.46	0.49
TOTAL	98.63	97.73	86.56	97.93	97.14	95.12	96.76	98.45	98.02	99.03
LOI	16.5	18.2	13.72	15.9	15.0	3.07	2.43	2.75	3.60	3.28
H_2O^+	-	-	-	-	-	-	-	-	-	-
CO_2	-	-	-	-	-	-	-	-	-	-
Trace elements (ppm)										
Ni	126	172	125	190	218	-	-	243	247	220
Cr	236	283	178	645	517	-	-	587	593	333
V	388	401	274	522	461	-	-	248	253	250
Sc	36	34	31	53	43	-	-	38	36	34
Cu	53	55	48	70	66	-	-	61	91	77
Zn	157	132	96	71	135	-	-	77	76	75
Sr	732	631	1165	1302	1430	1360	970	1595	692	722
Rb	56	52	51	51	44	30	40	39	11	13
Zr	383	395	273	524	447	150	160	161	170	170
Nb	110	115	83	135	120	-	-	56	57	60
Ba	587	702	621	1058	943	-	-	592	573	698
Pb	8	11	0.5	5	4	<10	<10	<d.l.	0.7	0.9
Th	9	9	16	7	5	<10	15	15	10	10
La	96	109	86	110	95	-	-	62	60	62
Ce	177	193	142	214	184	-	-	93	89	93
Nd	68	75	61	82	76	-	-	39	39	40
Y	33	34	25	34	29	20	20	20	19	19

Table 11.3 a) Continued

CARBONIFEROUS – EARLY PERMIAN																				
F04-02-A		**Wanneperveen-1 (WAV-01)**									**De Wijk-7 (WYK-07)**								**Dwingelo-2 (DWL-02)**	**Corle-1 (COR-01)**	**Hupsel (GEL-03)**
4650	4654	2070	2015	2030-2070	2030-2070	2030-2070	2030-2070	2030-2070	2030-2070	2690	2440-2460	2440-2460	2440-2460	2440-2460	2440-2460	2445	2464	3797	970	1320
F04-8	**F04-9**	**WAV**	**WAV**	**NAM 1/1**	**NAM 1/4**	**NAM 1/13**	**NAM 1/17**	**NAM 1/19**	**NAM 1/21**	**WYK-7**	**NAM 3/1**	**NAM 3/4**	**NAM 3/8**	**NAM 3/12**	**NAM 3/11**	**WYK-14**	**WYK-15**	**DWL**	**COR**	**GEL-3**
Trachyte	Trachyte	Olivine gabbro	Gabbro	Dolerite	Dolerite	Dolerite	Picritic dolerite	Picritic dolerite	Picritic dolerite	Olivine gabbro	Dolerite	Dolerite	Dolerite	Dolerite	Dolerite (Syenite)	Olivine gabbro	Olivine gabbro	Olivine gabbro	Gabbro/ melaphyre	Leucophyre
4	**4**	**3**	**3**	**1**	**1**	**1**	**1**	**1**	**1**	**3**	**1**	**1**	**1**	**1**	**1**	**4**	**4**	**3**	**3**	**3**
64.17	65.92	40.87	45.15	51.94	56.82	45.82	45.08	44.15	43.86	45.99	47.95	47.66	48.88	48.44	65.60	46.67	48.44	41.32	46.38	37.61
16.67	15.58	10.45	16.23	17.42	17.00	16.92	12.66	11.67	11.06	16.14	16.51	16.21	15.97	16.25	14.35	15.62	16.33	11.07	15.44	18.95
7.09	6.24	7.21	3.79	8.35	7.94	12.97	13.61	14.58	15.22	4.81	12.07	12.25	11.44	11.90	4.39	11.83	11.95	3.70	4.69	3.82
-	-	9.11	7.84	-	-	-	-	-	-	6.52	-	-	-	-	-	-	-	8.79	8.03	9.69
0.29	0.27	15.31	8.25	6.74	6.15	9.76	16.22	18.51	19.00	8.11	7.48	7.02	8.64	8.62	2.02	7.75	8.47	19.88	7.38	4.22
0.67	0.69	7.12	3.99	9.44	8.06	6.45	6.15	5.31	5.07	9.70	11.51	11.71	6.92	9.36	3.44	10.81	10.08	6.78	8.49	5.29
4.90	4.46	2.88	5.29	2.68	2.44	3.95	2.14	2.17	1.80	2.51	2.63	2.68	2.52	2.96	6.57	2.78	2.88	2.90	4.23	2.69
5.84	5.54	0.92	1.88	0.30	0.22	0.90	0.93	0.65	0.65	0.66	0.28	0.30	2.89	0.77	1.45	0.37	0.90	0.39	0.88	0.38
0.78	0.69	1.00	0.49	1.00	0.95	2.24	1.61	1.65	1.53	0.42	0.94	1.12	1.20	1.08	0.81	1.06	1.10	0.26	0.90	0.24
0.02	0.04	trace		0.12	0.10	0.18	0.14	0.15	0.15		0.14	0.16	0.33	0.18	0.10	0.16	0.20	-	-	-
0.24	0.22	0.18	0.19	0.10	0.10	0.34	0.20	0.22	0.23	0.14	0.08	0.12	0.12	0.10	0.16	0.10	0.10	0.24	0.11	0.08
100.67	99.65	95.05	93.1	98.10	99.78	99.52	98.76	99.06	98.57	95.00	99.59	99.23	98.92	99.67	98.89	97.15	100.45	95.33	96.53	82.97
1.35	1.49			3.9	3.7	8.3	4.6	5.6	6.0		5.5	3.4	3.1	2.4	1.9	2.97	2.22	-	-	-
-	-	2.77	2.94	-	-	-	-	-	-	2.31	-	-	-	-	-	-	-	3.00	2.02	13.03
-	-	1.80	2.77	-	-	-	-	-	-	0.94	-	-	-	-	-	-	-	1.56	0.70	3.90
6.4	6.2	-	-	102	90	101	430	548	682	-	136	121	103	136	9	123	128	-	-	-
2.7	3	-	-	344	334	228	611	675	804	-	309	267	209	264	0	220	216	-	-	-
17	9.4	-	-	287	292	345	263	266	232	-	264	293	298	261	36	230	221	-	-	-
13	9.8	-	-	38	43	33	22	20	13	-	34	35	30	27	10	29	28	-	-	-
4.4	6.8	-	-	-	-	-	-	-	-	-	-	-	-	-	-	111	124	-	-	-
20	28	-	-	-	-	-	-	-	-	-	-	-	-	-	-	75	71	-	-	-
78	61	-	-	210	211	333	305	294	239	-	152	150	164	173	134	137	179	-	-	-
185	175	-	-	8	6	27	32	21	22	-	7	7	30	16	25	9.3	17	-	-	-
434	432	-	-	97	94	189	133	114	121	-	59	76	82	71	501	60	54	-	-	-
46	41	-	-	7	6	17	20	15	15	-	5	7	7	7	36	4.4	4.3	-	-	-
496	517	-	-	121	74	240	287	209	279	-	296	156	805	159	192	328	308	-	-	-
5.0	3.8	-	-	-	-	-	-	-	-	-	-	-	-	-	-	1.6	1.1	-	-	-
15	14	-	-	-	-	-	-	-	-	-	-	-	-	-	-	2.5	2.5	-	-	-
60	56	-	-	0	0	10	8	10	9	-	4	6	14	4	39	10	11	-	-	-
102	84	-	-	26	28	44	36	32	26	-	10	21	19	17	82	12	8.8	-	-	-
52	46	-	-	12	11	28	15	15	11	-	10	8	10	11	37	9.0	8.1	-	-	-
51	47	-	-	20	20	28	20	18	18	-	18	21	21	21	60	17	16	-	-	-

Table 11.3 b) Rare-earth-element concentrations in igneous rocks from offshore and onshore wells in the Netherlands

Igneous episode	LATE JURASSIC											CARBONIFEROUS – EARLY PERMIAN				
Well name	F10-01				Zuidwal-1 (ZDW-01)		Loon-op-Zand-1 (LOZ-01)		Andel-2 (AND-02)	Heinenoord-1 (HEI-01)		F04-02-A	Wanneperveen-1 (WAV-01)	De Wijk-7 (WYK-07)		
Depth (m)	n.a.	n.a.	3451	3458	n.a.	2180	n.a.	2590	1368	2237	2249	4654	2030-2070	2440-2460	2445	2464
Sample code	PL1/6	PL1/10	F10-6	F10-7	ZU5	ZDW-4	NAM2/8	LOZ-12	AND-19	HEI-16	HEI-18	F04-9	NAM1/1	NAM3/8	WYK-14	WYK-15
Rock type	Lamprophyre	Lamprophyre	Foidite	Foidite	Phonolite-Basanite	Altered andesite	Basanite	Altered basaltic andesite	Trachy-basalt	Basanite	Basanite	Trachyte	Dolerite	Dolerite	Olivine gabbro	Olivine gabbro
Reference	1	1	4	4	1	4	1	4	4	4	4	4	1	1	4	4
La	78	82	78	83	93	69	59	77	84	46	48	30	10	5.3	8.6	7.9
Ce	159	157	159	168	159	113	121	143	161	88	93	71	23	13	19	18
Pr	18	16	18	19	16	11	14	15	18	10	11	9.0	2.8	1.9	2.6	2.4
Nd	70	63	69	71	50	39	51	54	66	40	41	37	13	10	12	11
Sm	11	10	12	12	7.7	6.1	8.5	8.7	11	7.3	7.6	8.3	2.5	2.1	3.1	2.9
Eu	3.3	3.0	3.5	3.4	2.2	1.7	2.4	2.6	3.4	2.3	2.4	2.1	0.82	0.84	1.1	1.1
Tb	-	-	1.3	1.3	-	0.70	-	0.97	1.4	0.91	0.94	1.3	-	-	0.68	0.61
Gd	9.1	8.4	9.3	9.0	5.6	4.9	6.7	6.8	9.3	6.4	6.5	8.2	3.0	3.1	3.9	3.7
Dy	6.4	6.2	6.4	6.3	4.4	3.8	5.4	5.0	7.0	4.8	4.9	7.6	3.6	3.5	4.3	3.9
Ho	1.1	1.1	1.1	1.1	0.69	0.72	0.86	0.88	1.3	0.86	0.88	1.6	0.66	0.64	0.91	0.83
Er	2.9	2.7	2.7	2.8	1.5	2.0	2.1	2.2	3.3	2.1	2.2	4.6	1.9	1.8	2.6	2.3
Tm	-	-	0.37	0.38	-	0.30	-	0.29	0.44	0.29	0.29	0.72	-	-	0.38	0.34
Yb	2.1	2.1	2.2	2.3	1.5	1.9	1.78	1.8	2.7	1.7	1.8	4.7	1.9	1.8	2.4	2.1
Lu	0.31	0.30	0.31	0.32	0.21	0.29	0.25	0.25	0.39	0.24	0.25	0.71	0.28	0.26	0.35	0.31

the nearby northwest German Ems-Weser area, where a large number of 'spilitized diabases' show a dominance of intermediate compositions and a wide range between basaltic and rhyolitic rock types (Eckhardt, 1968, 1979). The least altered rocks define a continuous subalkaline to mildly alkaline series between basaltic and rhyolitic compositions, comparable to those of lower Rotliegend volcanics from other locations in northern Germany (Benek et al., 1996).

Overall, the Dutch occurrences fit into the general characteristics of Carboniferous-lower Permian igneous rocks of northwestern Europe, which are marked by a dominance of mafic compositions locally showing a bimodal distribution with felsic rocks, variable alkali contents ranging from subalkaline (tholeiitic) to highly alkaline, subtle variations in incompatible trace-element contents and a prominent within-plate signature. The geochemical signatures are consistent with derivation of relatively small magma volumes from variable low degrees of partial melting of heterogeneous mantle sources in local independent systems, whereas crystal fractionation and contamination/melting of crustal components may have further added to the compositional diversity (e.g. Aghabawa, 1993; Benek et al., 1996; Heeremans et al., 2004; Neumann et al., 2004; Obst et al., 2004; Kirstein et al., 2006).

Late Jurassic

In comparison to those of other periods, Late Jurassic igneous rocks are geochemically well documented. Major and trace-element compositions have been reported on multiple samples from offshore wells F10-01 (sample PL-1), K14-FA-103, L13-03, Zuidwal-1, and from onshore wells Loon-op-Zand-1, Andel-2, Andel-4 and Heinenoord-1 (Dixon et al., 1981; Eigenfeld & Eigenfeld-Mende, 1986; Latin, 1990; Helmers, 1991; this work). Taking the effects of alteration into account, all of these rocks are silica-undersaturated and are marked by high contents of alkalis. With the exception of the samples from the Zuidwal volcano, which represent more evolved members of an ultrapotassic suite, they are relatively mafic. The least altered rocks (LOI <5 wt.%) of Heinenoord-1 (West Netherlands Basin) and F10-01 (Rim Dutch Central Graben) illustrate the compositional diversity of the late Jurassic mantle-derived magmas. The analysed samples from both locations plot in the tephrite-basanite field of the TAS classification diagram (Fig. 11.18b), but the Heinenoord-1 rock is more sodic (nephelinitic) and has a higher Na_2O/K_2O ratio, higher CaO and lower TiO_2 and P_2O_5 contents than F10-01, which has an ultrapotassic affinity. Mafic samples from the other locations may well represent magmas with similar compositions but strong alteration likely

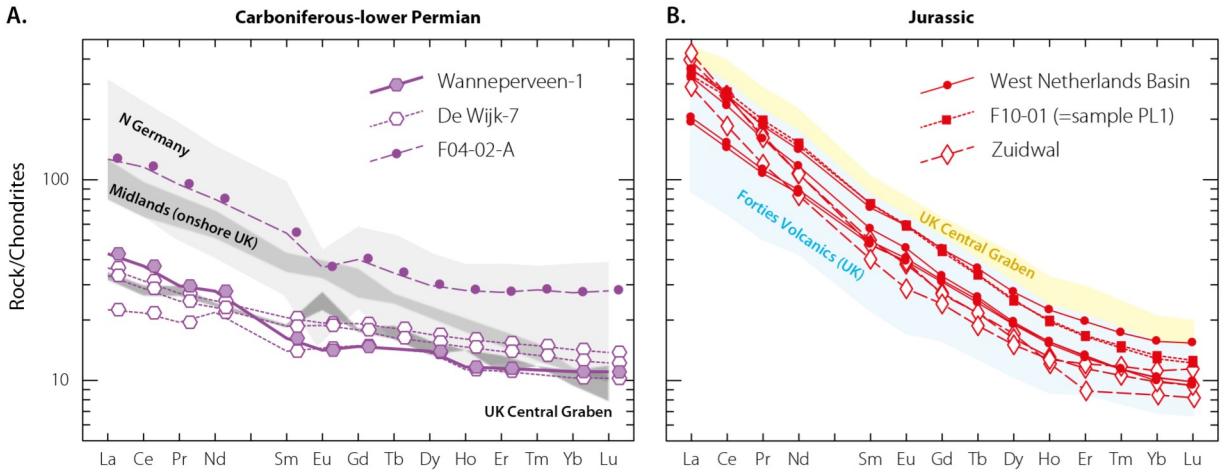

Figure 11.20. *Chondrite-normalized REE patterns for Carboniferous-lower Permian (a) and Jurassic(b) igneous rocks from Dutch exploration wells (data in Table 11.3b) in comparison with those for rocks from neighbouring regions in northwestern Europe. All Dutch rocks are basaltic except for the trachytic F04-02-A sample. Note the relative flat trends of the subalkaline-alkaline Carboniferous-lower Permian rocks and steep parallel trends of the ultra-alkaline Jurassic rocks. Data sources as in Fig. 11.18.*

affects the accuracy of their TAS classification. In the Nb/Y vs Zr/Ti diagram (Fig. 11.18d), all of the mafic rocks plot near the foidite-alkali basalt boundary whereas the Zuidwal rock series trends towards the tephri-phonolite field.

The geochemical compositions of the Dutch onshore and offshore occurrences mirror the differences between the subalkaline-alkaline, predominantly mafic rocks of the Forties Volcanics (or Rattray Volcanics) at the triple junction of the North Sea continental rift system (Gibb & Kanaris-Sotiriou, 1976; Woodhall & Knox, 1979; Dixon et al., 1981; Fall et al., 1982; Ritchie et al., 1988; Latin, 1990; Latin et al., 1990a; Latin & Waters, 1992; Quirie et al., 2019, 2020), and the more alkaline mafic centres in the west Central Graben (Latin, 1990; Latin et al., 1990a; Latin & Waters, 1992) (Fig. 11.13). Typically, the Central Graben tephrites-basanites are most enriched in alkalis and incompatible minor and trace elements (e.g. TiO_2, P_2O_5, Nb, Zr, REE) and contain lower amounts of Cr and Ni, which compares well with the ultrapotassic signature of F10-01 and the Zuidwal volcano. The nephelinitic alkali-basaltic rock of Heinenoord-1 has a closer affinity with the relatively alkaline varieties of the Forties Volcanics.

This regional difference in geochemical affinity also appears in REE patterns. In all cases they show almost straight trends with no Eu anomalies and enrichment of light REEs over heavy REEs (Fig. 11.20b), but the LREE/HREE ratios tend to be higher in the Central Graben area (including F10-01) than in the Forties region and Heinenoord-1. Similar systematics in Zr/Nb and Ce/Y ratios (Fig. 11.21b) suggest that if a common mantle source is assumed (Latin et al., 1990b), the latter group was generated by a higher degree of partial melting. Immobile-trace-element signatures further confirm a 'within-plate' tectonic affinity for all of the mafic rocks in these regions, as is illustrated in the Nb/Y-Ti/Y tectonic discrimination diagram of Fig. 11.21).

Magmagenesis and rifting

The inventory of igneous rocks in the Dutch subsurface provides insight into the intimate link between magmagenesis and rifting that has existed throughout the post-Devonian geological evolution of the (proto) North Sea region. A returning point of discussion concerns the geodynamic forces that controlled the rifting processes and to what extent signals from associated magmatism discriminate between different options. Possible involvement of mantle plumes is a subject of ongoing debate for both the Carboniferous-early Permian and the Jurassic episodes. In this section, some key issues on the two main magmatic episodes are summarized and briefly explained in a northwest European context, with emphasis on a petrological/geochemical perspective. The Cenozoic rifting period will not be treated since Dutch territories only host airborne products from volcanic activity outside the country.

Rifts can be distinguished into two main groups based on models for their origin and evolution: 'passive' rifts, developed as a result of lithospheric extension driven by far-field stresses (e.g. McKenzie & Bickle, 1988), and 'active' rifts, originated from thermal upwelling of the asthenosphere (White & McKenzie, 1995). In either case, volcanism accompanying rifting in continental settings is marked by a sequence ideally comprising the initial production of minor amounts of alkaline magma with a lithospheric imprint, followed by more voluminous sub-

alkaline magmas predominantly derived from upwelling mantle rock as stretching and/or thinning of continental lithosphere provides room for asthenosphere to rise. This adiabatic melting of asthenospheric mantle occurs when the accompanying perturbation of the local geotherm advances in such a way that it intersects the mantle solidus (i.e. the melting point is reached at a given pressure) and partial melting starts. The composition of the melt that ultimately escapes from a solid residue is a function of the original chemical and mineral composition of the mantle source, depth and degree of partial melting.

In a scenario where continental rifting is actively driven by deep mantle processes, a plume of solid mantle rock rises diapirically to the surface since it has a lower density than surrounding mantle, being hotter and/or different in composition. Impingement of a plume head from below may heat up, uplift and erode the lithosphere, which eventually can lead to tensional failure and continental breakup (e.g. Courtillot et al., 1999). Melting of mantle rock may occur in the centre of the rising plume by adiabatic decompression at higher potential temperature and/or in adjacent domains through heat transfer when a plume head cannot pass a physical barrier and spreads out below it. If the amount of melt produced becomes large enough it may escape to the surface and produce voluminous basaltic volcanism.

Carboniferous-early Permian

Magmatic activity occurred throughout Carboniferous and early Permian times over a wide region of the Variscan foreland in northwest Europe (Figs 11.3 and 11.7). The basement is a heterogeneous blend of relatively small crustal domains with Neoarchean to Neoproterozoic ages and low to high-grade metamorphic Caledonian belts, presumably bounded by major zones of deep-reaching faults. Hence, intrinsic variations in lithospheric thicknesses, thermal histories and other local controls explain differences in timing and nature of magma-producing events observed in individual areas. Decompression-induced low-degree partial melting of predominantly asthenospheric mantle rock is thought to have accompanied lithospheric extension, thinning and basin formation (see below for details on this mechanism). Magmatism was mostly marked by within-plate geochemical signatures, but locally with more arc-type imprints.

Early Carboniferous

Early Carboniferous (Dinantian) extension-related magmatism and basin formation from Ireland to Poland was driven by geodynamic events such as closure of the Rhenohercynian Ocean, accretion of a magmatic arc and amalgamation of microcontinents. In Ireland and the UK, where early Carboniferous magmatism peaked in the Visean, intrusive and extrusive rocks are mildly alkaline-transitional in composition (e.g. Smedley, 1986; Timmerman, 2004; Upton et al., 2004). Widespread manifestations of Namurian-Westphalian magmatic activity in the UK, centred in the Midland Valley of Scotland, the English Midlands and Derbyshire, includes alkaline and subalkaline varieties as well (Timmerman, 2004).

Minor volumes of tholeiitic to alkaline basaltic Visean volcanic rocks and Namurian-Westphalian dolerite sills with a typical within-plate signature in Derbyshire are thought to represent products of low-degree melting in isolated pockets of a heterogeneous mantle magma. They managed to reach the surface along fractures in attenuated crust (Macdonald et al., 1984; Timmerman, 2004).

Late Carboniferous

A similar scenario is conceivable for the presumably (late) Carboniferous dolerites found in Dutch onshore wells (e.g. Wanneperveen-1, De Wijk-7). Their geochemical signature tends to be mostly subalkaline but does not provide a uniform assessment of the tectonic setting. Discrimination diagrams suggest a within-plate signature for some of the rocks and magma derivation from a mantle source with possibly a modest subduction-related ('volcanic-arc') chemical imprint for others (Fig. 11.21). This diversity hints at small-scale heterogeneity of mantle sources that may include an earlier (Devonian?) back-arc spreading domain, perhaps related to the northward subduction of Rheic ocean crust.

Latest Carboniferous – early Permian

A conspicuous feature of the latest Carboniferous-early Permian period of voluminous magmatism is that it started almost simultaneously in different provinces over an extensive region north of the Variscan front. Magmatism coincided with a period of wrench-related lithospheric deformation in response to a fundamental change in the regional stress field that affected western and central Europe at the end of the Variscan orogenic activity (Ziegler, 1990) and is generally associated with lithospheric stretching and rifting.

Dated volcanic and plutonic rocks from the Oslo Graben, Scania, the North Sea area, Scotland, northern England and the northeast German Basin show that magmatic activity peaked in a rather narrow time interval around ca. 300 Ma, while centres in the internal Variscides as far south as Iberia and Italy have comparable ages (Heeremans et al., 2004; Neumann et al., 2004; Timmerman, 2004; Wilson et al., 2004; and references in caption to Fig. 11.7).

Bulk-rock compositions, often showing a bimodal distribution, are much more diverse than in later periods. In particular, the large abundance of intermediate and acid

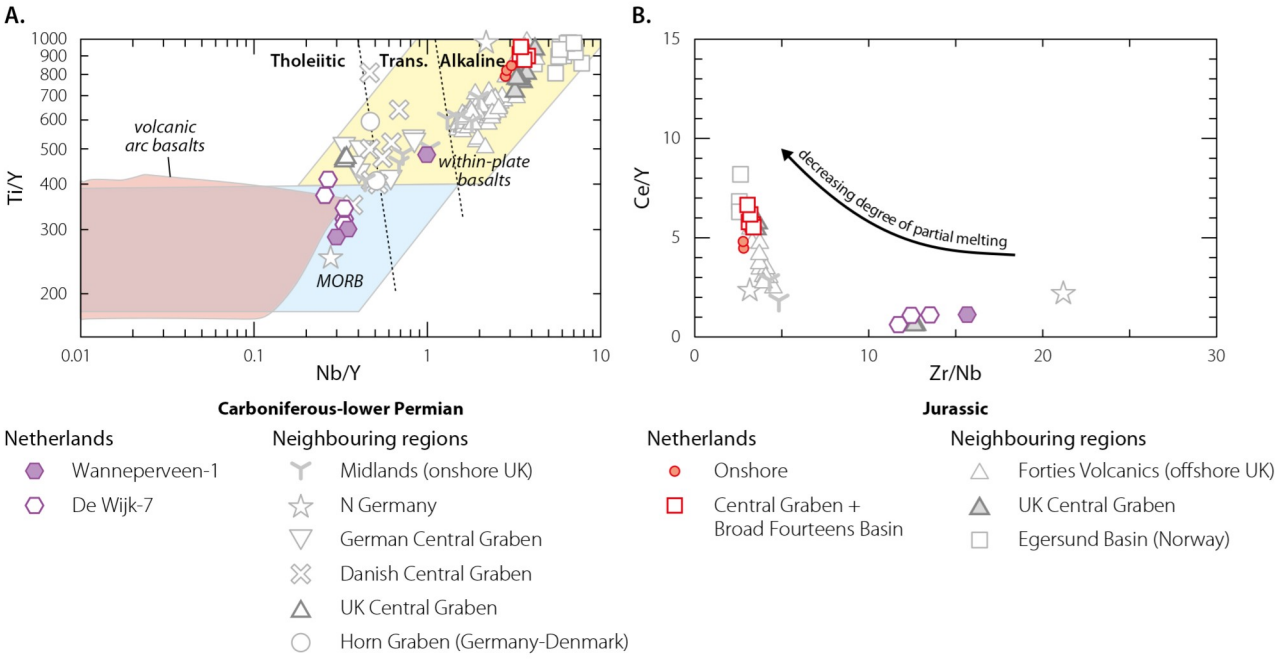

Figure 11.21. *Comparison of magmagenetic controls: a) Tectonic Nb/Y-Ti/Y discrimination diagram after Pearce (1982), illustrating an alkaline, within-plate signature of the Dutch Jurassic rocks and their difference with the transitional Carboniferous-lower Permian rocks, some of which trend towards the MORB or volcanic arc field; b) Zr/Nb vs. Ce/Y diagram for samples from Dutch onshore and offshore exploration wells, suggesting that the Jurassic mantle-derived magmas originated by lower degrees of melting than the Carboniferous-lower Permian magmas, assuming a reasonably similar source. Only relatively fresh samples (LOI<5 wt.%) of rocks with >5 wt.% MgO are shown. Data sources as in Fig. 11.18.*

varieties is noticeable. Although there tends to be a regional north-south trend from strongly alkaline in the Oslo Rift to mildly alkaline in the Variscan foredeep and calcalkaline in the Rhenohercynian orogenic belt (e.g. references in Ziegler, 1990), rock types vary widely both on regional and local scales. For example, basalts encompass the entire spectrum from highly alkaline to tholeiitic in the Oslo Graben (Neumann et al., 2004), while tholeiitic as well as alkali-rich basalts have also been found in North Sea wells (Heeremans et al., 2004).

'Rotliegend' volcanic rocks in Danish offshore and onshore wells and in surrounding areas are dominated by basaltic flows and pyroclastic ash flow deposits, while associated intermediate and acidic volcanic rocks are present in subordinate amounts (Aghabawa, 1993). There is a general tendency towards increasing alkalinity and degree of silica undersaturation from the Kattegat region in the east to the Central Graben in the west. The Horn Graben region is marked by a bimodal alkali/transitional basalt-rhyolite/rhyodacite suite. The trachytes from the Dutch Central Graben (well F04-02-A) fit in this scheme. Petrological modelling suggests that 'Rotliegend' basalts in the Danish North Sea and surroundings originate from variable-degree melting at different depths of a heterogeneous mantle or from separate mantle sources, including a depleted asthenospheric domain and an enriched lithospheric domain (Aghabawa, 1993).

Based on trace-element and isotopic signatures, Neumann et al. (2004) suggested that the main mantle source of magmatism in the Oslo Rift, Scania and possibly also the North Sea was similar to a Prevalent Mantle-type (PREMA) component residing in the lithospheric mantle. Melting was probably induced by local decompression and thinning of lithosphere in response to regional stretching north of the Variscan front, although the PREMA affinity implies that involvement of a mantle plume cannot be discarded.

Similar scenarios have been proposed for the northeast German Basin (e.g. Breitkreuz & Kennedy, 1999), where different structural domains and a heterogeneous basement added to geochemical diversity on a relatively small scale (Benek et al., 1996). Crustal thinning and block faulting facilitated the production of large volumes of intrusive and extrusive rocks. Magmas with a calcalkaline character could have been derived from a pre-existing subduction-influenced basaltic magma source (cf. Benek et al., 1996).

Locally, the thermal perturbation associated with Carboniferous-Permian magmatism may have been more pro-

nounced than in Jurassic times, as supported by the higher degrees of melting (~10%) inferred from trace-element signatures of the North Sea samples studied by Latin et al. (1990b). According to the data in Eckhardt (1979), particularly the Zr/Nb and Ce/Y ratios, a similar melting regime probably affected the Ems-Weser basalts in northwest Germany (and perhaps also the Dutch Permian volcanics) (Fig. 11.21b). A stronger thermal anomaly is also consistent with the widespread generation of the acidic magmas, which can be explained as the products of anatexis of the lower crust, possibly provoked by heat input from underplated basalt (Breitkreuz & Kennedy, 1999).

Ernst & Buchan (1997) noticed that the dyke swarms in the Oslo Rift, Scania, northeast England and Scotland radiate from a common triple junction in Denmark, which would localize the axis of a deep-mantle plume. From the large areal extent, volume, brevity of the activity interval and the convergent dyke swarms, Torsvik et al. (2008) connected the ~300 Ma igneous episode to that of a typical Large Igneous Province (LIP), sourced by a deep-sourced mantle plume below the Skagerrak. They proposed that mantle-derived basaltic magma originated at this centre and propagated over some 1000 km to Scotland and Northern England, where it formed the voluminous dike swarms and sills of the Midland Valley Rift, the Great Whin Sill and surrounding areas.

However, geochemical and tectonic evidence for a plume model is weak. In a geochemical study on dyke and sill intrusions across northern Europe, Kirstein et al. (2006) discussed a relationship between the depth of melting and lithosphere thickness, which strongly varies between the different areas and is difficult to reconcile with a region-wide plume control. Furthermore, radiogenic-isotope and trace-element signatures are not inconsistent with lithospheric mantle as a major source of the basaltic magma prior to decompression melting of the underlying asthenosphere, which would also be more in line with a local lithospheric extension rather than a single major plume as principal control (e.g. Neumann et al., 2004). Kirstein et al. (2006) suggested that the apparent dyke orientation is a relic of larger tectonic features (emplaced sub-parallel to the Caledonian trend, terrane boundaries in the Pre-Cambrian basement, or coeval extensional structures), and concluded that there is no evidence for a thermally anomalous mantle plume during Carboniferous-Permian magmatism in northern Europe.

Late Jurassic

The relation between late Jurassic magmatism and rifting in the Netherlands is best illustrated in conjunction with the igneous manifestations in other parts of the North Sea Basin (Fig. 11.13). Variations in timing, location, volume and composition allow the construction of a coherent magmagenetic framework for the entire region (Latin et al., 1990a, b; Latin & Waters, 1992). The Forties basaltic province (or Rattray Volcanic Province), situated at the triple junction between the Viking Graben, Central Graben and Moray Firth rift basins, can be seen as the focal point of the magmatic activity within the main rift system. Two phases of activity, possibly in a series of fissure eruptions from linear vents, produced an up to 1.5 km thick succession of subaerial basaltic lavas and hyaloclastites in a terrestrial-lacustrine environment over an area of ca. 7400 km², and ended with a minor intrusive suite (Quirie et al., 2019, 2020).

The occurrences in the Dutch Central Graben and Egersund Basin are much less voluminous, are located on the flanks of the main rift system or in minor sub-basins and are more silica-undersaturated and alkaline (ultrapotassic of nephelinitic) than the Forties basalts. All of these magmas were produced during the syn-rift phase of basin development, but none were derived from an asthenospheric mantle source similar to that producing mid-ocean-ridge basalts. Instead, the mantle sources were variably enriched in incompatible elements and have often been referred to as OIB-type (Oceanic Island Basalt) or E-MORB-type (Enriched Mid Ocean Rich Basalt) mantle without, however, necessarily implying a similar setting. The Forties basalts (mildly alkaline and mildly silica-undersaturated) represent the largest-degree melts of the entire sedimentary rock succession in the North Sea Basin. They did originate from asthenospheric mantle, but their trace-element and isotope signatures indicate that an enriched component is involved as well, either as heterogeneities in the asthenosphere or in the form of mixed-in lithospheric melt. The other magmas (highly alkaline and strongly silica-undersaturated), including those of the Netherlands, must have formed by lower-degree melting of a volatile- and incompatible-trace-element-enriched region of the mantle, which had remained isolated from the asthenosphere for hundreds of millions of years. Therefore, these magmas originated in a separate source, of which continental lithosphere is the most plausible domain (Latin & Waters, 1992).

The Zuidwal volcano likely represents a case of extension-driven melt generation in the continental lithosphere, as is illustrated in the generalized model of Fig. 11.11d, e (cf. Herngreen et al., 1991), wherein a schematic cross section of the magma system and a hypothetical P-T diagram visualize the potential controls. Given the small size of the Vlieland pull-apart basin, it is improbable that decompression was sufficient to cause melting of dry asthenosphere. Therefore, a more realistic scenario is that magma formed mainly at the base of the lithosphere, which must have been enriched in volatiles (H_2O and

CO_2) and incompatible elements in order to shift its solidus to sufficiently lower temperature for melting to occur. The nature and timing of this enrichment are unknown but may be related to an older melt-infiltration event on a regional scale. Localized stretching of the lithosphere, controlling the development of this basin, may have led to uplift of the asthenosphere-lithosphere boundary to a point where the geotherm crossed the solidus. The inferred limited degree of melting would be in line with the small size of the basin. The evolved compositions of the Zuidwal volcanics (Fig. 11.18b) and indications for a caldera structure (Perrot & Van der Poel, 1987) suggest that mantle-derived melt accumulated and fractionated in a crustal magma reservoir at relatively shallow depth before and during the period of eruptive activity.

Magmagenetic interpretations are consistent with the rift setting. The Forties basalts (Fig. 11.13) occur in a region that experienced the maximum lithospheric stretching at the rift triple junction. Major zones of weakness in the lithosphere may have further facilitated their rise to the surface. This would explain the only scattered volcanic occurrences in the adjacent Viking and North Sea Central grabens, where the degree of extension was slightly smaller. It is conceivable that asthenospheric melts were produced here as well, but that these solidified at depth and were not able to reach the surface. Melt generation in the Netherlands and on the flanks of the Central Graben, where the amount of stretching was much smaller, may have been facilitated by special conditions connected to the intersection of the graben with pre-existing and long-lived stable highs such as the Texel-IJsselmeer High and the Mid North Sea High (Fig. 11.13). At these locations, enriched continental lithosphere could have been partially molten in contact with small amounts of asthenospheric melts to create magma batches sufficiently voluminous to reach the surface.

Stratigraphic information from well data (e.g., detection of unconformities, absence of syn-rift sediments, erosion of pre-rift sediments), has been used to argue for a regional thermally driven doming event in Jurassic times, with the Forties basaltic province as focal point (Ziegler, 1990; Underhill & Partington, 1993). If valid for Zuidwal and the other Jurassic alkaline occurrences of the Netherlands, such a scenario would imply that localized low-degree partial melts originated in response to this regional heat pulse and/or uplift, and that ascent to shallow crustal levels was facilitated by crustal-scale faulting.

A model of active rifting driven by impingement of a mantle plume predicts that doming will be followed by volcanism and subsequent or simultaneous rift formation (e.g. Courtillot et al., 1999). Based on chronostratigraphic data and assuming a middle Jurassic age for North Sea volcanism, it has been contended that the sequence of events follows this scheme and supports a scenario of doming and deflation of a transient, warm plume head or 'blob' (Underhill & Partington, 1993). However, from a detailed paleogeographic study in the area of the Forties basaltic province, Quirie et al. (2020) suggested that subsidence already started before the onset of volcanism. Also, the amount and areal extent of regional uplift associated with a plume control have been contested and, if radiometric ages are taken into account, there are other uncertainties as to the chronology of magmatism relative to the main phase of faulting (Latin, 1990).

The entire set of available radiometric ages might suggest a southward migration of magmatism from the Forties basaltic province towards the Netherlands in the course of time, possibly connected to propagation of the rift system in the same direction. It may also point to northwards motion of the European plate over a fixed hot-spot (Latin et al., 1990a,b), which would be consistent with a plume model. However, if only the most reliable $^{40}Ar/^{39}Ar$ age dates on fresh samples are considered (see Fig. 11.8), the apparent geographic systematics of a hot-spot trail disappears, as ages tend to cluster around 160-150 Ma in the igneous provinces from the Forties triple junction to the Netherlands (Latin, 1990). This crude absolute age bracket places the timing of North Sea magmatism in the late Jurassic instead of the middle Jurassic inferred from stratigraphic interpretations. Consequently, magmatic activity would not precede but largely coincide with the main phases of extension and subsidence, which seems to discard a key argument against the passive rifting model (cf. Latin, 1990).

Also, the observed volume of basalts produced at the triple junction is much lower than modelling of decompression melting of a hot mantle plume, rising beneath stretched and thinned lithosphere in a rift setting, predicts (White & Latin, 1993; White & McKenzie, 1995). Significant uncertainty, inherent to some of the assumptions and input parameters on which this modelling approach relies, makes outcomes not always conclusive. In particular, the amount of stretching and associated vertical movements in the North Sea area have been subject of considerable debate (White & Latin, 1993 and references therein). Finally, available Sr-Nd-Pb isotope data are not sufficiently diagnostic (see discussion in Latin, 1990). The isotope ratios point to a source that experienced time-integrated enrichment relative to MORB, but candidate mantle components could have been tapped from a deep mantle domain by a rising plume or could have resided in the subcontinental lithospheric mantle.

In summary, there is no compelling evidence from geochemical signatures, petrological constraints and radiometric age dating that Jurassic magmatism in the North

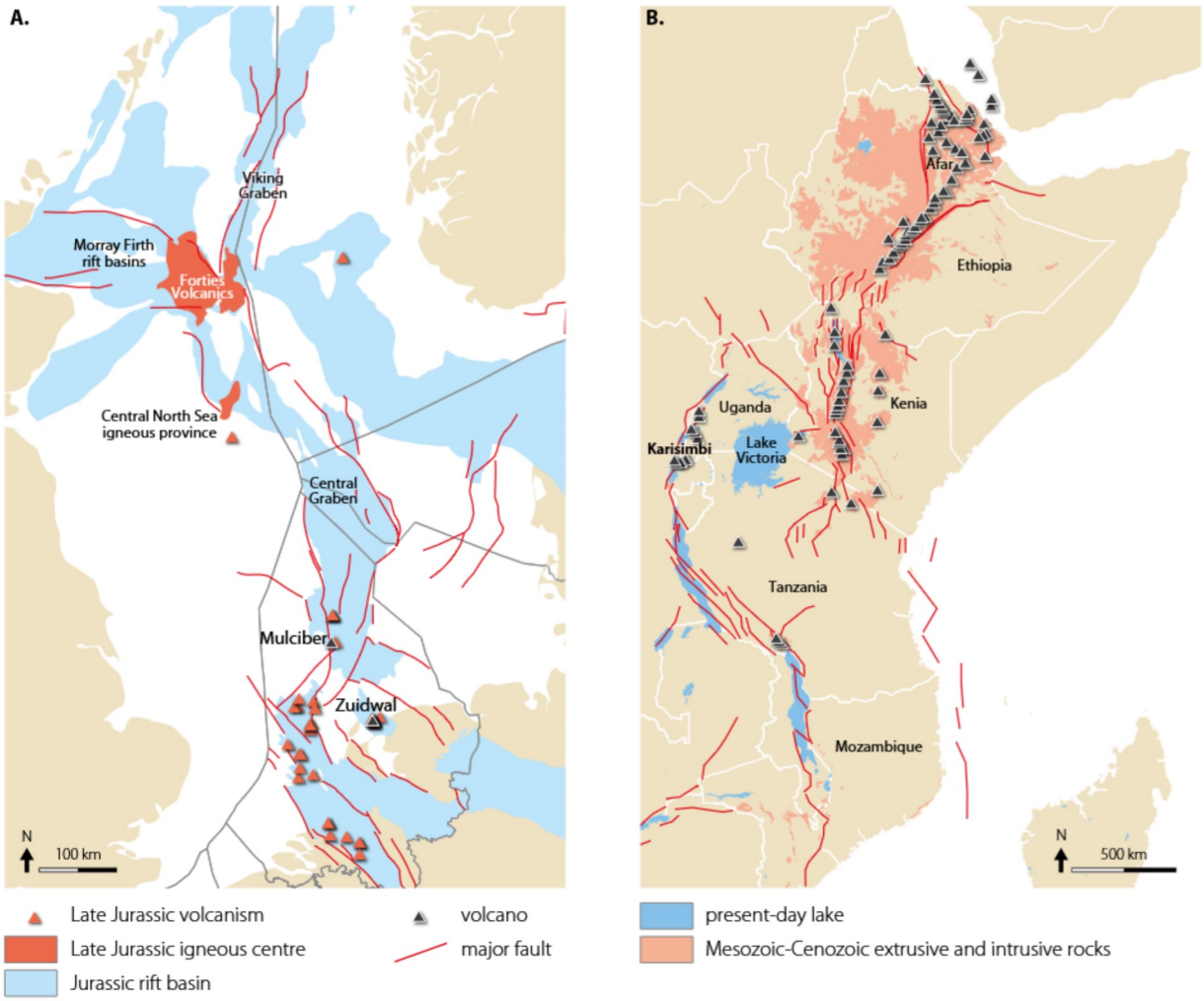

Figure 11.22. Linear distribution of known magmatic manifestations in the Jurassic of the North Sea Basin (a) compared with the chain of recently active volcanoes in the rift zone of East Africa (b). Note the difference in scale. Rift basins and faults in the North Sea region from Guterch et al. (2010), Kombrink et al. (2012) and Hopper et al. (2014). Faults, igneous rocks and volcanoes in the East African Rift Zone: Natural Environment Research Council, BGS Dataset ID: 13607585 and Global Volcanism Program (2023).

Sea region was controlled by the arrival of a major, deeply sourced mantle plume. A passive-rifting model adequately explains most of the observations, although minor effects from a modest, short-lived hot spot cannot be excluded, since the largest magma volume, degrees of partial melting and contributions of asthenospheric mantle material have all been inferred for the basalts in the triple-junction region. For the onshore and offshore subsurface occurrences in Dutch territory (Dutch Central Graben, Broad Fourteens Basin, West Netherlands Basin, Vlieland Basin), the subcontinental mantle lithosphere is the most likely source of the magmas. Melting can be explained in the context of passive stretching, thinning and rifting in the continental setting. If a distant mantle plume played a role in melt generation at all, it may only have acted as source of heat or as propagator of additional uplift.

Continental rifting and magmatism in East Africa: present-day analogue of the Jurassic North Sea region?

The magmatic manifestations from the Jurassic of the North Sea region show conspicuous similarities to those in the currently active rift zone of East Africa, both in distribution and in composition (Fig. 11.22). Parallels in fault patterns, volcanism and geological dimensions between the North Sea Graben system and the Kenyan-North Tanzanian segment of the East African Rift were already noticed by Dixon et al. (1981).

A row of (recently) active volcanoes in East Africa, all situated on continental basement, generally follow the branched rift structure from north to south. The northern termination in the Afar region and surrounding areas represents a triple junction (Fig. 11.22b) and can be seen as an evolution between continental rifting and sea floor

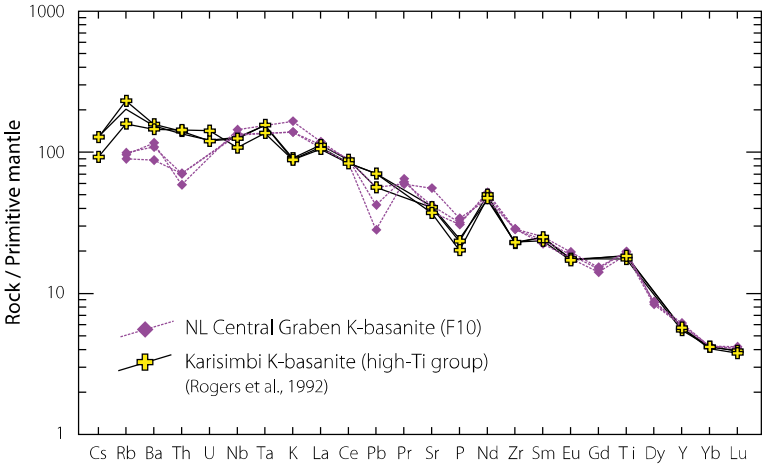

Figure 11.23. *Primordial-mantle normalized incompatible trace-element patterns illustrating similarity between the Jurassic alkaline rocks in Dutch onshore and offshore wells with Quaternary to Recent volcanics in the Virunga Volcanic Province and the Toro Ankole area, situated in the western arm of the East African Rift. Overlapping trends for K-basanites from the F10 well in the Dutch Central Graben (Table 11.3) and Karisimbi Volcano (Rogers et al., 1992) may indicate common petrogenetic controls.*

spreading in the Red Sea and Gulf of Aden. Magmatism in the East African Rift System (EARS) is generally marked by a systematic compositional evolution in space and time. While volcanics in a given sector tend to become less alkaline and more silica-saturated with time, there is also a gradual increase in alkalinity and silica under-saturation towards the south (Rooney, 2020 and references therein). This can be explained by differences in magma-contributing mantle sources: initial highly alkaline and silica-undersaturated magmas are derived from lithospheric subcontinental mantle, whereas continued lithospheric thinning ultimately allows melting of convecting upper mantle and the production of more silica-saturated, transitional to subalkaline magmas.

In this framework, the Forties volcanic field of the North Sea area, situated at the Moray Firth-Central North Sea Graben-Viking Graben triple junction (Fig. 11.22a) would have its counterpart in the Afar region. The tectonic setting, relatively high magma volumes and compositional affinity suggest a contribution from asthenospheric mantle. It is of interest to note that there is wide geochemical and geophysical support to regard magmatism in the Afar region (and possibly along the entire EARS) as a manifestation of mantle plume activity (e.g. Marty et al., 1996; Chang et al., 2020).

Quaternary to Recent volcanism of the Virunga Volcanic Province (Uganda-Rwanda-Congo border) in the western branch of the East African Rift system and the Toro Ankole Volcanic Province (west Uganda) produced alkali-rich rocks with compositions (Rogers et al., 1998; Pitcavage et al., 2021) very similar to the basanites, nephelinites and more evolved products of the Central Graben, Zuidwal and Dutch onshore occurrences, as is illustrated by incompatible trace-element patterns (Fig. 11.23). The parental magmas are thought to have originated from the subcontinental lithospheric mantle that had been variably modified by metasomatic agents and thus acquired a mineralogical composition that deviates substantially from common lherzolitic assemblages. Phlogopite is usually a prominent source component responsible for the (ultra) potassic nature of the volcanics. Results of melting experiments on phlogopite-clinopyroxenite rock (Lloyd et al., 1985) have shown that such a source can produce magma with compositions very close to those of the Central Graben (Latin, 1990). Also, metasomatically induced variability in the source mineralogy, inferred for the Ugandan rocks (Pitcavage et al., 2021), compares well with the compositional differences seen in the rocks from the Dutch wells on a similar spatial scale (e.g. Heinenoord-1, Zuidwal-1, F10-01). The volcanic setting of the western branch of the East African Rift system thus provides an attractive analogue for the manifestations of Jurassic volcanism in the Dutch subsurface. It is conceivable that Karisimbi or any other volcano in the Virunga area is a present-day equivalent of Zuidwal and Mulciber.

Concluding remarks

The igneous rocks encountered in ca. 100 wells in the Dutch subsurface represent a sequence of intermittent magmatic activity that fits well in the region-wide pattern of post-Caledonian melting events recorded in northwest Europe. There is no doubt about the relationship between magmatism and periods of extension and rifting since late Paleozoic times, but evidence for an accompanying role of mantle-plume activity as a driving force remains controversial, partly due to insufficient constraints from absolute age dating. This episodic magmatism in northwest Europe tends to be related to specific periods in the opening history of the North-East Atlantic Ocean (e.g. Woodhall & Knox, 1979; Ziegler, 1988). Since stretching, thinning and rifting did not lead to a full breakup and transition to seafloor spreading and MORB-type magmatism, the North

Sea region is a perfect example of a failed continental rift system (Ziegler, 1992).

The geographically widespread Carboniferous-Permian magmatism was voluminous and compositionally diverse, presumably because melting and assimilation of crustal components was promoted by the mobilization of large amounts of hot mantle-derived magma. In contrast, Jurassic magmatism was much less abundant, is predominantly basaltic in composition, and is typically confined to the Mesozoic rift system with the Forties (Rattray) triple junction as focal point. The preceding Triassic rifting was probably not accompanied by magmatic activity. The Cenozoic dyke swarms inferred to be present in the Southern North Sea are likely related to the final stages in the opening of the Northeast Atlantic.

Acknowledgements

We thank Neptune Energy (now ENI), Total Energies and NAM for supplying new data and photos. Pieter Vroon, Roel van Elsas, Bouke Lacet and Graham Hagen-Peter are thanked for their laboratory assistance at the VU Amsterdam. Kim Cohen of Utrecht University is thanked for data and feedback on Quaternary tephra distributions. David Latin helped us with interpreting sample codes in his PhD thesis, and Axel Gerdes shared details on the U-Pb age determination of the granite in well A17-01. Rixt Altenburg is thanked for mapping the distribution of igneous rocks of Mulciber in seismic data. We thank Johan ten Veen for a comprehensive review of an earlier draft of this chapter.

Digital map data

Spatial data of figures in this chapter for use in geographical information systems can be downloaded here: https://doi.org/10.5117/aup.28163870.

References

Á Horni, J., Hopper, J.R., Blischke, A., Geisler, W.H., Stewart, M., McDermott, K. & Árting, U., 2017. Regional distribution of volcanism within the North Atlantic Igneous Province. Geological Society, London, Special Publications 447(1): 105-125. DOI: 10.1144/SP447.18

Aghabawa, M.A., 1993. Petrology and geochemistry of the Rotliegendes Volcanic Rocks in Denmark and their tectonic implications. In: Stouge, S. & Vejbaek, O.V. (eds): Dynamisk/stratigrafisk analyse af Palaeozoikum i Denmark. EFP-89; Omrade 1: Olie og Naturgas 3, DGU Kunderapport. 351 pp.Andronikov, A.V., Van Hoesel, A., Andronikova, I.E. & Hoek, W.Z., 2016. Trace element distribution and implications in sediments across the allerød–younger dryas boundary in the Netherlands and Belgium. Geografiska Annaler: Series A, Physical Geography 98(4): 325-345. DOI: 10.1111/geoa.12140

Anonymous, 1992. Schichtenverzeichnis Balderhaar Z1. Preussag Erdöl und Erdgas GmbH, Provided by Landesamt für Bergbau, Energie und Geologie, LBEG (Hannover): 63 pp.

Autin, W.J., 2008. Stratigraphic analysis and paleoenvironmental implications of the Wijchen Member in the lower Rhine-Meuse Valley of the Netherlands. Netherlands Journal of Geosciences 87(4): 291-308. DOI: 10.1017/S0016774600023362

Benek, R., Kramer, W., McCann, T., Scheck, M., Negendank, J.F.W., Korich, D., Huebscher, H.D. & Bayer, U., 1996. Permo-Carboniferous magmatism of the Northeast German Basin. Tectonophysics 266(1-4): 379-404. DOI: 10.1016/S0040-1951(96)00199-0

Berendsen, H.J.A. & Stouthamer, E., 2001. Palaeogeographic development of the Rhine-Meuse delta, The Netherlands. Koninklijke van Gorcum B.V. (Assen): 268 pp.

Bischoff, A., Planke, S., Holford, S. & Nicol, A., 2021. Seismic Geomorphology, Architecture and Stratigraphy of Volcanoes Buried in Sedimentary Basins. In: Németh, K. (ed.): Updates in Volcanology - Transdisciplinary Nature of Volcano Science. IntechOpen: 1-34. DOI: 10.5772/intechopen.95282

Bless, M.J.M., Boonen, P., Bouckaert, J., Brauckmann, C., Conil, R., Dusar, M., Felder, P.J., Felder, W.M., Gökdag, H., Kockel, F., Laloux, M., Langguth, H.R., Van der Meer Mohr, C.G., Meessen, J.P.M.T., Op het Veld, F., Paproth, E., Pietzner, H., Plum, J., Poty, E., Scherp, A., Schulz, R., Streel, M., Thorez, J., Van Rooyen, P., Vanguestaine, M., Vieslet, J.L., Wiersma, D.J., Winkler Prins, C.F. & Wolf, M., 1981. Preliminary report on Lower Tertiary-Upper Cretaceous and Dinantian-Famennian rocks in the boreholes Heugem-1-1a and Kastanjelaan-2 (Maastricht, the Netherlands). Mededelingen Rijks Geologische Dienst 35(15): 333-415

Boenigk, W. & Frechen, M., 2006. The Pliocene and Quaternary fluvial archives of the Rhine System. Quaternary Science Reviews 25(5-6): 550-574. DOI: 10.1016/j.quascirev.2005.01.018

Bouroullec, R., Verreussel, R.M.C.H., Geel, C.R., De Bruin, G., Zijp, M.H.A.A., Kőrösi, D., Munsterman, D.K., Janssen, N.M.M. & Kerstholt-Boegehold, S.J., 2018. Tectonostratigraphy of a rift basin affected by salt tectonics: synrift Middle Jurassic-Lower Cretaceous Dutch Central Graben, Terschelling Basin and neighbouring platforms, Dutch offshore. Geological Society of London, Special Publications 469(1): 269-303. DOI: 10.1144/SP469.22

Bradshaw, M.J., 1975. Origin of montmorillonite bands in the Middle Jurassic of Eastern England. Earth and Planetary Science Letters 26(2): 245-252.

Bredewout, J.W., 1989. The character of the Erkelenz intrusive as derived from geophysical data. Geologie en Mijnbouw 68(4): 445-454.

Breitkreuz, C. & Kennedy, A., 1999. Magmatic flare-up at the

Carboniferous/Permian boundary in the NE German Basin revealed by SHRIMP zircon ages. Tectonophysics 302(3-4): 307-326.

Breitkreuz, C., Kennedy, A., Geissler, M., Ehling, B.-C., Kopp, J., Muszynski, A., Protas, A. & Stouge, S., 2007. Far Eastern Avalonia: its chronostratigraphic structure revealed by SHRIMP zircon ages from Upper Carboniferous to Lower Permian volcanic rocks (drill cores from Germany, Poland and Denmark). GSA Special Paper 423: 173-190.

Brown, G., Platt, N.H. & McGrandle, A., 1994. The geophysical expression of Tertiary dykes in the southern North Sea. First Break 12(3): 137-145.

Brugmans, S.J., 1784. Natuurkundige verhandeling over een zwavelagtigen nevel den 24 Juni 1783 in de provintie van Stad en Lande en naburige landen waargenomen. Petrus Doekema (Groningen): 74 pp.

Burger, A.W., 1979. Sedimentpetrologisch onderzoek van boring Lievelde 41 B/73 (No. 645). Rijks Geologische Dienst (Haarlem).

Burger, A.W., 1992. Sedimentpetrologisch onderzoek aan boring Beltrum 34D/232 (No. 960). Rijks Geologisch Dienst (Haarlem).

Busschers, F.S., Kasse, C., Van Balen, R.T., Vandenberghe, J., Cohen, K.M., Weerts, H.J.T., Wallinga, J., Johns, C., Cleveringa, P. & Bunnik, F.P.M., 2007. Late Pleistocene evolution of the Rhine-Meuse system in the southern North Sea basin: imprints of climate change, sea-level oscillation and glacio-isostacy. Quaternary Science Reviews 26: 3216-3248. DOI: 10.1016/j.quascirev.2007.07.013

Carver, F., Cartwright, J., McGrandle, A., Kirkham, C. & Pryce, E., 2023. The continuation of the Mull Dyke Swarm into the Southern North Sea. Journal of the Geological Society 180(6): jgs2023-039. DOI: 10.1144/jgs2023-039

Chambers, L.M., Pringle, M., Fitton, G., Larsen, L.M., Pedersen, A.K. & Parrish, R., 2003. Recalibration of the Palaeocene–Eocene boundary (P-E) using high precision U-Pb and Ar-Ar isotope dating. Presented at the EGS-AGU-EGU Joint Assembly, Nice.

Chang, S.-J., Kendall, E., Davaille, A. & Ferreira, A.M.G., 2020. The Evolution of Mantle Plumes in East Africa. Journal of Geophysical Research: Solid Earth 125(12): e2020JB019929. DOI: 10.1029/2020JB019929

Cohen, K.M. & Stouthamer, E., 2012. Digitaal Basisbestand Paleogeografie van de Rijn-Maas Delta. DANS Data Station Archaeology 5. DOI: 10.17026/dans-x7g-sjtw

Corfu, F. & Dahlgren, S., 2008. Perovskite U–Pb ages and the Pb isotopic composition of alkaline volcanism initiating the Permo-Carboniferous Oslo Rift. Earth and Planetary Science Letters 265(1): 256-269. DOI: 10.1016/j.epsl.2007.10.019

Corfu, F. & Larsen, B.T., 2020. U-Pb systematics in volcanic and plutonic rocks of the Krokskogen area: Resolving a 40 million years long evolution in the Oslo Rift. Lithos 376-377: 105755. DOI: 10.1016/j.lithos.2020.105755

Cottençon, A., Parant, B. & Flacelière, B., 1975. Lower Cretaceous Gas-fields in Holland. In: Woodland, A.W. (ed.): Petroleum and the continental shelf of northwest Europe. Applied Science Publications (London) 1-30: 403-412

Courtillot, V., Jaupart, C., Manighetti, I., Tapponnier, P. & Besse, J., 1999. On causal links between flood basalts and continental breakup. Earth and Planetary Science Letters 166(3): 177-195. DOI: 10.1016/S0012-821X(98)00282-9

Cremer, H., Bunnik, F.P.M., Donders, T.H., Hoek, W.Z., Koolen-Eekhout, M., Koolmees, H.H. & Lavooi, E., 2010. River flooding and landscape changes impact ecological conditions of a scour hole lake in the Rhine-Meuse delta, The Netherlands. Journal of Paleolimnology 44: 789-801. DOI: 10.1007/s10933-010-9452-2

Crommelin, R.D., 1963. Een vulkanisch sediment in de ondergrond van de Betuwe. Netherlands Journal of Geosciences-Geologie en Mijnbouw 42(4): 112-113.

Dahlgren, S., Corfu, F. & Heaman, L.M., 1996. U–Pb time constraints, and Hf and Pb source characteristics of the Larvik plutonic complex, Oslo Paleorift. Geodynamic and geochemical implications for the rift evolution. VM Goldschmidt Conference. Journal of Conference Abstracts 1 (Cambridge Publications).

Davies, S.M., Hoek, W.Z., Bohncke, S.J.P., Lowe, J.J., Pyne-O'Donnell, S. & Turney, C.S.M., 2005. Detection of Lateglacial distal tephra layers in the Netherlands. Boreas 34: 123-135. DOI: 10.1080/03009480510012944

De Bruin, G., Bouroullec, R., Geel, K., Abdul Fattah, R., Van Hoof, T., Pluymaekers, M., Van der Belt, F., Vandeweijer, V.P. & Zijp, M., 2015. New petroleum plays in the Dutch northern offshore. TNO (Utrecht), Report No. 2015 R10920. https://www.nlog.nl/sites/default/files/2018-11/NORTHERN_OFFSHORE_TNO_report_2015_R10920_0.pdf

De Jager, J., Van Ojik, K. & Smit, J., 2025. Geological development. In: J.H. Ten Veen, G.-J. Vis, J. De Jager & Th.E. Wong (eds): Geology of the Netherlands, second edition. Amsterdam University Press (Amsterdam): 21-51. DOI: 10.5117/9789463728362_ch01

De Vos, W., Feldrappe, H., Pharaoh, T.C., Smith, N.J.P., Vejbæk, O.V., Verniers, J., Nawrocki, J., Poprawa, P. & Bełka, Z., 2010. Pre-Devonian. In: Doornenbal, J.C. & Stevenson, A.G. (eds): Petroleum Geological Atlas of the Southern Permian Basin Area. EAGE Publications B.V. (Houten): 59-69.

Dewey, J.F. & Windley, B.F., 1988. Palaeocene-Oligocene tectonics of NW Europe. In: Morton, A.C. & Parsons, L.M. (eds): Early Tertiary volcanism and the opening of the NE Atlantic. Geological Society of London, Special Publications 39: 25-31.

Dirkzwager, J.B., Stephenson, R.A. & Legostaeva, O.V., 2000. The pre-Permian residual gravity field for the Dutch onshore and adjacent offshore. Global and Planetary Change 27(1-4): 53-66.

Dixon, J.E., Fitton, J.G. & Frost, R.T.C., 1981. The tectonic significance of post-Carboniferous igneous activity in the North Sea

Basin. In: Illing, L.V. & Hobson, G.D. (eds): Petroleum Geology of the continental Shelf of North-West Europe: Proceedings of the 2nd Conference. Institute of Petroleum (London): 121-137.

Donato, J.A., 1993. A buried batholith and the origin of the Sole Pit Basin, UK Southern North Sea. Journal of the Geological Society 150: 255-258.

Donato, J.A., Martindale, W. & Tully, M.C., 1983. Buried granites within the Mid North Sea High. Journal of the Geological Society 140: 825-837.

Donato, J.A., 2020. Gravity modelling across two postulated granite batholiths within the UK onshore East Midlands Shelf. UK Onshore Geophysical Library: 14 pp.

Dusar, M. & Langenaeker, V., 1992. De oostrand van het Massief van Brabant, met beschrijving van de geologische verkenningsboring te Martenslinde. Belgische Geologische Dienst: 22 pp.

Eckhardt, F.J., 1979. Der permische Vulkanismus Mitteleuropas. Geologisches Jahrbuch D35: 3-84.

Eckhardt, F.J., 1968. Vorkommen und Petrogenese spilitisierter Diabase des Rotliegenden im Weser-Ems-Gebiet. Geologisches Jahrbuch 85: 227-264.

Egger, H. & Brückl, W., 2006. Gigantic volcanic eruptions and climatic change in the early Eocene. International Journal of Earth Sciences 95(6): 1065-1070. DOI: 10.1007/s00531-006-0085-7

Eigenfeld, R.W.F. & Eigenfeld-Mende, I., 1986. Niederländische permokarbone basische Magmatite als Fortsetzung der spilisierten Effusiva in NW-Deutschland. Mededelingen Rijks Geologische Dienst 40(1): 11-21.

Erkens, G., 2009. Sediment dynamics in the Rhine catchment - Quantification of fluvial response to climate change and human impact. PhD thesis Utrecht University, Netherlands Geographical Studies 388: 278 pp.

Ernst, R.E. & Buchan, K.L., 1997. Giant radiating dyke swarms: their use in identifying pre-Mesozoic large igneous provinces and mantle plumes. In: Large Igneous Provinces: Continental, Oceanic, and Planetary Flood Volcanism. American Geophysical Union: 297-334.

Erren, H. & Bredewout, J.W., 1991. Model calculations on intrusive cooling and related coalification of the Peel-Erkelenz coalfield (The Netherlands and Germany). Geologie En Mijnbouw 70(3): 243-252.

Fall, H.G., Gibb, F.G.F. & Kanaris-Sotiriou, R., 1982. Jurassic volcanic rocks of the northern North Sea. Journal of the Geological Society 139(3): 277-292. DOI: 10.1144/gsjgs.139.3.0277

Fekiacova, Z., Mertz, D.F. & Renne, P.R., 2007. Geodynamic Setting of the Tertiary Hocheifel Volcanism (Germany), Part I: 40Ar/39Ar geochronology. In: Ritter, J.R.R. & Christensen, U.R. (eds): Mantle Plumes: A Multidisciplinary Approach. Springer (Berlin, Heidelberg): 185-206. DOI: 10.1007/978-3-540-68046-8_6

Foulger, G.R. & Anderson, D.L., 2005. A cool model for the Iceland hotspot. Journal of Volcanology and Geothermal Research 141(1): 1-22. DOI: 10.1016/j.jvolgeores.2004.10.007

Frezzotti, M.L., 1992. Fluid and melt inclusion study (No. XUM/090; 15 pp.). Nederlandse Aardolie Maatschappij B.V. (Assen): 15 pp.

Frost, R.T.C., Fitch, F.J. & Miller, J.A., 1981. The age and nature of the crystalline basement of the North Sea Basin. In: Illing, L.V. & Hobson, G.D. (eds): Petroleum Geology of the continental Shelf of North-West Europe: Proceedings of the 2nd Conference. Institute of Petroleum (London): 43-57.

Furnes, H., Elvsborg, A. & Malm, O.A., 1982. Lower and Middle Jurassic alkaline magmatism in the Egersund sub-basin, North Sea. Marine Geology 46(1-2): 53-69.

Gaina, C., Medvedev, S., Torsvik, T.H., Koulakov, I. & Werner, S.C., 2014. 4D Arctic: A Glimpse into the Structure and Evolution of the Arctic in the Light of New Geophysical Maps, Plate Tectonics and Tomographic Models. Surveys in Geophysics 35(5): 1095-1122. DOI: 10.1007/s10712-013-9254-y

Galavazi, M.A., 1999. Study of volcanic fragments in cuttings samples of the lower Delfland, wells P9-8 and P12-8 (No. G307b-1). PanTerra Geoconsultants B.V. for Clyde Petroleum Exploration B.V.: 7 pp. https://www.nlog.nl/brh-web/rest/brh/document/605736932

Gast, R.E., Dusar, M., Breitkreuz, C., Gaupp, R., Schneider, J.W., Stemmerik, L., Geluk, M.C., Geißler, M., Kiersnowski, H., Glennie, K.W., Kabel, S. & Jones, N.S., 2010. Rotliegend. In: Doornenbal, J.C. & Stevenson, A.G. (eds): Petroleum Geological Atlas of the Southern Permian Basin Area. EAGE Publications B.V. (Houten): 100-121.

Gauer, M.B., Upton, A.J. & McGrandle, A., 2004. Identification and interpretation of igneous sills in the Zechstein of the Southern North Sea Basin. Extended Abstract presented at PETEX: 23-25 pp.

Geluk, M.C., 1997. Palaeogeographic maps of Moscovian and Artinskian: contributions from the Netherlands. In: Crasquin-Soleau, S. & De Wever, P. (eds): Peri-Tetheys stratigraphic correlations. Geodiversitas 19: 229-234.

Gibb, F.G.F. & Kanaris-Sotiriou, R., 1976. Jurassic igneous rocks of the Forties Field. Nature 260: 23-25.

Glennie, K.W., 1997. Recent advances in understanding the southern North Sea Basin: a summary. In: Ziegler, K., Turner, P. & Daines, S.R. (eds): Petroleum Geology of the Southern North Sea: Future Potential. Geological Society of London: 17-29. DOI: 10.1144/GSL.SP.1997.123.01.03

Global Volcanism Program, 2023. [Database] Volcanoes of the World. Smithsonian Institution: v. 5.1.2. DOI: 10.5479/si.GVP.VOTW5-2023.5.1

Gradstein, F.M., Ogg, J.G. & Smith, A.G., 2004. A Geologic Time Scale 2004. Cambridge University Press (Cambridge): 589 pp.

Guterch, A., Grad, M., Krawczyk, C.M., Wybraniec, S., Ziegler, P.A. & De Vos, W., 2010. Crustal structure and structural framework. In: Doornenbal, J.C. & Stevenson, A.G. (eds): Petroleum Geological Atlas of the Southern Permian Basin Area. EAGE Publications B.V. (Houten): 10-23.

Hamilton, M. & Pearson, G., 2011. Precise U-Pb Age for the Great Whin Dolerite Complex, N.E. England and Its Significance: 495-507. DOI: 10.1007/978-3-642-12496-9_26

Harrison, R.K., Jeans, C.V. & Merriman, R.J., 1979. Mesozoic igneous rocks, hydrothermal mineralisation and volcanogenic sediments in Britain and adjacent regions. Bulletin of the Geological Survey of Great Britain 70: 57-69.

Heeremans, M., Timmerman, M.J., Kirstein, L.A. & Faleide, J.I., 2004. New constraints on the timing of late Carboniferous - early Permian volcanism in the central North Sea. In: Wilson, M., Neumann, E.-R., Davies, G.R., Timmerman, M.J., Heeremans, M. & Larsen, B.T. (eds): Permo-Carboniferous magmatism and rifting in Europe 223: 177-194. DOI: 10.1144/GSL.SP.2004.223.01.08

Helmers, H., 1991. Ultramafic alkalibasalt of the Heinenoord-1 drilling. Vrije Universiteit for NAM (Assen): 29 pp.

Hernandez Casado, J. & Underhill, J.R., 2013. Consequences of intrusions for sub-salt, sub-basalt exploration and development. 75th EAGE Conference and Exhibition (London). EAGE (Houten): cp-348-00615. DOI: 10.3997/2214-4609.20130141

Herngreen, C.F.W., 1985. Resultaten van het palynologisch onderzoek van de kernen 1 en 2 van boring F3-7 (No. 2167-A; 2 pp.). Rijks Geologische Dienst: 2 pp.

Herngreen, G.F.W., Smit, R. & Wong, Th.E., 1991. Stratigraphy and tectonics of the Vlieland basin, The Netherlands. In: Spencer, A.M. (ed.): Generation, accumulation and production of Europe's hydrocarbons. Special Publication of the European Association of Petroleum Geoscientists (Berlin) 1: 175-192.

Hole, M.J. & Natland, J.H., 2020. Magmatism in the North Atlantic Igneous Province; mantle temperatures, rifting and geodynamics. Earth-Science Reviews 206: 102794. DOI: 10.1016/j.earscirev.2019.02.011

Hopper, J. R., Funck, T., Stoker, M., Árting, U., Péron-Pinvidic, G., Doornenbal, H. & Gaina, C. (eds), 2014. Tectonostratigraphic Atlas of the North-East Atlantic Region. Geological Survey of Denmark and Greenland (GEUS) (Copenhagen, Denmark): 339 pp.

Huis in 't Veld, R. & Den Hartog Jager, D., 2025. Late Carboniferous. In: Ten Veen, J.H., Vis, G.-J., De Jager, J. & Wong, Th.E. (eds): Geology of the Netherlands, second edition. Amsterdam University Press (Amsterdam): 95-125 DOI: 10.5117/9789463728362_ch03

Jacqué, M. & Thouvenin, J., 1975. Lower Tertiary tuffs and volcanic activity in the North Sea. In: Woodland, A.W. (ed.): Petroleum and the continental shelf of northwest Europe. Applied Science Publications (London) 1-30: 455-465.

Jeans, C.V., Merriman, R.J. & Mitchell, J.G., 1977. Origin of Middle Jurassic and Lower Cretaceous fuller's earths in England. Clay Minerals 12: 11-44.

Jeans, C.V., Wray, D.S., Merriman, R.J. & Fisher, M.J., 2000. Volcanogenic clays in Jurassic and Cretaceous strata of England and the North Sea Basin. Clay Minerals 35(1): 25-55.

Jung, C., Jung, S., Hoffer, E. & Berndt, J., 2006. Petrogenesis of Tertiary Mafic Alkaline Magmas in the Hocheifel, Germany. Journal of Petrology 47(8): 1637-1671. DOI: 10.1093/petrology/egl023

Jung, S., Vieten, K., Romer, R.L., Mezger, K., Hoernes, S. & Satir, M., 2012. Petrogenesis of Tertiary Alkaline Magmas in the Siebengebirge, Germany. Journal of Petrology 53(11): 2381-2409. DOI: 10.1093/petrology/egs047

Juvigné, E., 1999. Téphrostratigraphie du Quaternaire en Belgique. Geologica Belgica 2/3: 73-87. DOI: 10.20341/gb.2014.011

Juvigné, E. & Semmel, A., 1981. Un tuf volcanique semblable à l'Eltviller Tuff dans les loess de Hesbaye (Belgique) et du Limbourg néerlandais. E&G Quaternary Science Journal 31(1): 83-90. DOI: 10.3285/eg.31.1.08

Kettel, D., 1983. The East Groningen Massif - Detection of an intrusive body by means of coalification. Geologie En Mijnbouw 62(1): 203-210.

Kimbell, G.S. & Williamson, J.P., 2015. A gravity interpretation of the Central North Sea. British Geological Survey (Nottingham, UK), Commissioned Report No. CR/15/119: 75 pp.

Kimpe, W.F.M., 1953. Doleritic and gabbroic instrusives in the Autunian (Lower Permian) of the boring Wanneperveen 1, eastern Netherlands. Geologie en Mijnbouw 15: 57-65.

King, A.D., Marshall, K.L. & Burton, C.A., 1985. Well P/6-B1 Stratigraphical Report (Interval 1545-1850 m). Paleoservices Ltd. for Mobil Producing Netherlands Inc., Report No. 1523: 18 pp. https://www.nlog.nl/brh-web/rest/brh/document/910480758

Kirstein, L.A., Davies, G.R. & Heeremans, M., 2006. The petrogenesis of Carboniferous–Permian dyke and sill intrusions across northern Europe. Contributions to Mineralogy and Petrology 152(6): 721-742. DOI: 10.1007/s00410-006-0129-9

Kirton, S.R. & Donato, J.A., 1985. Some buried Tertiary dykes of Britain and surrounding waters deduced by magnetic modelling and seismic reflection methods. Journal of the Geological Society 142(6): 1047-1057. DOI: 10.1144/gsjgs.142.6.1047

Klaver, M., Blundy, J.D. & Vroon, P.Z., 2018. Generation of arc rhyodacites through cumulate-melt reactions in a deep crustal hot zone: Evidence from Nisyros volcano. Earth and Planetary Science Letters 497: 169-180. DOI: 10.1016/j.epsl.2018.06.019

Knox, R.W.O., 1997. The late Paleocene to early Eocene ash layers of the Danish Mo-Clay (Fur Formation): stratigraphic and tectonic significance. In: Thomsen, E. & Pedersen, S.A.S. (eds): Geology and palaeontology of the Mo-clay. Aarhus Geoscience 6: 7-11.

Knox, R.W.O. & Morton, A.C., 1988. The record of early Tertiary N Atlantic volcanism in sediments of the North Sea Basin. Geological Society Special Publication 39: 407-419.

Kombrink, H., Doornenbal, J.C., Duin, E.J.T., Den Dulk, M., Ten Veen, J.H. & Witmans, N., 2012. New insights into the geological structure of the Netherlands; results of a detailed mapping project. Netherlands Journal of Geosciences 91(4): 419-446. DOI: 10.1017/S0016774600000329

Kortekaas, M., Böker, U., Van der Kooij, C. & Jaarsma, B., 2018.

Lower Triassic reservoir development in the northern Dutch offshore. Geological Society of London, Special Publications 469: 149-168. DOI: 10.1144/SP469.19

Krueger, 1982. Potassium-Argon age determination of a sample from borehole K12-05-S1. Krueger Enterprises Inc., Geochron Laboratories Division (Cambridge), Report No. R-6006: 1 pp. https://www.nlog.nl/brh-web/rest/brh/document/3881042201

Kuijper, R.P., 1991. Petrology of a dolerite in Netherlands offshore well G/17-2. Scripta Geologica 97 (Journal Article): 33-97.

Kuijper, R.P., 2003. Petrography of igneous rocks in E18-5. Goal Olie- en Gasexploratie B.V. for Wintershall Noordzee B.V., Report No. 2003/025: 14 pp. https://www.nlog.nl/brh-web/rest/brh/document/3831683293

Larsen, L.M., Fitton, J.G. & Pedersen, A.K., 2003. Paleogene volcanic ash layers in the Danish Basin: compositions and source areas in the North Atlantic Igneous Province. Lithos 71(1): 47-80. DOI: 10.1016/j.lithos.2003.07.001

Latin, D.M., Dixon, J.E. & Fitton, J.G., 1990a. Rift-related magmatism in the North Sea basin. In: Blundell, D.J. & Gibbs, A.D. (eds): Tectonic Evolution of the North Sea Rifts. Oxford Science Publications (Oxford): 101-144.

Latin, D.M., Dixon, J.E., Fitton, J.G. & White, N., 1990b. Mesozoic magmatic activity in the North Sea Basin: implications for stretching history. Tectonic Events Responsible for Britain's Oil and Gas Reserves 55: 207-227.

Latin, D.M., 1990. The relationship between extension and magmatism in the North Sea Basin. PhD thesis, University of Edinburgh: 404 pp.

Latin, D.M. & Waters, F.G., 1992. Basaltic magmatism in the North Sea and its relationship to lithospheric extension. Tectonophysics 208(1-3): 77-90. DOI: 10.1016/0040-1951(92)90337-6

Le Maitre, R. W., Streckeisen, A., Zanettin, B., Le Bas, M. J., Bonin, B. & Bateman, P. (eds), 2002. Igneous Rocks: A Classification and Glossary of Terms: Recommendations of the International Union of Geological Sciences Subcommission on the Systematics of Igneous Rocks. Cambridge University Press (Cambridge): 2nd ed. DOI: 10.1017/CBO9780511535581

Lester, M.J., 1985. Biostratigraphical analysis of the Amoco F/16-2 Well, offshore Netherlands. Amoco Netherlands Petroleum Company (Surrey): 25 pp.

Linnemann, U., Herbosch, A., Liégeois, J.P., Pin, C., Gärtner, A. & Hofmann, M., 2012. The Cambrian to Devonian odyssey of the Brabant Massif within Avalonia: A review with new zircon ages, geochemistry, Sm-Nd isotopes, stratigraphy and palaeogeography. Earth-Science Reviews 112: 126-154. DOI: 10.1016/j.earscirev.2012.02.007

Lippolt, H.J., Hess, J.C. & Burger, K., 1984. Isotopische Alter von pyroklastischen Sanidinen aus Kaolin-Kohlentonsteinen als Korrelationsmarken für das mitteleuropäische Oberkarbon. Fortschritte in Der Geologie von Rheinland Und Westfalen 32: 119-150.

Lloyd, F.E., Arima, M. & Edgar, A.D., 1985. Partial melting of a phlogopite-clinopyroxenite nodule from south-west Uganda: an experimental study bearing on the origin of highly potassic continental rift volcanics. Contributions to Mineralogy and Petrology 91(4): 321-329. DOI: 10.1007/BF00374688

Lohne, Ø.S., Mangerud, J. & Birks, H.H., 2013. Precise 14C ages of the Vedde and Saksunarvatn ashes and the Younger Dryas boundaries from western Norway and their comparison with the Greenland Ice Core (GICC05) chronology. Journal of Quaternary Science 28(5): 490-500. DOI: 10.1002/jqs.2640

Lundmark, A.M., Gabrielsen, R.H., Austrheim, H., Flaat, K., Strand, T. & Ohm, S.E., 2012. Late Devonian rifting in the central North Sea: Evidence from altered felsic volcanic rocks in the Embla oil field. Marine and Petroleum Geology 29: 204-218. DOI: 10.1016/j.marpetgeo.2011.06.002

Lundmark, A.M., Gabrielsen, R.H. & Brown, J.F., 2011. Zircon U–Pb age for the Orkney lamprophyre dyke swarm, Scotland, and relations to Permo- Carboniferous magmatism in northwestern Europe. Journal of the Geological Society 168: 1233-1236.

Lundmark, A.M., Gabrielsen, R.H., Strand, T. & Ohm, S.E., 2018. Repeated post-Caledonian intra-cratonic rifting in the central North Sea: Evidence from the volcanic record in the Embla oil field. Marine and Petroleum Geology 92: 505-518. DOI: 10.1016/j.marpetgeo.2017.11.018

Lyngsie, S.B. & Thybo, H., 2007. A new tectonic model for the Laurentia-Avalonia-Baltica sutures in the North Sea: A case study along MONA LISA profile 3. Tectonophysics 429(3-4): 201-227. DOI: 10.1016/j.tecto.2006.09.017

Macdonald, R., Gass, K.N., Thorpe, R.S. & Gass, I.G., 1984. Geochemistry and petrogenesis of the Derbyshire Carboniferous basalts. Journal of the Geological Society 141: 147-159.

Mansy, J.L., Everaerts, M. & De Vos, W., 1999. Structural analysis of the adjacent Acadian and Variscan fold belts in Belgium and northern France from geophysical and geological evidence. Tectonophysics 309(1-4): 99-116. DOI: 10.1016/S0040-1951(99)00134-1

Marty, B., Pik, R. & Gezahegn, Y., 1996. Helium isotopic variations in Ethiopian plume lavas: nature of magmatic sources and limit on lower mantle contribution. Earth and Planetary Science Letters 144(1): 223-237. DOI: 10.1016/0012-821X(96)00158-6

McKenzie, D. & Bickle, M.J., 1988. The Volume and Composition of Melt Generated by Extension of the Lithosphere. Journal of Petrology 29(3): 625-679. DOI: 10.1093/petrology/29.3.625

Meadows, N. & Hrycyszyn, A., 1992. A sedimentological and petrographical evaluation of 17.90 m of core from Bow Valley Industries LTD. Well M/3-1, southern North Sea, Netherlands sector. Geochem Group NAM (Assen), Report No. 5435/0004: 91 pp. https://www.nlog.nl/brh-web/rest/brh/document/1784665012

Mees, R.P.R. & Meijs, E.P.M., 1984. Note on the presence of pre-weichselian loess deposits along the Albert Canal near Kesselt

and Vroenhoven (Belgian Limbourg). Geologie en Mijnbouw 63(1): 7-11.

Meijs, E., Mücher, H.J., Ouwerkerk, G., Romein, A. & Stoltenberg, H., 1983. Evidence of Presence of the Eltville Tuff Layer in Dutsch and Belgian Limbourg and the Consequences for the Loess Stratigraphy. Eiszeitalter Und Gegenwart: Jahrbuch Der Deutschen Quartärvereinigung 33: 59 pp.

Meijs, E.P.M., 2011. The Veldwezelt site (province of Limburg, Belgium): environmental and stratigraphical interpretations. Netherlands Journal of Geosciences 90 (2-3): 73-94. DOI: 10.1017/S0016774600001037

Meijs, E.P.M., 1980. A short note on the presence of the Eltville-tuff layer in the surroundings of Maastricht. Geologie en Mijnbouw 59(4): 409-410.

Meijs, E.P.M., 1985. Loess stratigraphical research at the Palaeolithic site Maastricht-Belvédère. Mededelingen Rijks Geologische Dienst 39(1): 31-34.

Meyer, R., Wijk, J. & Gernigon, L., 2007. The North Atlantic Igneous Province: A review of models for its formation. The Geological Society of America, Special Paper 430: 525-552.

Milton-Worssell, R.J., Smith, K., McGrandle, A., Watson, J. & Cameron, D., 2010. The search for a Carboniferous petroleum system beneath the Central North Sea. Petroleum Geology Conference Series 7: 57-75. DOI: 10.1144/0070057

Mitchell, J.G., Rands, P.N. & Ineson, P.R., 1989. Perturbation of the K-Ar age system in the Cleveland dyke, U.K.: Evidence of an Early Eocene age for barite mineralisation in the Magnesian Limestone of County Durham. Chemical Geology: Isotope Geoscience Section 79(1): 49-64. DOI: 10.1016/0168-9622(89)90006-7

Monaghan, A.A. & Pringle, M.S., 2004. 40Ar/39Ar geochronology of Carboniferous-Permian volcanism in the Midland Valley, Scotland. Geological Society, London, Special Publications 223(1): 219-241. DOI: 10.1144/GSL.SP.2004.223.01.10

Monaghan, A.A. & Parrish, R.R., 2006. Geochronology of Carboniferous-Permian magmatism in the Midland Valley of Scotland: implications for regional tectonomagmatic evolution and the numerical time scale. Journal of the Geological Society 163(1): 15-28. DOI: 10.1144/0016-764904-142

Morgan, W.J., 1971. Convection Plumes in the Lower Mantle. Nature 230(5288): 42-43. DOI: 10.1038/230042a0

Morton, A.C. & Knox, R.O.B., 1990. Geochemistry of late Palaeocene and early Eocene tephras from the North Sea Basin. Journal of the Geological Society 147(3): 425-437. DOI: 10.1144/gsjgs.147.3.0425

Neumann, E.-R., Olsen, K.H., Baldridge, W.S. & Sundvoll, B., 1992. The Oslo Rift: a review. Tectonophysics 208(1-3): 1-18. DOI: 10.1016/0040-1951(92)90333-2

Neumann, E.-R., Wilson, M., Heeremans, M., Spencer, E.A., Obst, K., Timmerman, M.J. & Kirstein, L., 2004. Carboniferous-Permian rifting and magmatism in southern Scandinavia, the North Sea and northern Germany: a review. Permo-Carboniferous Magmatism and Rifting in Europe 223: 11-40.

NITG, 1998. Geological Atlas of the subsurface of the Netherlands (1:250,000), Explanation to Map Sheet X Almelo–Winterswijk. Netherlands Institute of Applied Geoscience (NITG-TNO, Haarlem): 134 pp.

NITG, 2000. Geological Atlas of the subsurface of the Netherlands (1:250,000), Explanation to Map Sheet VI Veendam Hoogeveen. Netherlands Institute of Applied Geoscience (NITG-TNO, Utrecht): 152 pp.

Obst, K., Ansorge, J., Matting, S. & Hüneke, H., 2015. Early Eocene volcanic ashes on Greifswalder Oie and their depositional environment, with an overview of coeval ash-bearing deposits in northern Germany and Denmark. International Journal of Earth Sciences 104(8): 2179-2212. DOI: 10.1007/s00531-015-1203-1

Obst, K., Hammer, J., Katzung, G. & Korich, D., 2004. The Mesoproterozoic basement in the southern Baltic Sea: insights from the G 14-1 off-shore borehole. International Journal of Earth Sciences 93(1): 1-12. DOI: 10.1007/s00531-003-0371-6

Park, C. & Schmincke, H., 2009. Apokalypse im Rheintal. Spektrum Der Wissenschaft 2: 78-87.

Parnell, J., 1988. Migration of biogenic hydrocarbons into granites: a review of hydrocarbons in British plutons. Marine and Petroleum Geology 5(4): 385-396. DOI: 10.1016/0264-8172(88)90032-3

Pearce, J.A., 1996. A users guide to basalt discrimination Diagrams. In: Wyman, D.A. (ed.): Trace element geochemisty of volcanic rocks: Application for massive sulphide exploration. Geological Association of Canada, Short Course Notes 12: 79-113.

Pearce, J.A., 1982. Trace element characteristics of lavas from destructive plate boundaries. In: Thorpe, R.S. (ed.): Orogenic andesites and related rocks. John Wiley and Sons (Chichester, England): 528-548.

Pedersen, L.E., Heaman, L.M. & Holm, P.M., 1995. Further constraints on the temporal evolution of the Oslo Rift from precise U-Pb zircon dating in the Siljan-Skrim area. Lithos 34(4): 301-315. DOI: 10.1016/0024-4937(94)00014-S

Peniguel, G., Acheriteguy, J., Bignoumba, J., Dugue, O., Euvrard, B., Gout, C., Janisek, J.M., Mathis, B., Meyer, A., Neumann, C., Nicolas, G. & Philippe, B., 1992. E/12-3 (The Netherlands offshore – Block E12) – Laboratory studies. Société Nationale Elf Aquitaine Production (France), Report No. 92/013: 59 pp.

Perrot, J. & Van der Poel, A.B., 1987. Zuidwal - a Neocomian gas field. In: Brooks, J. & Glennie, K. (eds): Petroleum Geology of North-West Europe. Graham & Trotman (London): 325-335.

Pharaoh, T.C., Dusar, M., Geluk, M.C., Kockel, F., Krawczyk, C.M., Krzywiec, P., Scheck-Wenderoth, M., Thybo, H., Vejbæk, O.V. & Van Wees, J.-D., 2010. Tectonic Evolution. In: Doornenbal, J.C. & Stevenson, A.G. (eds): Petroleum Geological Atlas of the Southern Permian Basin Area. EAGE Publications B.V. (Houten): 24-57.

Pharaoh, T.C., England, R. & Lee, M.K., 1995. The concealed Caledonide basement of Eastern England and the southern North

Sea - A review. Sudia Geophysica et Geodaetica 39: 330-346. DOI: 10.1007/BF02295826

Pharaoh, T.C., Winchester, J.A., Verniers, J., Lassen, A. & Seghedi, A., 2006. The Western Accretionary Margin of the East European Craton: an overview. In: Gee, D.G. & Stephenson, R.A. (eds): European Lithosphere Dynamics. Geological Society of London Memoirs 32: 291-312. DOI: 10.1144/GSL.MEM.2006.032.01.17

Pitcavage, E., Furman, T., Nelson, W.R., Kalegga, P.K. & Barifaijo, E., 2021. Petrogenesis of primitive lavas from the Toro Ankole and Virunga Volcanic Provinces: Metasomatic mineralogy beneath East Africa's Western Rift. Lithos 396-397: 106192. DOI: 10.1016/j.lithos.2021.106192

Plein, E., 1995. Norddeutsches Rotliegendbecken; Rotliegend-Monographie Teil II. Stratigraphie von Deutschland I. Courier Forschungsinstitut Senckenberg 183.

Pouclet, A. & Juvigne, E., 2009. The Eltville Tephra, a late Pleistocene widespread tephra layer in Germany, Belgium and the Netherlands; symptomatic compositions of the minerals. Geologica Belgica 12(1-2): 93-103.

Pouclet, A., Juvigné, E. & Pirson, S., 2008. The Rocourt Tephra, a Widespread 90-74 ka stratigraphic marker in Belgium. Quaternary Research 70(1): 105-120. DOI: 10.1016/j.yqres.2008.03.010

Preusser, F., 2008. Characterisation and evolution of the River Rhine system. Netherlands Journal of Geosciences 87(1): 7-19.

Przybyla, T., Pfänder, J.A., Münker, C., Kolb, M., Becker, M. & Hamacher, U., 2018. High-resolution 40Ar/39Ar geochronology of volcanic rocks from the Siebengebirge (Central Germany)—Implications for eruption timescales and petrogenetic evolution of intraplate volcanic fields. International Journal of Earth Sciences 107(4): 1465-1484. DOI: 10.1007/s00531-017-1553-y

Quirie, A.K., Schofield, N., Hartley, A., Hole, M.J., Archer, S.G., Underhill, J.R., Watson, D. & Holford, S.P., 2019. The Rattray Volcanics: Mid-Jurassic fissure volcanism in the UK Central North Sea. Journal of the Geological Society 176(3): 462-481. DOI: 10.1144/jgs2018-151

Quirie, A.K., Schofield, N., Jolley, D.W., Archer, S.G., Hole, M.J., Hartley, A., Watson, D., Burgess, R., Pugsley, J.H., Underhill, J.R. & Holford, S.P., 2020. Palaeogeographical evolution of the Rattray Volcanic Province, Central North Sea. Journal of the Geological Society 177(4): 718-737. DOI: 10.1144/jgs2019-182

Reinig, F., Wacker, L., Jöris, O., Oppenheimer, C., Guidobaldi, G., Nievergelt, D., Adolphi, F., Cherubini, P., Engels, S., Esper, J., Land, A., Lane, C., Pfanz, H., Remmele, S., Sigl, M., Sookdeo, A. & Büntgen, U., 2021. Precise date for the Laacher See eruption synchronizes the Younger Dryas. Nature 595(7865): 66-69. DOI: 10.1038/s41586-021-03608-x

Riber, L., Dypvik, H. & Sørlie, R., 2015. Altered basement rocks on the Utsira High and its surroundings, Norwegian North Sea. Norwegian Journal of Geology 95(1). DOI: 10.17850/njg95-1-04

Rieffe, E.C. & Van Lil, R., 1992. Optical analyses of igneous rock samples from 45 wells in the Netherlands and the Dutch part of the continental shelf. MSc thesis. Vrije Universiteit Amsterdam/NAM (Assen): 41 pp.

Rijkers, R. & Duin, E., 1994. Crustal observations beneath the southern North Sea and their tectonic and geological implications. Tectonophysics 240(1-4): 215-224.

Rijks Geologische Dienst, 1993. Geological atlas of the subsurface of the Netherlands (1 : 250 000). Explanation to Map sheet V Sneek- Zwolle. Rijks Geologische Dienst (Haarlem) 127.

Ritchie, J.D., Swallow, J.L., Mitchell, J.G. & Morton, A.C., 1988. Jurassic ages from intrusives and extrusives within the Forties igneous province. Scottish Journal of Geology 24(1): 81-88. DOI: 10.1144/sjg24010081

Ritter, J.R.R., Jordan, M., Christensen, U.R. & Achauer, U., 2001. A mantle plume below the Eifel volcanic fields, Germany. Earth and Planetary Science Letters 186(1): 7-14.

Rogers, N.W., De Mulder, M. & Hawkesworth, C.J., 1992. An enriched mantle source for potassic basanites: evidence from Karisimbi volcano, Virunga volcanic province, Rwanda. Contributions to Mineralogy and Petrology 111(4): 543-556. DOI: 10.1007/BF00320908

Rogers, N.W., James, D., Kelley, S.P. & De Mulder, M., 1998. The Generation of Potassic Lavas from the Eastern Virunga Province, Rwanda. Journal of Petrology 39(6): 1223-1247. DOI: 10.1093/petroj/39.6.1223

Rooney, T.O., 2020. The Cenozoic magmatism of East Africa: Part V – Magma sources and processes in the East African Rift. Lithos 360-361: 105296. DOI: 10.1016/j.lithos.2019.105296

Saunders, A.D., Fitton, J.G., Kerr, A.C., Norry, M.J. & Kent, R.W., 1997. The north Atlantic igneous province. In: Mahony, J.J. & Coffin, M.F. (eds): Large Igneous Provinces: Continental, Oceanic and Planetary. Geophysical Monograph-American Geophysical Union (Washington, D.C.) 100: 45-94.

Scheck, M. & Bayer, U., 1999. Evolution of the Northeast German Basin – inferences from a 3D structural model and subsidence analysis. Tectonophysics 313(1-2): 145-169. DOI: 10.1016/S0040-1951(99)00194-8

Schmincke, H.-U., Park, C. & Harms, E., 1999. Evolution and environmental impacts of the eruption of Laacher See Volcano (Germany) 12,900 a BP. Quaternary International 61(1): 61-72. DOI: 10.1016/S1040-6182(99)00017-8

Searle, M.P., Shail, R.K., Pownall, J.M., Jurkowski, C., Watts, A.B. & Robb, L.J., 2024. The Permian Cornubian granite batholith, SW England; Part 1: Field, structural, and petrological constraints. Geological Society of America Bulletin 136 (9-10), 4301-4320. DOI: 10.1130/B37457.1

Senglaub, Y., Littke, R. & Brix, M.R., 2006. Numerical modelling of burial and temperature history as an approach for an alternative interpretation of the Bramsche anomaly, Lower Saxony Basin. International Journal of Earth Sciences 95: 204-224. DOI: 10.1007/s00531-005-0033-y

Sissingh, W., 2004. Palaeozoic and Mesozoic igneous activity

in the Netherlands: a tectonomagmatic review. Netherlands Journal of Geosciences 83 (2): 113-134. DOI: 10.1017/S0016774600020084

Sissingh, W., 2003. Tertiary paleogeographic and tectonostratigraphic evolution of the Rhenish Triple Junction. Palaeogeography, Palaeoclimatology, Palaeoecology 196(1-2): 229-263. DOI: 10.1016/S0031-0182(03)00320-1

Slagstad, T., Davidsen, B. & Daly, J.S., 2011. Age and composition of crystalline basement rocks on the Norwegian continental margin: offshore extension and continuity of the Caledonian–Appalachian orogenic belt. Journal of the Geological Society 168(5): 1167-1185. DOI: 10.1144/0016-76492010-136

Slater, T.H.A., 1980. Potassium-Argon age dating and petrographic analysis of a core piece sample from the Union Oil F/4-2A well, Dutch North Sea (No. 4503P/C; 3 pp.). Robertson Research International Limited (Gwynedd, Wales): 3 pp.

Smedley, P.L., 1986. The relationship between calc-alkaline volcanism and within-plate continental rift volcanism: evidence from Scottish Palaeozoic lavas. Earth and Planetary Science Letters 77(1): 113-128. DOI: 10.1016/0012-821X(86)90137-8

Smit, J., Van Wees, J.-D. & Cloetingh, S., 2016. The Thor suture zone: From subduction to intraplate basin setting. Geology 44(9): 707-710. DOI: 10.1130/G37958.1

Smit, J., Van Wees, J.-D. & Cloetingh, S., 2018. Early Carboniferous extension in East Avalonia: 350 My record of lithospheric memory. Marine and Petroleum Geology 92(1): 1010-1027. DOI: 10.1016/j.marpetgeo.2018.01.004

Smith, K. & Ritchie, J.D., 1993. Jurassic volcanic centres in the Central North Sea. In: Parker, J.R. (ed.): Petroleum Geology of North-West Europe: Proceedings of the 4th Conference. Geological Society of London: 519-531.

Stemmerik, L., Ineson, J.R. & Mitchell, J.G., 2000. Stratigraphy of the Rotliegend Group in the Danish part of the Northern Permian Basin, North Sea. Journal of the Geological Society 157 (6): 1127-1136. DOI: 10.1144/jgs.157.6.1127

Stokke, E.W., Liu, E.J. & Jones, M.T., 2020. Evidence of explosive hydromagmatic eruptions during the emplacement of the North Atlantic Igneous Province. Volcanica 3(2): 227-250. DOI: 10.30909/vol.03.02.227250

Storey, M., Duncan, R.A. & Swisher, C.C., 2007. Paleocene-Eocene Thermal Maximum and the Opening of the Northeast Atlantic. Science 316(5824): 587-589. DOI: 10.1126/science.1135274

Tappe, S., Smart, K.A., Stracke, A., Romer, R.L., Prelević, D. & Van den Bogaard, P., 2016. Melt evolution beneath a rifted craton edge: 40Ar/39Ar geochronology and Sr-Nd-Hf-Pb isotope systematics of primitive alkaline basalts and lamprophyres from the SW Baltic Shield. Geochimica et Cosmochimica Acta 173: 1-36. DOI: 10.1016/j.gca.2015.10.006

Teichmüller, M. & Teichmüller, R., 1971. Inkohlung im Rhein-Ruhr-Revier. Fortschritte Geologie Rheinland und Westfalen 19: 69-72.

Tesch, P., 1925. Over een intrusie in het Carboon van oostelijk Gelderland. Verslag Vergadering van 22 Maart 1924. Geologie Sectie Geologisch Mijnbouwkundig Genootschap van Nederland en Koloniën 3(4).

Tesch, P., 1928. On the occurrence of igneous rocks in the Dutch Carboniferous. Le Congres pour l'Avancement des Études de Stratigrafie Carbonifère, Compte Rendu: 731-732.

Tesch, P. & Van Voorthuysen, J.H., 1944. Nog drie intrusies in het Carboon van Oost-Gelderland. Geologie en Mijnbouw 5: 56-57.

Thiadens, A.A., 1963. The Palaeozoic of The Netherlands. Verhandelingen van Het Koninklijk Nederlands Geologisch Mijnbouwkundig Genootschap, Geologische Serie 21(1): 9-28.

Thordarson, Th. & Self, S., 1993. The Laki (Skaftár Fires) and Grímsvötn eruptions in 1783-1785. Bulletin of Volcanology 55(4): 233-263. DOI: 10.1007/BF00624353

Timmerman, M.J., 2004. Timing, geodynamic setting and character of Permo-Carboniferous magmatism in the foreland of the Variscan Orogen, NW Europe. In: Wilson, M., Neumann, E.R., Davies, S.J., Timmerman, M.J., Heeremans, M. & Larsen, B.T. (eds): Permo-Carboniferous Magmatism and Rifting in Europe. Geological Society of London, Special Publications 223: 41-74. DOI: 10.1144/GSL.SP.2004.223.01.03

TNO-GDN, 2022. Emmen Volcanic Formation. Stratigraphic Nomenclature of the Netherlands, TNO – Geological Survey of the Netherlands. https://www.dinoloket.nl/en/stratigraphic-nomenclature/emmen-volcanic-formation

TNO-GDN, 2024. De Wijk Member. Stratigraphic Nomenclature of the Netherlands, TNO – Geological Survey of the Netherlands. https://www.dinoloket.nl/en/stratigraphic-nomenclature/de-wijk-member

Tomkeieff, S. & Tesch, P., 1931. On a dolerite in the Dutch Carboniferous. Geological Magazine 68(5): 231-236.

Torsvik, T.H., Mosar, J. & Eide, E.A., 2001. Cretaceous–Tertiary geodynamics: a North Atlantic exercise. Geophysical Journal International 146(3): 850-866. DOI: 10.1046/j.0956-540x.2001.01511.x

Torsvik, T.H., Smethurst, M.A., Burke, K. & Steinberger, B., 2008. Long term stability in deep mantle structure: Evidence from the ~300 Ma Skagerrak-Centered Large Igneous Province (the SCLIP). Earth and Planetary Science Letters 267(3): 444-452. DOI: 10.1016/j.epsl.2007.12.004

Underhill, J.R., 2009. Role of intrusion-induced salt mobility in controlling the formation of the enigmatic Silverpit Crater, UK Southern North Sea. Petroleum Geoscience 15(3): 197-216. DOI: 10.1144/1354-079309-843

Underhill, J.R. & Partington, M.A., 1993. Jurassic thermal doming and deflation in the North Sea: implications of the sequence stratigraphic evidence. In: Parker, J.R. (ed.): Petroleum Geology of Northwest Europe: Proceedings of the 4th Conference. Geological Society of London, Petroleum Geology Conference Series 4: 337-345. DOI: 10.1144/0040337

Upton, B.G.J., Stephenson, D., Smedley, P.M., Wallis, S.M. & Fitton, J.G., 2004. Carboniferous and Permian magmatism in Scotland. Geological Society of London, Special Publications 223(1):

195-218. DOI: 10.1144/GSL.SP.2004.223.01.09

Van Amerom, H.W.J., 1972. Das karbonische Alter der Tiefbohrung Wanneperveen 1, eine Revision. Geologie En Mijnbouw 51(4): 491-495.

Van Bergen, M.J. & Sissingh, W., 2007. Magmatism in the Netherlands:expression of the north-west European rifting history. In: Wong, Th.E., Batjes, D.A.J.& De Jager, J. (eds): Geology of the Netherlands. Royal Netherlands Academy of Arts and Sciences (KNAW, Amsterdam): 197-222.

Van Buggenum, J.M. & Den Hartog Jager, D.G., 2007. Silesian. In: Wong, Th.E., Batjes, D.A.J.& De Jager, J. (eds): Geology of the Netherlands. Royal Netherlands Academy of Arts and Sciences (KNAW, Amsterdam): 43-62.

Van den Bogaard, P. & Schmincke, H.-U., 1990. Die Entwicklungsgeschichte des Mittelrheinraumes und die Eruptionsgeschichte des Osteifel-Vulkanfeldes. In: Schirmer, W. (ed.): Rheingeschichte zwischen Mosel und Maas. Deuqua-Führer 1 (Hannover): 166-190.

Van den Bosch, M., 2015. Lithostratigraphy of the Oligocene in the Almelo-Winterswijk area, eastern Netherlands. Eburon Publishers (Delft): 164 pp.

Van der Sijp, J.W.C.M., 1953. Intrusive rocks in the Berkel well. Geologie en Mijnbouw 15: 65-66.

Van Voorthuysen, J.H., 1944. Hoornblendediabaas-intrusie in het Wealden van Oost-Nederland. Geologie en Mijnbouw 6: 24-26.

Van Wijhe, D.H., Lutz, M. & Kaasschieter, J.P.H., 1980. The Rotliegend in The Netherlands and its gas accumulations. Geologie En Mijnbouw 59(1): 3-24.

Vandenberghe, N., De Craen, M. & Wouters, L., 2014. The Boom clay geology - from sedimentation to present-day occurrence – a review. Memoirs of the Geological Survey of Belgium 60: 1-76.

Verbraeck, A., 1984. Toelichtingen bij de Geologische kaart van Nederland, schaal 1 : 50.000, bladen Tiel West (39W) en Tiel Oost (390). Rijks Geologische Dienst (Haarlem).

Verweij, J.M., Nelskamp, S. & Hegen, D., 2016. Geochemical composition and origin of natural gas in onshore and offshore Netherlands TNO (Utrecht), Report No. R10599: 182 pp.

Vis, G.-J., Houben, A.J.P., Debacker, T.N. & Geel, C.R., 2025. The geological foundation of the Netherlands: the early Carboniferous, Devonian and older. In: Ten Veen, J.H., Vis, G.-J., De Jager, J. & Wong, Th.E. (eds): Geology of the Netherlands, second edition. Amsterdam University Press (Amsterdam): 53-93. DOI: 10.5117/9789463728362_ch05

Wall, M., Cartwright, J., Davies, R. & McGrandle, A., 2010. 3D seismic imaging of a Tertiary Dyke Swarm in the Southern North Sea, UK. Basin Research 22: 181-194.

Watts, A.B., Xu, C., Searle, M.P., Jurkowski, C. & Shail, R.K., 2024. The Permian Cornubian granite batholith, SW England; Part 2: Gravity anomalies, structure, and state of isostasy. Geological Society of America Bulletin 136 (9-10), 4381-4397. DOI: 10.1130/B37459.1

Wedepohl, K.H., Gohn, E. & Hartmann, G., 1994. Cenozoic alkali basaltic magmas of western Germany and their products of differentiation. Contributions to Mineralogy and Petrology 115(3): 253-278. DOI: 10.1007/BF00310766

White, N. & Latin, D., 1993. Subsidence analyses in the North Sea 'triple-junction'. Journal of the Geological Society 150(3): 473-488.

White, R.S. & McKenzie, D., 1995. Mantle plumes and flood basalts. Journal of Geophysical Research 100(B9): 17543-17585. DOI: 10.1029/95jb01585

Wilkinson, C.M., Ganerød, M., Hendriks, B.W.H. & Eide, E.A., 2017. Compilation and appraisal of geochronological data from the North Atlantic Igneous Province (NAIP). Geological Society of London, Special Publications 447(1): 69-103. DOI: 10.1144/SP447.10

Wilson, M., Neumann, E.-R., Davies, G.R., Timmerman, M.J., Heeremans, M. & Larsen, B.T., 2004. Permo-Carboniferous Magmatism and Rifting in Europe. In: Wilson, M., Neumann, E.-R., Davies, G.R., Timmerman, M.J., Heeremans, M. & Larsen, B.T. (eds): Permo-Carboniferous Magmatism and Rifting in Europe. Geological Society of London, Special Publications 223: 1-10.

Wolf, M. & Bless, M.J.M., 1987. Coal-petrographic investigations on samples from the boreholes Thermae 2000 and Thermae 2002 Valkenburg a/d Geul, The Netherlands. Annales de La Société Géologique de Belgique 110: 77-84.

Woodhall, D. & Knox, R.W.O., 1979. Mesozoic volcanism in the northern North Sea and adjacent areas. Bulletin of the Geological Survey of Great Britain 70: 34-56.

Wörner, G. & Schmincke, H.-U., 1984. Mineralogical and Chemical Zonation of the Laacher See Tephra Sequence (East Eifel, W. Germany). Journal of Petrology 25(4): 805-835. DOI: 10.1093/petrology/25.4.805

Wright, J.E., Hull, J.H., McQulllan, R. & Arnold, S.E., 1971. Irish Sea investigations 1969-70. Natural Environment Research Council.

Zagwijn, W.H., 1985. An outline of the Quaternary stratigraphy of The Netherlands. Geologie en Mijnbouw 64 (1): 17-24.

Zens, J., Zeeden, C., Römer, W., Fuchs, M., Klasen, N. & Lehmkuhl, F., 2017. The Eltville Tephra (Western Europe) age revised: Integrating stratigraphic and dating information from different Last Glacial loess localities. Palaeogeography, Palaeoclimatology, Palaeoecology 466: 240-251. DOI: 10.1016/j.palaeo.2016.11.033

Ziegler, P.A., 1990. Tectonic and palaeogeogaphic development of the North Sea Rift system. In: Blundell, D.J. & Gibbs, A.D. (eds): Tectonic Evolution of the North Sea Rifts. Oxford Science Publications (Oxford): 1-36.

Ziegler, P.A., 1988. Evolution of the Arctic, North Atlantic and western Tethys. American Association of Petroleum Geologists Memoir. 43: 198 pp.

Ziegler, P.A., 1992. North Sea rift system. Tectonophysics 208(1-3): 55-75. DOI: 10.1016/0040-1951(92)90336-5

Ziegler, P.A. & Dèzes, P., 2005. Evolution of the lithosphere in the

area of the Rhine Rift System. International Journal of Earth Sciences 94(4): 594-614.
Zimmerle, W., 1993. On the lithology and provenance of the Rupelian Boom Clay in northern Belgium, a volcaniclastic deposit. Bulletin de La Société Belge de Géologie 102: 91-103.